2014

Pervious Concrete Piles: Development and Investigation of an Innovative Ground Improvement System

Lusu Ni
Lehigh University

PERVIOUS CONCRETE PILES: DEVELOPMENT AND INVESTIGATION OF AN INNOVATIVE GROUND IMPROVEMENT SYSTEM

By

Lusu Ni

A Dissertation

Presented to the Graduate and Research Committee

Of Lehigh University

In Candidacy for the Degree of

Doctor of Philosophy

In

Civil Engineering

Lehigh University

September, 2014

Lusu Ni

PERVIOUS CONCRETE PILES: DEVELOPMENT AND INVESTIGATION OF AN INNOVATIVE GROUND IMPROVEMENT SYSTEM

Approved and recommended for acceptance as a dissertation in partial fulfillment of the requirements for the degree of Doctor of Philosophy.

_____
Defense Date

_____
Accepted Date

_____
Muhannad T. Suleiman

Committee Members:

_____
Sibel Pamukcu

_____
Clay J. Naito

_____
Anne M. Raich

_____
Mesut Pervizpour

ACKNOWLEDGEMENT

First of all, I would like to express my thanks to my advisor, Dr. Muhannad Suleiman, for his guidance, support and generosity. It was my great fortune to work with such a diligent, high self-demand, passionate researcher.

My thanks go to all other members of my committee members for their insightful and valuable advices and encouragement: Dr. Sibel Pamukcu, Dr. Clay Naito, Dr. Mesut Pervizpour, Dr. Anne Raich.

I would like to appreciate all members in our research group at Lehigh University for their assistance in laboratory testing and discussions: Hai Lin, Suguang Xiao, Ehsan Ghazanfari, Pierre Bick and Caleb Davis; and also the undergraduate students from Lafayette College: Matthew D O'Loughlin, Martin Anderson. I would never forget the days and nights we spent together to study and figure out the problems.

I also would like to acknowledge the Lehigh University and National Science Foundation for supporting this research.

Last, but by no means least, I would like to thank my family for their unconditional love and encouragement, which are always my inspiration and courage during my study.

TABLE OF CONTENTS

LIST OF FIGURES

LIST OF TABLES

ABSTRACT

Permeable granular piles are used to increase the time rate of consolidation, reduce liquefaction potential, improve bearing capacity, and reduce settlement. However, the behavior of granular piles depends on the confinement provided by surrounding soil, which limits their use in very soft clays and silts, and organic and peat soils. This research effort aims to develop a new ground-improvement method using pervious concrete piles. Pervious concrete piles provide higher stiffness and strength which are independent of surrounding soil confinement, while offering permeability comparable to granular piles. This proposed ground-improvement method can improve the performance of different structures supported on poor soils.

To achieve the goal of the research project, a series of pervious concrete sample mixing has been conducted to investigate the pervious concrete material properties. Four vertical load tests were performed on one granular pile and three pervious concrete piles. The vertical load responses of pervious concrete and aggregate piles are compared and the variation of soil stresses and displacement during pile installation are discussed. Two lateral load tests were conducted on a precast pervious concrete pile and on a cast-in-place pile. The behavior of pervious concrete piles and the effects of installation on their response under lateral loading were investigated. In addition, a finite element model simulation account for the installation effect has been used to further investigate the behavior of the pervious concrete pile and surrounding soil under vertical load condition.

CHAPTER 1

INTRODUCTION

1.1 BACKGROUND

Ground improvement methods are widely used to enhance soil strength, allow for drainage path, mitigate total and differential settlements, and to reduce construction time. Based on different conditions, various ground improvement methods are available (i.e., prefabricated vertical drains, vacuum consolidation, deep soil mixing, grouting, and vibro-compaction). As one of the most commonly used ground improvement methods, granular piles have been used extensively in several geotechnical engineering applications (Mitchell 1981; Barksdale and Bachus 1983; Aboshi and Suematsu 1985; Bergado et al. 1994; Baez 1995; Terashi and Juran 2000; Okamura et al. 2006). The sections below will discuss different types of granular piles and their installation, properties and failure mechanisms. In addition, this chapter presents the properties of pervious concrete. Furthermore, the motivation and goals of research are presented in this chapter.

1.1.1 Granular Piles

The term 'granular piles' refers to columns composed of compacted sand or gravel. The three common granular piles are sand compaction piles, stone columns, and rammed aggregate piers (Geopiers®). Granular piles provide higher stiffness and strength than surrounding soil. In addition, the piles provide high permeability allowing for soil drainage and consolidation.

The construction of granular piles will change the soil stresses and accelerate pore water pressure dissipation, resulting in consolidation, which leads to the improvement of surrounding soil. Granular piles have been used to increase the time rate of consolidation, increase the bearing capacity, reduce liquefaction potential, and reduce settlement (Mitchell 1981; Barksdale and Bachus 1983; Aboshi and Suematsu 1985; Bergado et al. 1994; Baez 1995; Terashi and Juran 2000; Okamura et al. 2006).

Construction Techniques

Depending on soil types, water level, equipment availability, local practice and construction company ownership, various technical methods have been developed to install different types of granular piles. (Mitchell 1981; Barksdale and Bachus 1983; Bergado 1994; Lin and Wong 1999; Terashi and Juran 2000; Elias et al. 2006). These main installation methods are briefly described as below:

1. *Vibro-compaction Method*

In this method, a vibroflot with water jetting and vibration penetrate into soil to predetermined depth, and then the vibroflot is withdrawn gradually with granular backfill inserted near the ground surface by top feeding method. This specific method is usually used in the cohesionless granular soils (Figure 1.1).

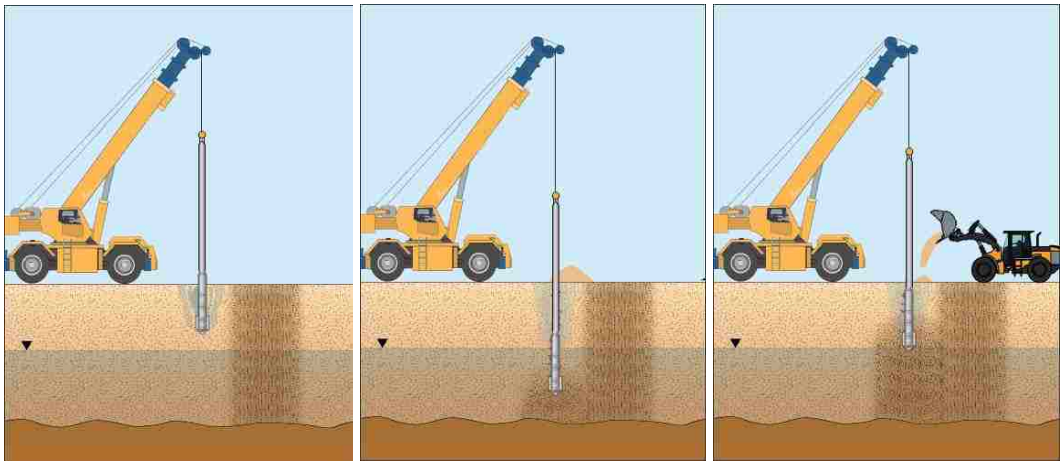

(a) Step 1 **(b) Step 2** **(c) Step 3**

Figure 1.1 Constructions of granular piles by Vibro-compaction Method: (1) Step 1; (2) Step 2; (3) Step 3. (www.HaywardBaker.com)

2. Vibro-replacement Method

This method uses a vibroflot that sinks into the ground under its own weight and with assistance of water (wet top feeding). In wet top feeding method, when the vibroflot reaches the designed depth, it is withdrawn and the uncased hole is flushed out and filled in stages with 12-75 mm size imported gravel. It is mainly used in cohesive soils with high groundwater level and with more than 18% passing No. 200 sieve (Figure 1.2).

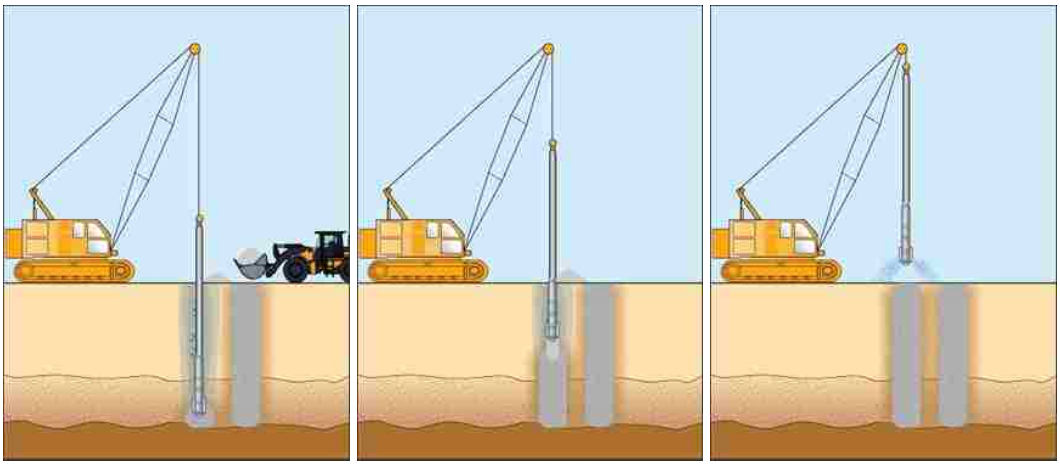

(a) Step 1 **(b) Step 2** **(c) Step 3**

Figure 1.2 Constructions of granular piles by Vibro-replacement Method (Top feeding method): (1) Step 1; (2) Step 2; (3) Step 3. (www.HaywardBaker.com)

3. Vibro-displacement Method

This method is similar to the vibro-replacement method, however, the difference is that the soil is penetrated without water jetting and can be either top feeding method (short piles) or bottom feeding (deep piles). In the bottom feeding, the aggregate is fed gradually through a feeding pipe attached to the vibrator as showed in Figure 1.3. Because of the dry process without water jetting, this method is suitable for soft clay with undrained shear strength more than 40 kN/m^2 and low groundwater level.

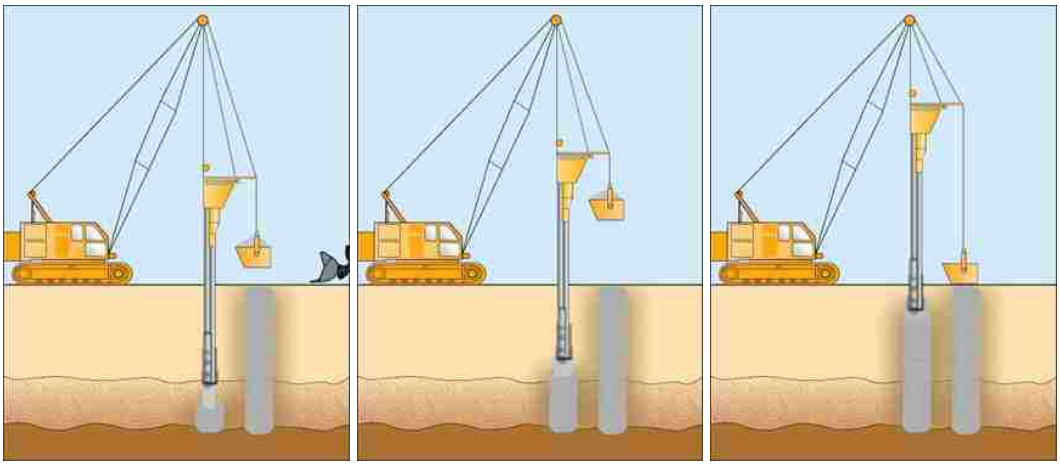

(a) Step 1 **(b) Step 2** **(c) Step 3**

Figure 1.3 Constructions of granular piles by Vibro-displacement Method (Bottom feeding method): (1) Step 1; (2) Step 2; (3) Step 3. (www.HaywardBaker.com)

4. Aggregate Ramming Method

Rammed aggregate piers is a method using a beveled tamper to compact the loose aggregate into the prebored hole in stages. The compaction process results in a high density and stiffness aggregate pier (Figure 1.4). With the beveled tamper, the surrounding soil is densified and horizontal stresses are increased to further support

the piers. Rammed aggregate piers can be used in soft clay and silt, loose sand and soils below the groundwater level.

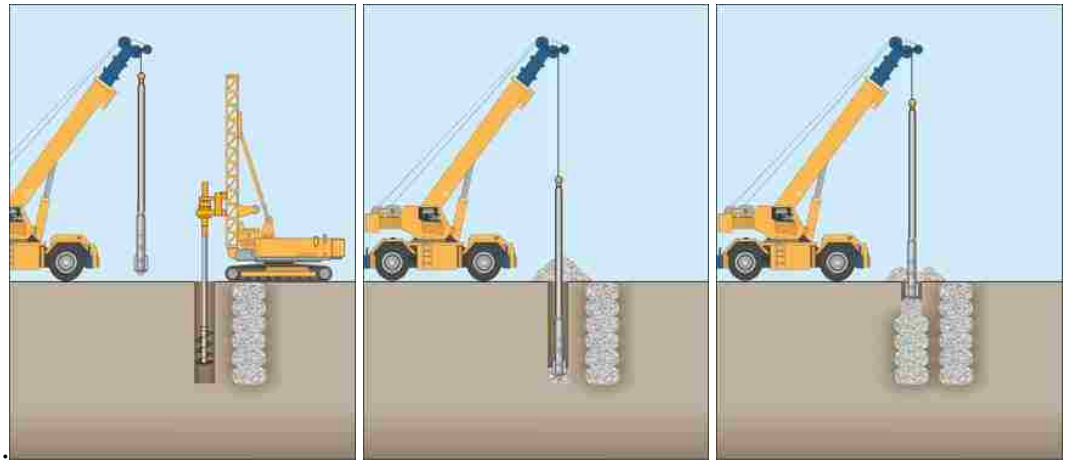

(a) Step 1 **(b) Step 2** **(c) Step 3**

Figure 1.4 Constructions of rammed aggregate piers: (1) Step 1; (2) Step 2; (3) Step 3. (www.HaywardBaker.com)

5. *Vibro-compozer Method*

This method is mainly used to install sand compaction piles (Bergado et al. 1988, 1994; Aboshi et al. 1974, 1985). As shown in Figure 1.5, a casing pipe is driven into the soil with a vertical vibratory hammer. The casing pipe with an open end cone will be used to transport sands down to the bottom and the casing is then repeatedly extracted and partially re-driven to compact the sand below. When the pipe is driven in, the cone at the tip of the casing pipe is kept close. As the pipe is extracted, the cone will open under the weight of feeding sand. This method is suitable to be used in soft clay with high groundwater level.

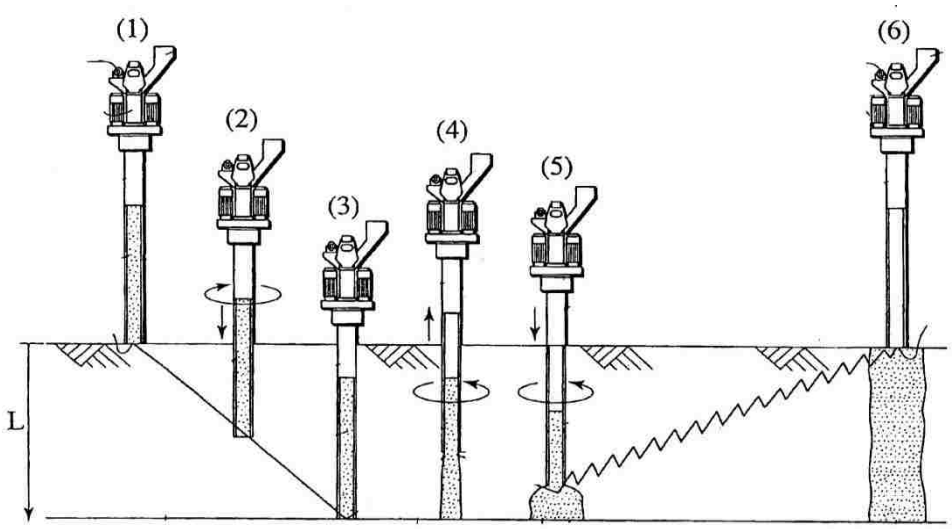

Figure 1.5 Constructions of sand compaction pile (Kitazume, 2005)

Failure Mechanism

As shown in Figure 1.6, regardless of the used construction method, single isolated granular piles under vertical load fail in bulging, shear, or punching (Barksdale and Bachus 1983). For typical granular pile length-to-diameter (L/D) ratios, the most common failure mechanism is bulging, which is usually observed over a distance of 2 to 3 pile diameters (2 to 3D) below the soil surface (Barksdale and Bachus 1983; Bergado et al. 1994). In this failure mechanism, the granular pile bulges into the surrounding soil (Figure 1.6a). Therefore, the ultimate vertical resistance of the column depends upon the lateral confining stress provided by the surrounding soil. Shear failure is possible to occur in short piles bearing on a firm support layer. This is similar to the general shear bearing capacity failure occurring in shallow foundations. Punching failure occurs in a short pile (less than 3 D in length) with a floating end installed in soft soils. The ultimate capacities of the first two failure mechanisms are summarized in Table 1.1. Note that the third failure

mechanism is similar to that experienced by rigid deep foundations subjected to vertical loading.

When subjected to lateral load, such as in slope stabilization, the granular piles fail in direct shear along the failure surface. The shear strength is calculated as the average shear strength of the soil/granular piles composite materials along the failure surface (Mitchell 1981; Barksdale and Bachus 1983; Bergado et al. 1994).

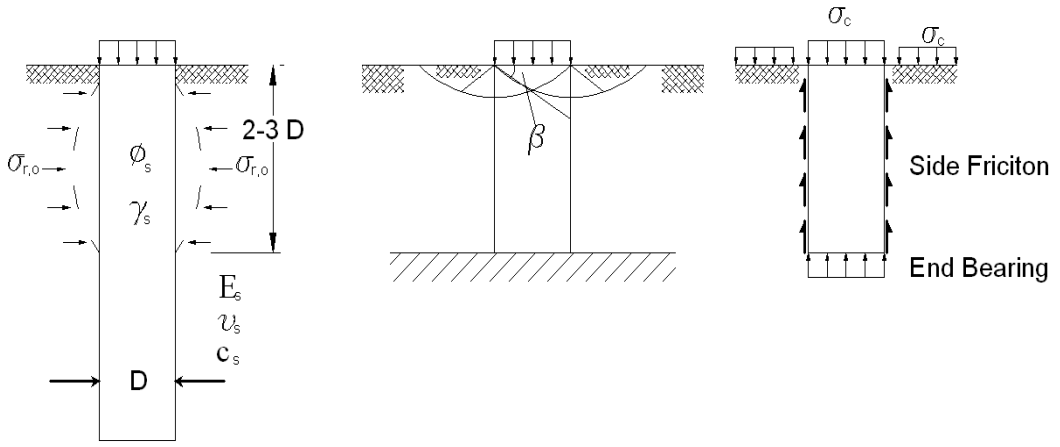

(a) Bulging Failure **(b) Shear Failure** **(c) Punching Failure**

Figure 1.6 Failure mechanisms of single granular piles

Table 1.1 Ultimate capacity for different failure mechanisms of granular piles

Mode of failure	Derived formula	References
Bulging	$q_{ult} = \left\{\sigma_{r,o} + c_s\left[1 + \ln\frac{E_s}{2c_s(1+\nu_s)}\right]\right\}\tan^2(45 + \frac{\phi_c}{2})$ Where, $\sigma_{r,o}$: the total radial confining stress; c_s: undrained shear strength of soil; ϕ_c:the friction angle of aggregate material; E_s: undrained modulus of soil; ν_s: Poisson's ratio of soil	Barksdale and Bachus 1983
Shear	$q_{ult} = \frac{1}{2}\gamma_c B tan^3\beta + 2c_s tan^2\beta + 2(1 - a_s)c_s tan\beta$ $\beta = 45° + \frac{\tan^{-1}\mu_s a_s tan\phi_c}{2}$; Where, γ_c: saturated or wet unit weight of the cohesive soil; B: foundation (including surrounding soil) width; β: failure surface inclination; a_s: the area replacement ratio; μ_s the stress concentration factor for granular piles; c_s: undrained shear strength within the unreinforced cohesive soil;	Barksdale & Bachus 1983

Properties of Granular Piles

The properties of granular piles (i.e. sand compaction piles, stone columns, rammed aggregate piers) are summarized in Table 1.2. As shown in the table, the modulus of granular piles ranges from 25 to 190 MPa and the permeability ranges from 0.05 to 2.0 cm/sec.

Table 1.2 Summaries of the properties of granular piles

Granular pile	Friction Angle (°)	Modulus (MPa)	Stress Concentration ratio	Permeability (cm/sec)	Reference
Sand Compaction Piles	30-36	25-40	1.5-6.0	0.05-0.65	Aboshi et al. 1979; Bergado et al. 1988, 1994
Stone Columns	35-45	30-70	2.0-8.5	0.09-2.0	Mitchell 1981; Barksdale and Bachus 1983; Baez 1995
Rammed Aggregate Piers	47-52	60-190	2.0-10	1.90	Hoevelkamp 2002; White and Suleiman 2004; Suleiman et al. 2014a

1.1.2 Pervious Concrete

Pervious concrete is a special concrete made primarily of single-size aggregate (Figure 1.7). Pervious concrete has been used in pavements to reduce the quantity of storm water runoff and perform initial treatment of water quality by allowing water to penetrate through the porous surface. The pervious concrete is mainly used in pavement application, including sidewalks, parking lots, tennis courts, and low traffic density areas (Tennis et al. 2004; and Suleiman et al. 2011).

(a) (b)

Figure 1.7 Pervious concrete: (a) Pervious concrete sample; (b) Pervious concrete pavement surface. (Concrete Technology Forum Focus on Pervious Concrete Conference, NRMCA, 2006)

As summarized in Table 1.3, the pervious concrete has porosity ranging from 11% to 42%, 28-days compressive strength 5.5 MPa to 26.5 MPa and permeability 0.01 cm/sec to 1.50 cm/sec (Kajio et al. 1998; Beeldens et al. 2003; Tennis et al. 2004; Park and Tia 2004; and Suleiman et al. 2006; Kevern et al. 2008).

Table 1.3 Summary of the properties of pervious concrete material

Porosity (%)	Permeability (cm/sec)	28-days Compression Strength (MPa)	Reference
11-15	0.025-0.18	N/A	Kajio, 1998
19	N/A	26.0	Beeldens, 2003
N/A	N/A	19.0	Tamai and Yoshida, 2003
15-25	0.2-0.53	5.5-20.7	Tennis, et al. 2004
18-31	N/A	11.0-25.0	Park and Tia, 2004
12-42	0.03-1.50	11.9-25.3	Schaefer, et al., 2006
19-33	0.18-1.50	10.4-22.3	Suleiman et al., 2006
15-33	0.01-1.18	17.3-26.5	Kevern et al., 2008

1.2 MOTIVATION

1.2.1 Pervious Concrete Ground Improvement Piles

The various installation methods and improvement benefits allow granular piles to be used to improve a wide range of poor soils. However, when compared with other pile types (e.g., steel and concrete piles), the strength and stiffness of granular piles are lower and depend on the properties of the surrounding soil. For conditions where the surrounding soil cannot provide the confining pressure around granular piles to ensure developing the required stiffness and strength, the use of granular piles is limited (Venema 1991). For example, Barksdale and Bachus (1983) reported that when a stratum of poor soil (very soft clays and silts, peat and other organic materials) with a thickness greater than 1 column diameter, granular piles is not suitable to improve the soil. Therefore, granular piles have limited use in very soft clays and silts, and organic and peat soils.

Comparing the properties of granular piles (Table 1.2) with those of the pervious concrete material (Table 1.3), pervious concrete can develop a much higher unconfined compressive strength and maintain a relatively similar permeability of granular piles. According to the studies of other ground improvement techniques (Suleiman et al. 2003; Han and Gabr 2002), the stress concentration ratio of pervious concrete piles is expected to be 3 to 4 times that of granular piles in embankment applications. Higher stress concentration ratio indicates that the stresses carried by soils and the area replacement ratio in the field will be reduced. Meanwhile, the relative high permeability ensures accelerated consolidation and dissipation of pore water pressure. Furthermore, the stiffness of pervious concrete pile is not depending

on surrounding soil. These advantages are expected to result in an enhanced ground improvement system that can be used in a wider range of soil types.

1.2.2 Pile Installation Effects

During pile installation or constructions, the soil surrounding the pile experience significant change of displacement and stress and its properties also be changed correspondingly. The changes due to the pile installation influence the subsequent load-displacement response of the pile. Therefore, the effects of pile installation have been investigated by several researchers (Yu 1990 and 2000; Shublaq 1992; Klotz and Coop 2001; Hunt et al. 2002; Lee et al. 2004; White and Bolton 2004; Dijkstra et al. 2006 and 2008; Suleiman and White 2006; Pham and White 2007; Salgado and Prezzi 2007; Chen et al. 2009; Said et al. 2009; Basu et al. 2010; Castro and Karstunen 2010; Thompson and Suleiman 2010; Yi et al. 2010; Dijkstra et al. 2011; Pucker and Grabe 2012; and Lundberg et al. 2013).

Different approaches have been used by these researchers to investigate the effects of pile installation on surrounding soils, including cavity expansion analysis, numerical modeling methods, experimental methods with pressure measurement at soil-pile interface, soil density measurement, shear wave velocity measurement and movement around the pile.

Shublaq (1992) and Dijkstra et al. (2008) used thermal probe density measurement to investigate the installation effect of driven pile in sand and showed that sand was compacted with 0.6 to 28.6% density increase in a zone of 7D (diameter) around the pile tip. Klotz and Coop (2001) conducted a series of model

pile tests in a centrifuge and investigated the effects of changing soil density and stresses on pile capacity. They concluded that the shaft friction increase by approximately 12% due to the increase of horizontal stresses. Hunt et al. (2002) measured the shear wave velocity change and investigated the changes of soil properties surrounding piles driven in soft clay through a comprehensive testing program. The testing results show that the soil zone affected by pile installation extends to 3.5D (3.5 x pile diameter) from pile center and that the soil stiffness of the soil adjacent to pile increased by10 to 15% due to pile installation. Lee et al. (2004), who performed centrifuge tests, reported that the soil horizontal stresses and pore water pressure changes by 30 to 100% within 6D surrounding the pile during the installation of sand compaction piles in soft clay. Yi et al. (2010) investigated the effects of installation of sand compaction piles on soil shear strength using the same centrifuge test setting-up as Lee et al. (2004). The results showed that the increase of the shear strength of the soil at 1.5D from pile center ranged from 25% to 200% along the pile length. White and Bolton (2004) investigated the penetration mechanism of a displacement pile using an image-cased deformation measurement technique, and the results demonstrate that the soil displacement extended to 15D, which were amplified by the testing boundary. Yu (1990 and 2000) and Salgado and Prezzi (2007) used the cavity expansion theory and cone penetration tests to investigate the stress development in pile installation. However, the cavity expansion theory assumed an large effected zone (70 to 100 times of cavity diameter) for available calculation. Lundberg et al. (2013) observed the displacement of soil during pile installation through the Plexiglas wall of test container and the results showed the displacement

occurs within 2D from pile centers due to pile installation. However, none of these approaches, directly and simultaneously measured the variation of soil stresses and soil movement during pile installation. Therefore, Lundberg et al. (2013) reported that there is a lack of direct combined measurements of soil stresses and movement surrounding piles in general.

Numerical simulation methods have been also utilized to investigate the effects of pile installation on soil properties, displacement and stress (Dijkstra et al. 2006; Ambily and Ganhdi 2007; Pham and White 2007; Chen et al. 2009; Said et al. 2009; Basu et al. 2010; Castro and Karstunen 2010; Thompson and Suleiman 2010; Dijkstra et al. 2011; Pucker and Grabe 2012). However, due to the complexity of the pile installation effects and lack of direct measurements on soil and pile, the modelling results are difficult to be validated (Dijkstra 2011; Pucker and Grabe 2012). In addition, very few researches have investigated the change of soil properties due to pile installation (Wehnert and Vermeer 2004a and 2004b; Said et al. 2009) in numerical simulation. Therefore, the numerical simulation needs to be improved and validate calculation results with the experimental measurement. In addition, very few researchers have been investigating the installation effects on the behavior of laterally loaded piles (Lunberg et al. 2013). The installation effects on laterally loaded pile and soil require further investigation.

In this research, the installation effects on pile and soil behavior will be investigated utilizing both experimental method and numerical modeling method.

1.3 GOALS AND OBJECTIVES

The goal of this research is to develop an innovative ground improvement alternative that uses pervious concrete piles and investigate the pile installation effect. The pervious concrete piles should be able to provide higher stiffness and strength that are independent of the surrounding soil properties while offering permeability comparable to granular piles, to support structures and highway facilities constructed on a wide range of poor soil conditions, including very soft clays and silts, and peat and organic soils. In addition, the effect of pile installation on soil properties, displacement and stress was directly measured in tests. The installation effects are analyzed by experimental and numerical approaches.

The objectives of this research are:

1. Investigating the pervious concrete material properties and developing suitable mixing procedures and mixing proportions for pervious concrete pile casting;
2. Developing installation technique for pervious concrete pile and investigating the effects of pile installation effects on soil and pervious concrete pile properties, soil-pile interactions, and on pile behavior;
3. Evaluating the response of pervious concrete piles when subjected to different loading conditions;
4. Developing appropriate analytical methods to simulate the pervious pile behavior, soil-pile interaction and installation effects.

1.4 ORGNIZATION

The Dissertation begins with Chapter 1, in which the back ground information, the motivation and research goal has been introduced.

Chapter 2 discusses the investigation of pervious concrete material properties, and provides an optimized mixing procedure and mixing proportion design for casting pervious concrete piles.

Chapter 3 describes the soil-pile interaction and behavior of pervious concrete piles subjected to vertical loading and the effects of pile installation on the sepsonse under vertical loading.

Chapter 4 presents the soil-pile interaction and behavior of pervious concrete piles under lateral loads, including the pile behavior with respect to lateral capacity, pile and soil displacements, soil-pile interactions and the effects of installation.

Chapter 5 focuses on numerical modeling of pervious concrete piles under vertical load including the effects of installation.

Chapter 6 summarizes the general conclusions and provides recommendations for further studies.

CHAPTER 2

INVESTIGATION OF PERVIOUS CONCRETE PROPERTIES

2.1 INTRODUCTION

In Chapter 1, the use of pervious concrete in pavement and sidewalk applications were introduced and the properties of pervious concrete from literatures were summarized in Table 1.3, which shows a wide range of strength and permeability. For ground improvement applications, a pervious concrete material need to be improved with high stiffness and strength, and permeability comparable to granular piles (ranged from 0.05 to 2.0 cm/s).

To develop a mixture suitable for ground improvement application, a series of pervious concrete mixtures was prepared to obtain an adequate compressive strength and permeability. Pervious concrete cylinder samples were tested to measure the porosity, permeability, compressive strength, elastic modulus, and split tensile strength. The porosity was measured using ASTM C1688 (ASTM 2009e), the compressive strength was determined using ASTM C39 (ASTM 2009b), the elastic modulus was measured using ASTM C469 (ASTM 2009j), and the split tensile strength was measured using ASTM C496 (ASTM 2009i). In addition, the permeability was measured using an in house designed falling-head as shown in Figure 2.1. The permeameter has a transparent tube with scale for recording the water level. The tube has an inside diameter of 76 mm and height of 914 mm. The sample was installed at the bottom of the tube. Duct Seal (DS-130, Gardner Bender) was used to seal the both sides of the sample to prevent water leakage along the sides of the

sample. The falling-head test was performed for several times to obtain an average value of permeability.

Pervious concrete properties are significantly affected by the mixing procedure, aggregate type, compaction (vibrating) times, water/cement ratio, and sand/aggregate ratio (Schaefer et al. 2006; Suleiman 2006; Kevern 2008). The effects of these variables on pervious concrete strength and permeability were investigated and will be discussed next.

Figure 2.1 Falling head permeameter used for the permeability testing

2. 2 MIXING DESIGN INVESTIGATION

The materials used for pervious concrete mixing include aggregate, cement (Portland cement type II from Lafarge North America Inc.), sand (fine play sand available in home improvement store), water, air enhancement admixture (AEA, Daravair 1000) and high range water reducer (HRWR, V-MAR VSC 500). The investigation focuses on mixing procedure, aggregate type, compaction time, water/cement ratio, and sand/aggregate ratio. Mixtures were prepared using

water/cement ratios ranging from 0.21 – 0.28 and sand/aggregate ratios ranging from 0.05 – 0.17 using two mixing procedures, four different types of aggregate and four different compaction times.

2.2.1 Mixing Procedure

The main procedure of pervious concrete mixing follows the normal concrete mixing procedure in the ASTM C192 (2009a). Two procedures have been used for pervious concrete mixing as summarized in Table 2.1. The main difference between two mixing procedures is in the Step 2 and Step 4 as show in table. Two mixtures were prepared using the two mixing procedures. The first mixture has the following mixing design: sand/aggregate ratio of 0.07, water/cement ratio of 0.26, 343 kg/m^3 cement, 1,510 kg/m^3 coarse aggregate, 0.49 kg/m^3 AEA, and 0.96 kg/m^3 HRWR. The sec.ond mixing design is 0.11 sand/aggregate ratio, 0.21 water/cement ratio, 343 kg/m^3 cement, 1,440 kg/m^3 coarse aggregate, 2.47 kg/ m^3 AEA, and 4.94 kg/m^3 HRWR. Both mixtures used Nazareth gravel, which was locally available in Lehigh Valley. The aggregate was sieved and the portion passing the 9.5 mm sieve (3/8 in. sieve) and retained on the 4.75 mm sieve (No.4 sieve) was used (Schaefer et al. 2006). For both mixtures, a compaction time of 10 sec. was used.

The compressive strength and permeability comparison of mixture using these two mixing procedures are summarized in the Figure 2.1. The results shows that the compressive strength of mixtures prepared by procedure 1 (13.8 MPa as average) is higher than that of mixtures prepared by procedure 2 (9.6 MPa as average). The permeability of samples prepared suing procedure 2 (2.1 cm/sec.) is higher than that

in procedure 1 (1.7 cm/sec.). Further investigation on mixing proportion adjustment shows that the compressive strength can be improved by optimization of mixing proportion, while the permeability is more difficult to be improved by changing the mixing proportion if the aggregate size is kept the same. It is worth noting that the mixing of cement in step 4 of procedure 1 may cause cement clumps as shown in Figure 2.2, which may affect the pervious concrete properties. As shown in Figure 2.4, the failure surface of samples prepared by procedure 2 passes through the aggregate, while the failure surface of samples prepared by procedure 1 mainly passes through cement or the interface between the cement and aggregate. This phenomenon indicates that the sample prepared by procedure 2 may achieve a higher strength with better quality aggregate material. Based on the above observations and analysis, the mixing procedure 2 was selected for further mixing.

Table 2.1 Mixing procedure

Procedure 1:	
Step 1	Mix water, AEA, and HRWR together
Step 2	**Add sand, aggregate, and 2/3 of water mixture to mixer**
Step 3	Mix together for 1 minute
Step 4	**Add cement and last 1/3 of water mixture to mixer**
Step 5	Mix thoroughly for 3 minutes
Step 6	Allow to rest for 3 minutes
Step 7	Mix for an additional 2 minutes

Procedure 2:	
Step 1	Mix water, AEA, and HRWR together
Step 2	**Add Aggregate and 5 – 10% cement**
Step 3	Mix together for 1 minute
Step 4	**Add sand, water mixture, and rest of cement to mixer**
Step 5	Mix thoroughly for 3 minutes
Step 6	Allow to rest for 3 minutes
Step 7	Mix for an additional 2 minutes

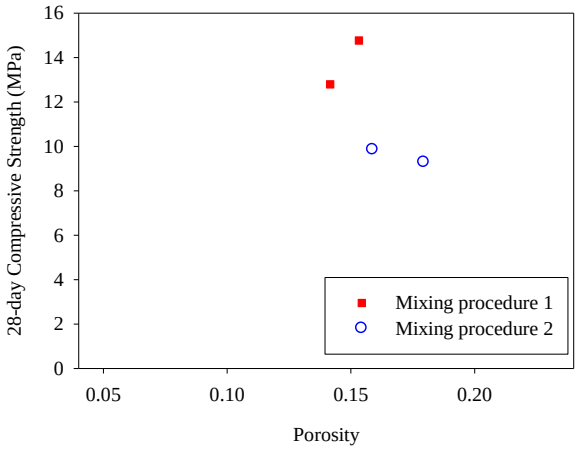

(a)

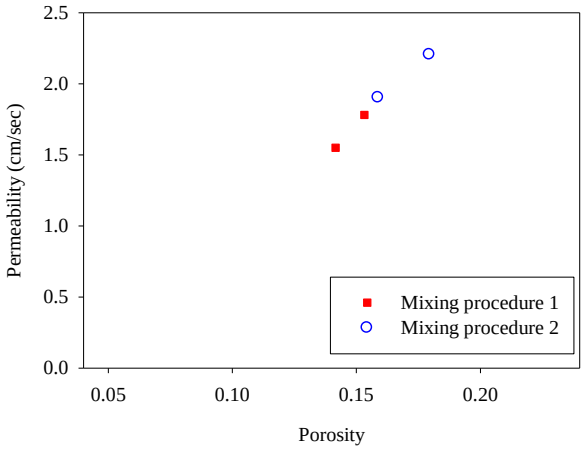

(b)

Figure 2.2 Pervious concrete properties for mixtures prepared using different mixing procedures: (a) 28-day compressive strength; (b) permeability

Figure 2.3 Pervious concrete properties for mixtures

(a) (b)

Figure 2.4 Failure surface of samples prepared using the two mixing procedure: (a) Mix procedure 1; (b) Mix procedure 2

2.2.2 Sand/Aggregate Ratio

Four different sand/aggregate ratios (0.05, 0.08, 0.11 and 0.17) have been used. The samples were mixed using the mixing procedure 2, sieved Nazareth aggregate, and 10 sec. compaction time. The material proportion for mixing is water/cement ratio of 0.21, 343 kg/m^3 cement, 1,523 kg/m^3 coarse aggregate for ratio 0.05 (1,477 kg/m^3 for ratio 0.08, 1,440 kg/m^3 for ratio 0.11, and 1,329 kg/m^3 for ratio 0.17), 0.49 kg/m^3 AEA, and 0.96 kg/m^3 HRWR.

The results in Figure 2.5 show that the mixing with sand/aggregate ratio with 0.11 can provide the highest compressive strength of 13.6 MPa. The permeability of the mixtures with different sand/aggregate ratio is higher than 1.6 cm/s which is comparable to granular piles (up to 2.0 cm/sec.). Therefore, the sand/aggregate ratio of 0.11 was selected for further investigation.

Other mixtures were prepared using the sieved Pea gravel with sand/aggregate ratios of 0.07 and 0.11. The mixtures have water/cement ratio of 0.21, 343 kg/m^3

cement, 1,440 kg/m^3 coarse aggregate, 0.74 kg/m^3 AEA, and 4.06 kg/m^3 HRWR. The compressive strengths of mixtures with 0.07 and 0.11 sand/aggregate ratios were 22.2 and 29.0 MPa, respectively. The permeability was 1.68 cm/sec. of mixture with 0.07 sand/aggregate ratio and 1.45 cm/sec. of mixture with 0.11 sand/aggregate ratio. Therefore, the sand/aggregate ratio of 0.11 was selected for further mixing investigation.

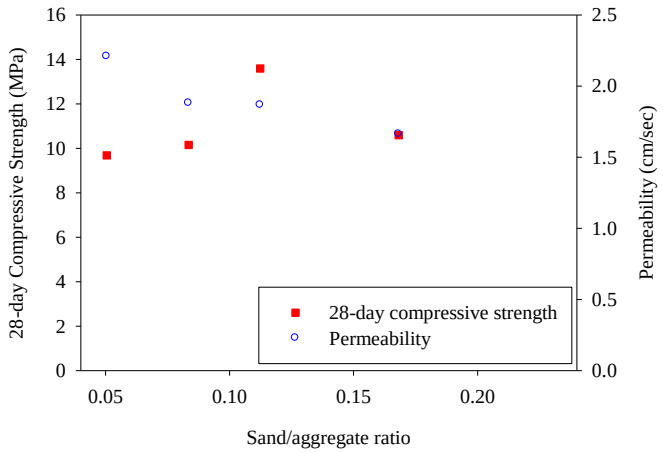

Figure 2.5 Pervious concrete compressive strength and permeability for mixtures prepared using different sand/aggregate ratios

2.2.3 Water/Cement Ratio

Four different water/cement ratios (0.21, 0.23, 0.27 and 0.28) were used for pervious concrete mixtures. The samples were mixed using mixing procedure 2 and with sand/aggregate ratio of 0.11, water/cement ratio of 0.21, 377 kg/m^3 cement, 1,440 kg/m^3 coarse aggregate, 2.47 kg/m^3 AEA, and 4.94 kg/m^3 HRWR. The aggregate used for these mixtures was sieved Nazareth gravel. The compaction time of 10 sec. was used for these samples.

As shown in Figure 2.6, the water/cement ratio of 0.21 provides higher compressive strength (18.3 MPa) for mixing sample. The increase of water/cement ratio to 0.27 decreases the compressive strength up to 25%. In addition, the sample with 0.21 water/cement ratio has 1.33 cm/s permeability which is within the permeability range of granular piles (0.05 to 2.0 cm/sec.).

The sample mixing with water/cement ratio less than 0.21 has also been tried. During the mixing, the mixture was dry, which indicated that water was not enough for cementation development. Therefore, the mixing of water/cement ratio less than 0.21 was stopped and the water/cement ratio was adjusted to 0.21.

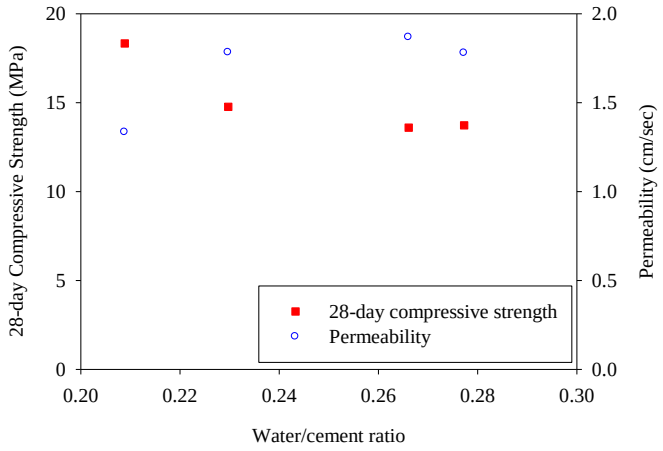

Figure 2.6 Pervious concrete compressive strength and permeability for mixtures prepared using different water/cement ratios

2.2.4 Aggregate Type

Four different aggregate types, including Nazareth gray gravel, Marble gravel, Pea gravel and New Jersey aggregate, have been used during the pervious concrete mixing preparation. The properties of aggregate are summarized in the Table 2.2 and their gradations are presented in Figure 2.7. The aggregates were washed and sieved,

and the portion passing the 9.5 mm sieve (3/8 in. sieve) and retained on the 4.75 mm sieve (No.4 sieve) was used for all mixtures. The samples were mixed using mixing procedure 2, compaction time of 10 sec., and sand/aggregate ratio of 0.11, water/cement ratio of 0.21, 377 kg/m^3 cement, 1,440 kg/m^3 coarse aggregate, 2.47 kg/m^3 AEA, and 4.94 kg/m^3 HRWR.

The compressive strength and permeability versus porosity are presented in the Figure 2.8. The testing results show that aggregate type has great effect on the pervious concrete mixture properties. The mixture using New Jersey aggregate provides the highest compressive strength and permeability. However, this type material can only be obtained from one manufacture in New Jersey. The quantity obtained by research team is not enough for further mixing. Among the mixtures of the other three aggregates, the samples mixed with Pea gravel have higher strength (20.8 MPa) and permeability (1.75 cm/sec.) comparable to granular piles (up to 2.0 cm/sec.). In addition, the pea gravel is available from home improvement stores. Therefore, the Pea gravel was chosen for further investigation.

Table 2.2 Properties of aggregates used for the pervious concrete mixing

Aggregate Type	Nazareth Gray Gravel	Marble Gravel	Pea Gravel	New Jersey Aggregate
Unit Weight (kN/m^3)	14.9	16.2	16.1	16.1
Voids (%)	40	35	33	43
Specific Gravity	2.62	2.62	2.48	2.90
Absorption (%)	1.8	1.6	0.7	0.9
Abrasion Mass Loss (%)	12.1	-	14.1	10.9

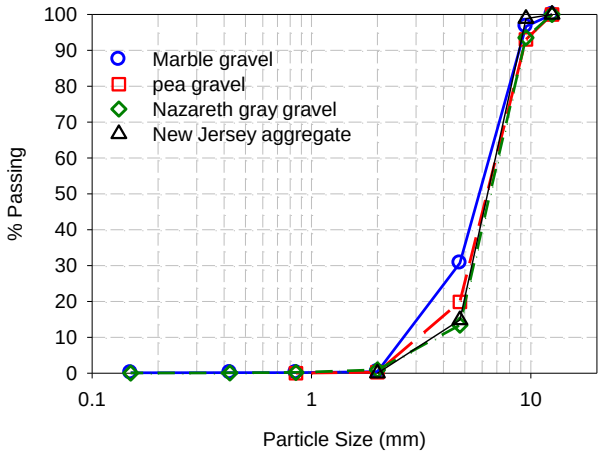

Figure 2.7 The gradation of aggregates used for pervious concrete mixing

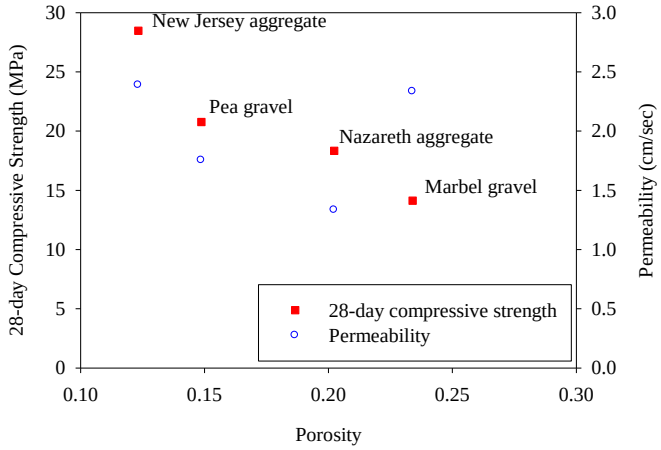

Figure 2.8 Pervious concrete compressive strength and permeability for mixtures prepared using different aggregate

2.2.5 Compaction Time

The pervious concrete samples were compacted using a vibrating table (HUMBOLDT, 60 Hz with amplitude 0.86 mm). The samples were mixed using sieved Pea gravel and mixing procedure 2 with 0.11 sand/aggregate ratio, 0.21 water/cement ratio, 377 kg/m^3 cement, 1,440 kg/m^3 coarse aggregate, 2.47 kg/m^3 AEA and 4.94 kg/m^3 HRWR. Four different compaction times (5 sec., 10 sec., 30 sec.

and 60 sec.) have been used to investigate the compaction time effect on pervious concrete properties.

As shown in Figure 2.9a, the samples with compaction time of 10 sec. have uniform distribution of materials, while samples with 30 and 60 sec.. compaction time have segregation at the bottom. This segregation may affect the permeability of the pervious concrete sample and the pile as well as the strength. The 28-day compressive strength and permeability presented in Figure 2.9b, the sample compacted by 10 sec.. has highest strength (33.3 MPa) and a comparable permeability (1.1 cm/sec.) to granular piles. Therefore, compaction time with 10 sec. was selected for further investigation. It should be noted that the permeability increase of samples with 30 and 60 sec. compaction times shown in Figure 2.9b was determined after cutting the segregation part at the bottom of the samples.

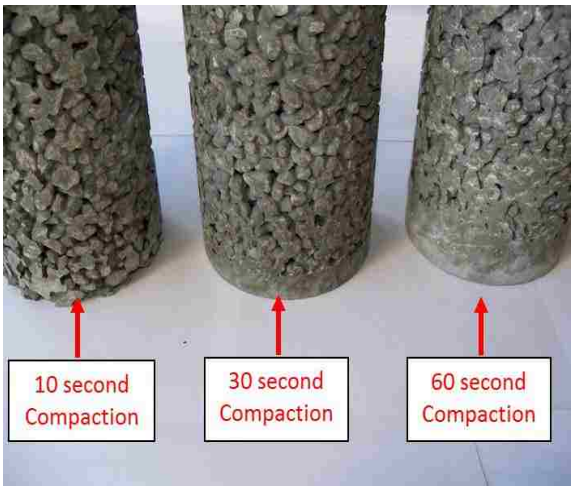

(a)

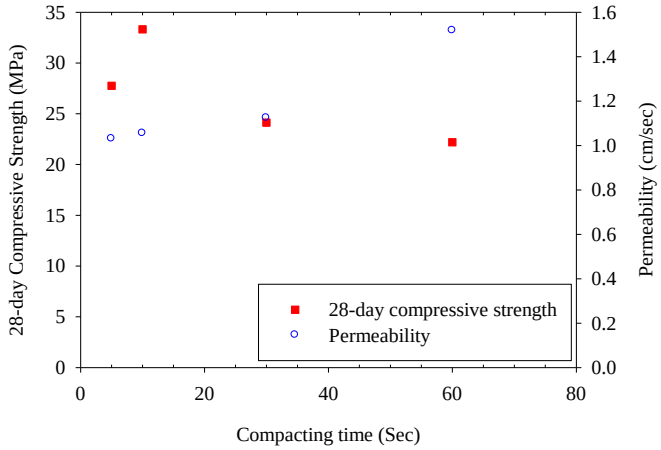

(b)

Figure 2.9 pervious concrete mixtures with different compacting times: (1) samples compacted with 10 sec., 30 sec. and 60 sec.; (2) compressive strength and permeability versus porosity

2.2.6 Mixing for Pervious Concrete Pile

For all mixtures prepared as part of this study, the 28-day compressive strength and permeability as a function of porosity of the pervious concrete mixings are summarized in the Figure 2.10. This figure includes different mixing procedure, sand/aggregate ratio, water/cement ratio, aggregate type and compaction time. Among all the mixtures, the improved mixing design selected for pervious concrete pile casting has the following mixing design: water/cement ratio of 0.21, sand/aggregate ratio of 0.11, 377 kg/m^3 cement, 1,440 kg/m^3 coarse aggregate, 2.47 kg/m^3 AEA and 4.94 kg/m^3 HRWR.

When comparing the material properties of the pervious concrete sample with the granular piles, it was found that the unconfined compressive strength of the pervious concrete material was more than 10 times greater than that of the confined granular piles; and the permeability coefficient of the pervious concrete sample and granular columns were comparable (Suleiman et al. 2014a).

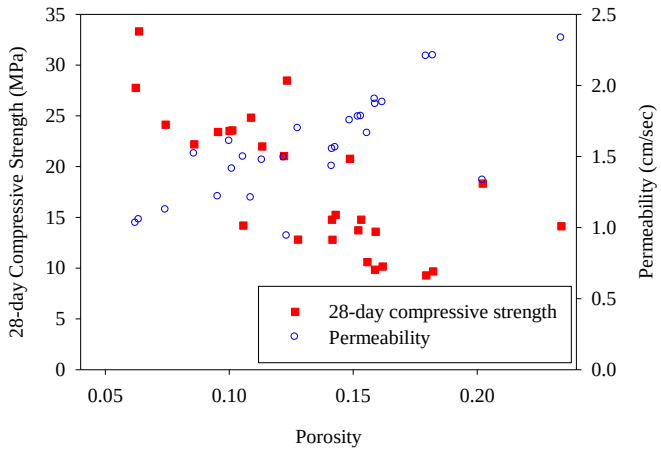

Figure 2.10 pervious concrete compressive strength and permeability versus the porosity

2.3 BEAM TEST

2.3.1 Beam Test Set Up

The purpose of the beam test is to obtain the moment-curvature relationship of the pervious concrete pile cross section. The test follows the procedure of ASTM C78 (2009f). A load increment of 89 N was used and each load was hold for 1 minute. The test was stopped when the pile displacement increased continuously under a constant load.

The pervious concrete pile shown in Figure 2.11 was cast using the mixing design mentioned at the end of the previous section. The pervious concrete mixing has a porosity of 0.11, permeability of 1.21 cm/s, 28-day compressive strength of 24.8 MPa, split tensile strength of 2,260 kPa and elastic modulus of 16.3 GPa. The pile has 101 mm diameter and 1,524 mm length. The pile had one No.4 rebar installed at pile center and one groove along the pile was made for Shape Acceleration Arrays (SAA) installation (Figure 2.11b).

As shown in Figure 2.11, the beam was loaded at two symmetric points, which was located at 1/3 and 2/3 length of pile. The moment at the section between these two loading points is keep constant. The pile was instrumented with Shape Acceleration Arrays (SAA) at middle along the pile to measure the pile deformation during the test. Four dial gauges had been set to verify the SAA measurements.

Figure 2.11 Beam test setting up of pervious concrete pile: (a) pervious concrete pile setting up; (b) SAA and dial gauge setting up; (c) hydraulic load on beam

2.3.2 Test Results

The ultimate load of the beam test was 5,204N with maximum displacement of 18.7 mm at the middle of the pile. Figure 2.12 shows the pile deformation during the test. Based on the measurement values of the load and the displacement along the pile, the moment curvature relationship was calculated and presented in Figure 2.13. The maximum moment is 1,322N·m with curvature of 0.0019. Theoretical method results based on SAP2000 was compared with the moment-curvature response calculated using the measured displacement of the pile, which shows very good

agreement. The slope of the moment-curvature curve shows that EI (elastic modulus multiplied by inertia) value of pile section decreased from 130 kN m^2 to 18 kN m^2. This moment-curvature relationship will be used to model the behavior of the pervious concrete pile cross section.

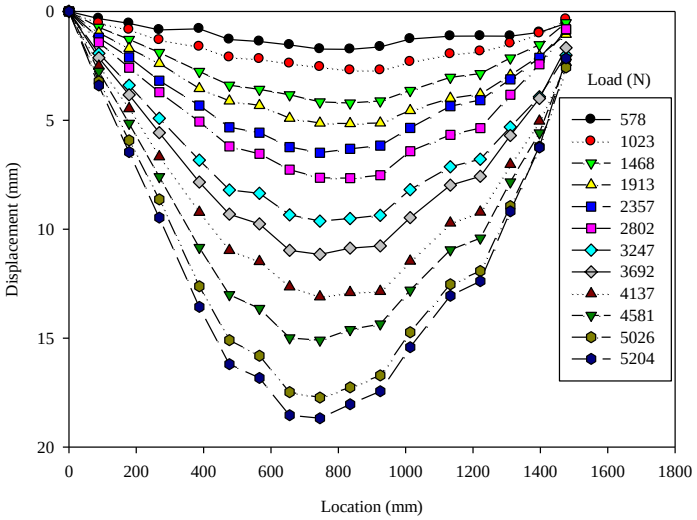

Figure 2.12 The deformation of pervious concrete pile in beam test

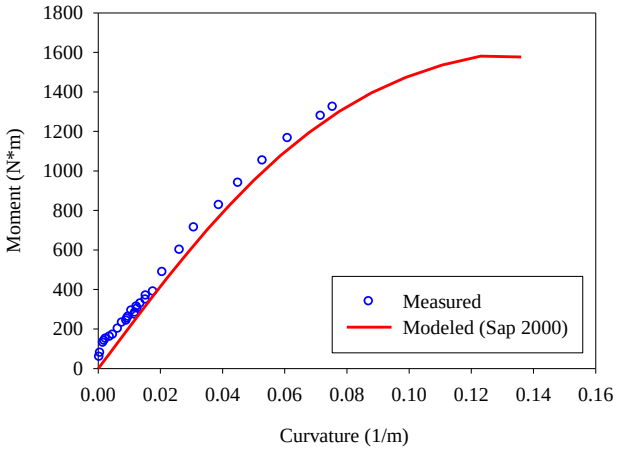

Figure 2.13. The moment curvature relationship of pervious concrete pile

2.4 SUMMARY AND CONCLUSIONS

In this chapter, the pervious concrete properties have been investigated. A mixing design targeted higher strength and comparable permeability of granular pile The moment-curvature properties have been investigated using the beam tests. Based on the discussion of the experimental results presented in this chapter, the conclusions on pervious concrete properties are made as follow:

1. The mixing initial step of the additional 1 min. mixing of aggregate and 5-10% cement improved the coating of aggregate w and improved the mixing quality.
2. Sand/aggregate ratio of 0.11 provides higher compressive strength in the range of 0.05 to 0.17, and comparable permeability to granular piles.
3. Water/cement ratio of 0.21 provides highest compressive strength (18.3 MPa) comparing to other water/cement ratio and permeability of 1.33 cm/sec.
4. Aggregate type has great effect on concrete strength and permeability. Pea gravel, which provides high strength (20.8 MPa) and comparable permeability (1.75 cm/sec.), was chosen for pervious concrete pile mixing.
5. The 10 second compaction time c prevent segregation of cement at bottom and provide adequate strength and permeability. The sample has compressive strength of 33.3 MPa and a comparable permeability of 1.1 cm/sec.

6. The moment-curvature curve of pervious concrete pile has been developed using beam test and proved that the calculation procedure for normal concrete to develop moment-curvature can be used for pervious concrete section.

CHAPTER 3

DEVELOPMENT OF PERVIOUS CONCRETE PILE GROUND-IMPROVEMENT ALTERNATIVE AND BEHAVIOR UNDER VERTICAL LOADING

3.1 INTRODUCTION

Numerous structures and highway facilities, including embankments and bridges, are often constructed on poor soils (i.e., soft or loose soils as well as organic/peat soils). In order to facilitate construction, achieve allowable settlements, and avoid failures, poor soils are often improved using ground improvement technologies. A common ground improvement technique involves using permeable granular piles (aggregate piers), which include sand compaction piles, stone columns and rammed aggregate piers, to improve soil strength and provide a drainage path. The use of permeable granular piles increases the time rate of consolidation, reduces liquefaction potential, improves bearing capacity and reduces settlement (Barksdale and Bachus, 1983; Mitchell, 1981; Aboshi and Suematsu, 1985; Bergado, 1994; Baez, 1995; Terashi and Juran, 2000; and Okamure et al., 2006). However, when compared to other pile types (i.e., steel and concrete piles), the strength and stiffness of granular piles are lower and depend on the properties of the surrounding soil. Therefore, granular piles have limited use in very soft clays and silts, and organic and peat soils. This research effort proposes the use of pervious concrete piles that can provide higher stiffness and strength, which are independent of the surrounding soil properties, while offering permeability comparable to granular piles, to support structures and highway facilities constructed on poor soils.

The goal of this research is to develop an innovative ground improvement alternative that uses pervious concrete piles. This chapter focuses on: (1) presenting the material properties of pervious concrete and describing the developed installation method for pervious concrete piles; (2) comparing the response of pervious concrete and aggregate piles when subjected to vertical loading; (3) comparing the vertical loading response of precast pervious concrete pile with that of cast-in-place pervious pile constructed using the developed installation method; and (4) briefly discussing the variation of soil stresses and displacement (or movement) during installation.

3.2 BACK GROUND

3.2.1 Permeable granular piles

Permeable granular piles are often used as a ground improvement technique to support structures, embankments and highway facilities constructed on poor soils. The term "permeable granular column" describes any columnar foundation element made of sand or gravel, including sand compaction piles, stone columns, and rammed aggregate piers. The effective use of permeable granular piles in supporting structures and highway facilities subjected to static and seismic loading is well documented (e.g., Mitchell, 1981; Barksdale and Bachus, 1983; Welsh, 1987; Bergado et al., 1994; Baez, 1995; Mitchell et al., 1995; Yasuda et al., 1996; Schaefer et al., 1997; Lawton, 1999; Lawton, 2000; Terashi and Juran, 2000; Ashford et al., 2000; Okamura et al., 2003; White and Suleiman, 2004; Ohtsuka et al., 2004; Krishna et al., 2006; and Suleiman and White, 2006). The benefits of permeable granular piles include

increasing the time rate of consolidation, reducing liquefaction potential, improving bearing capacity, and reducing settlement.

Many construction methods, including vibro-composer, vibro-compaction, vibro-replacement, impact, and ramming compaction, are used to install permeable granular piles (Aboshi et al., 1979; Mitchell, 1981; Barksdale and Bachus, 1983; Bergado et al., 1994; Moseley and Kirsch, 2004; White and Suleiman, 2004; and Geopier Foundation Company, 2012). These construction methods change the soil stresses resulting in horizontal consolidation, which leads to the improvement of surrounding soil (Handy, 2001; Basu et al., 2011; and Lundberg et al., 2013). The effects of granular piles construction on soil stresses and displacement have been investigated by several researchers (Shublaq, 1992; Hunt, et al., 2002; Lee, et al., 2004; Suleiman and White, 2006; Ambily and Ganhdi, 2007; Guetif et al., 2007; Elshazly et al., 2008; Chen et al., 2009; Yi et al., 2010; Dijkstra, et al., 2011; Thompson and Suleiman, 2010; and Frikha et al., 2013). Different approaches have been used to evaluate the effects of granular column installation on surrounding soils, including cavity expansion analysis, numerical modeling methods, cone penetration tests before and after installation, and shear wave velocity measurements. None of these approaches, however, directly and simultaneously measured the variation of soil stresses and soil movement during pile installation. Lundberg et al. (2013) reported that there is a lack of direct combined measurements of soil stresses and movement surrounding displacement piles in general; a knowledge gap that is partially addressed as part of this chapter for the installation method used to construct pervious concrete piles. Further experimental tests measuring the variation of soil stresses and lateral

movement during installation along with analytical modeling are being performed by the research team.

The method used to install granular piles affects their properties. Table 3.1 provides a comparison of published properties of sand compaction piles, stone columns and rammed aggregate piers. For the range of design loads, the friction angle of sand compaction piles, stone columns and rammed aggregate piers ranges from 30–36 °, 35–45 ° and 48–52 °, respectively. White and Suleiman (2004) conducted triaxial tests on different types of compacted aggregates used in constructing granular piles and reported an average friction angle of 48.5 ° and a cohesion of 30 kPa. Table 3.1 also shows that the initial elastic modulus of granular piles ranges from 25 to 120 MPa and the measured stress concentration ratios range from 1.5 to 10, while the permeability measured using laboratory and field tests ranges from 0.05 cm/sec. to 2.0 cm/sec.

Regardless of the used construction method, single isolated granular piles fail in bulging, shear, or punching (Barksdale and Bachus, 1983). For typical granular column length to diameter (L/D) ratios, the most common failure mechanism is bulging, which is usually observed over a distance of 2 to 3 pier diameters below the soil surface (Barksdale and Bachus, 1983; Bergado et al., 1994). The ultimate vertical load capacity for a bulging failure mechanism of granular piles depends on the confinement provided by the surrounding soil (Hughes and Withers, 1974). For this reason, the use of granular piles is limited in very poor soils, where minimum confinement is provided by the surrounding soil (Barksdale and Bachus, 1983; and Bergado et al., 1994). This research effort proposes an innovative ground

improvement method using pervious concrete piles that offer adequate permeability and material properties, which are independent of soil confinement, allowing it to be used in a wide range of poor soils including very soft, loose, and peat and organic soils.

Table 3.1 Properties of three types of granular piers

Granular Pier	Friction Angle ( )	Initial Elastic Modulus (MPa)	Stress Concentration ratio	Permeability (cm/sec)	Reference
Sand Compaction Piles	30-36	25-40	1.5-6.0	0.05-0.65	Bergado, 1988&1994; Aboshi et al., 1979
Stone Columns	35-45	30-70	2.0-8.5	0.09-2.0	Mitchell, 1981;Barksdale and Bachus, 1983; Baez, 1995
Rammed Aggregate Piers	48-52	60-190	2.0-10	N/A	Hoevelkamp, 2002; White and Suleiman, 2004

3.2.2 Pervious Concrete Material

Pervious concrete is a special concrete product made primarily of a single-sized aggregate. Pervious concrete has been used in pavements to reduce storm water runoff quantities and perform initial water quality treatment by allowing water to penetrate through the surface. In the United States, pervious concrete is mainly used in pavement applications, including sidewalks, parking lots, tennis courts, pervious base layers under heavy duty pavements and low traffic density areas (Tennis et al., 2004; and Suleiman et al., 2011). Based on previous material studies (Kajio et al., 1998; Beeldens et al., 2003; Tennis, et al,. 2004; Park and Tia, 2004; and Suleiman et al. 2006), pervious concrete material has a porosity ranging from 11% to 31%, a 28-day compressive strength between 5.5 MPa and 26.0 MPa and a permeability coefficient ranging from 0.25 to 0.54 cm/sec. Recent material tests performed by

Kevern et al. (2008) indicated that the 28-day compressive strength of pervious concrete ranged from 17.0 MPa to 26.5 MPa and the permeability coefficient ranged from 0.02 to 1.03 cm/sec.

To investigate the benefits of the proposed pervious concrete pile ground improvement method, four vertical load tests were conducted in a Soil-Structure Interaction (SSI) facility. The Test units included one granular column (Test unit 1) and three pervious concrete piles (Test units 2, 3, and 4). All the Test units were installed in loose well-graded sand. Test units 1 and 2 were used to compare the behavior of a granular column to a pervious concrete pile. Test units 3 (precast) and 4 (cast-in-place or installed) were used to evaluate the effects of the installation method on the behavior of pervious concrete piles subjected to vertical loading. The following sections of this chapter focus on presenting the pervious concrete material properties; describing the installation method for pervious concrete piles; comparing the vertical loading response of pervious concrete and aggregate piles; comparing the vertical loading response of precast and installed pervious concrete piles; and briefly discussing the variation of soil stresses and movement during installation.

3.3 MATERIAL PROPERTIES

3.3.1 Pervious Concrete Properties

A series of pervious concrete mixtures were prepared in order to obtain an adequate compressive strength and permeability. Pervious concrete cylinder samples were tested to measure the porosity, permeability, compressive strength, elastic modulus, and split tensile strength. The compressive strength was determined using

ASTM C39 (2009a), the permeability was measured using an in-house designed falling head permeameter, the porosity was measured using ASTM C1688 (2009b), the elastic modulus was measured using ASTM C469 (2009c) and the split tensile strength was measured using ASTM C496 (2009d). Several aggregate types, sizes and compaction (vibration) times were investigated. Mixtures were prepared using water/cement ratios (w/c) ranging from 0.21 to 0.27 and sand/aggregate ratios ranging from 5% to 11% using two mixing procedures and three different compaction times.

Figure 3.1a summarizes the 28-day compressive strength and permeability coefficient results for pervious concrete mixtures that were prepared using a 10 second compaction time for different water/cement and sand/aggregate ratios, as a function of porosity. The results presented in Figure 3.1a indicate that the porosity ranged from 6% to 23% with the 28-day compressive strength ranging from 10.0 to 34.0 MPa and the permeability coefficient ranging from 1.0 to 2.4 cm/sec. Based on these results, two pervious concrete mixes with high compressive strength and adequate permeability (comparable to granular piles) were selected to cast the piles for the vertical load tests. Both mixtures used a 0.21 water/cement ratio, an 11% sand/aggregate ratio, 377 kg/m^3 cement and 1440 kg/m^3 coarse aggregate. Test units 1 and 2 used crushed Nazareth aggregate, which is locally available in eastern Pennsylvania. However, it was observed that the quality of this aggregate varies from one delivery to the other. To ensure more consistent results, pea river gravel (commercially available at home improvement stores) was used to conduct further material testing and to construct Test units 3 and 4. Both aggregates were washed and sieved, and the portion passing through a 9.5 mm sieve and retained on a No.4 (4.75

mm) sieve was used (see Figure 3.1b). The pervious concrete mixture used in preparing Test unit 2 had an average porosity of 20%, a permeability of 1.33 cm/sec., a 28-day compressive strength of 18.3 MPa, a split tensile strength of 2344 kPa, and an elastic modulus of 16.2 GPa. The pervious concrete mixture used in preparing Test units 3 and 4 had an average porosity of 12.5%, a permeability of 1.21 cm/sec., a 28-day compressive strength of 22.2 MPa, a split tensile strength of 2337 kPa, and an elastic modulus of 15.4 GPa.

Pervious concrete samples cut from Test units 3 and 4 were used to measure the porosity and permeability of these piles. The average porosity and permeability of the precast pile (Test unit 3) were 13.6% and 1.35 cm/sec., respectively. For the installed pile (Test unit 4), the average porosity and permeability were 11.2% and 1.06 cm/sec., respectively. Strength tests were not performed on the samples cut from the test piles because the cutting process affects the strength of pervious concrete as concluded by Suleiman et al. (2006).

Mixtures that used a compaction (vibration) time of 10 seconds per layer during sample preparation resulted in an adequate compressive strength and permeability with no or minimal segregation of cement and aggregate. By comparing the material properties of granular piles and the pervious concrete piles, the following observations can be made: (1) the unconfined compressive strength of the pervious concrete material is more than 10 times greater than that of the confined granular piles; and (2) the permeability coefficient of the pervious concrete piles and granular piles are comparable. Furthermore, according to the analytical work of Han and Gabr (2002) and Suleiman et al. (2003) for embankments supported on several ground

reinforcement techniques representing a wide range of modulus ratios (i.e., elastic modulus of pile/elastic modulus of soil), using a pile with a modulus similar to pervious concrete piles will increase the stress concentration ratio by approximately 3 times the ratio for granular piles. This will reduce the stress carried by poor foundation soils and reduce the area replacement ratio. Given that several researchers documented the successful use of granular piles in mitigating liquefaction, which is attributed to higher stiffness and permeability when compared to the surrounding soil (e.g., (Adalier et al., 2003; Adalier and Elgamal, 2004; Shenthan et al., 2004; and Shao et al. 2013), it is expected that pervious concrete piles will provide the same advantages under similar loading conditions.

3.3.2 Sand and Aggregate Properties

Due to the large soil quantity needed in the large-scale experiments and because it is easier to rain sandy soils and to achieve uniform soil properties in the soil box, the testing program focuses on pervious concrete piles installed in loose sand. However, pervious concrete piles can be used in different soil types including very soft clays, and peat and organic soils. The soil used in all vertical load tests was classified as well-graded sand (SW) according to the United Soil Classification System (Figure 3.1b). The minimum and maximum relative density vibrating table tests [ASTM D4254 (2009h), and ASTM D4253 (2009g)] were performed at oven dry conditions and the minimum and maximum unit weight of the sand were 15.1 kN/m^3 and 20.8 kN/m^3, respectively (i.e., maximum void ratio of 0.720 and minimum void ratio of 0.250). For each vertical load test, the soil was placed in the large soil box using soil storage and moving system. The dry unit weight and moisture content

of the sand placed in the soil box were measured using a nuclear density gauge. The placed soil had an average relative density of 32%, unit weight of 16.5 kN/m^3, and water content of 2%. The standard deviation of the unit weight measurements was 0.377 kN/m^3, which confirmed the uniformity of the placed soil. (Note: soil placement is described later in the chapter). To characterize the soil properties, consolidated drained (CD) triaxial tests were performed. The samples were prepared to achieve a relative density similar to that of the soil in the large soil box (i.e., 32% relative density or unit weight of 16.5 kN/m^3). The 70-mm diameter samples were tested at confining stresses of 15, 25, 35, 100 and 160 kPa. The measured deviator stress-axial strain and volume change during the CD triaxial tests are presented in Figure 3.1c. The initial modulus of the soil (E_i) as a function of confining pressure ($\sigma 3$) was evaluated using the power function suggested by Janbu (1963) [i.e., $E_i = k$ Pa $(\sigma_3/Pa)^n$, where Pa is the atmospheric pressure, *k* is the modulus number and *n* is the modulus exponent] and the calculated values of *k* and *n* were 82.3 and 0.95, respectively, as shown in Figure 3.1c. The K_f line presented in Figure 3.1d indicates that the peak friction angle of the soil equals to 38 °. The peak and critical friction angles of the used loose sand have the same value, which is consistent with the results presented by Mitchell and Soga (2005) for loose sands. The friction angle and permeability of Nazareth aggregate, which was used to construct Test unit 1 (granular column), was measured using CD triaxial tests and failing head permeability tests. The friction angle of the aggregate was 47 ° and the permeability was 1.90 cm/sec.

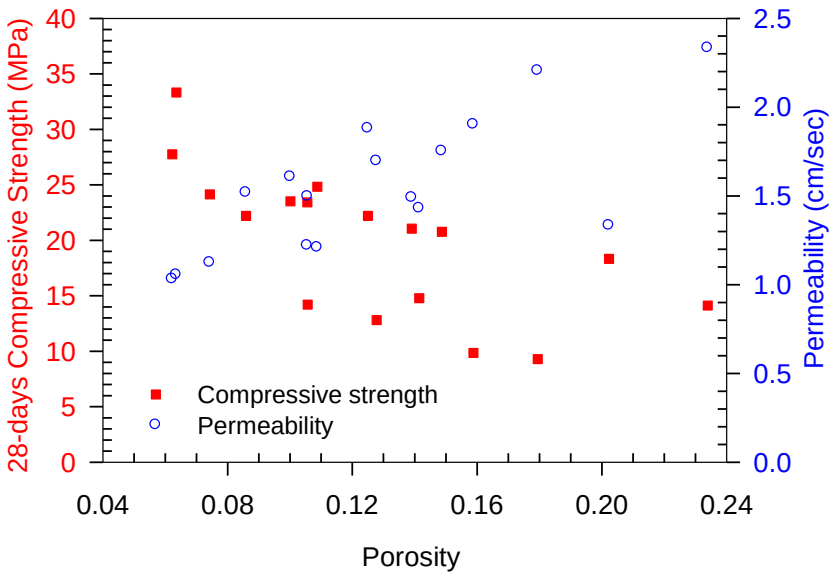

(a)

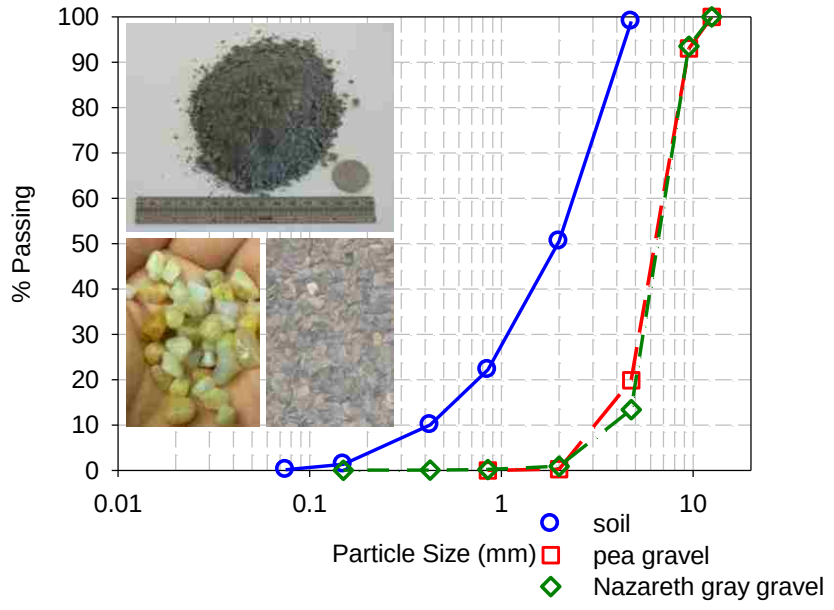

(b)

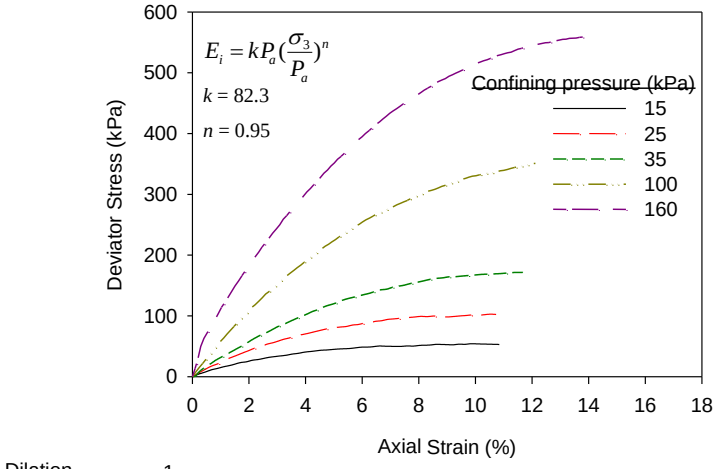

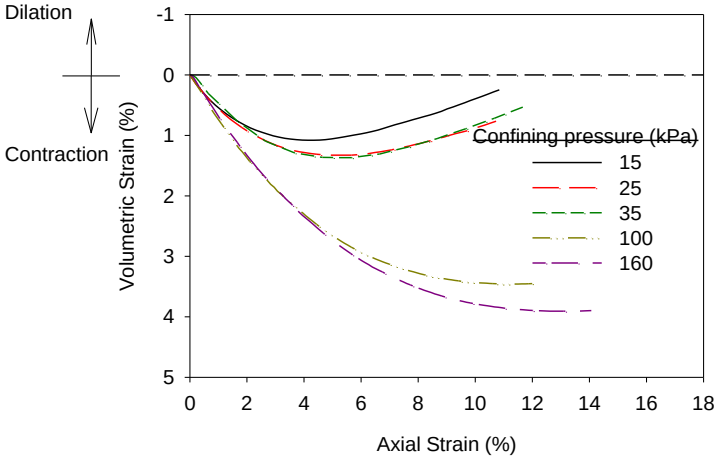

(c)

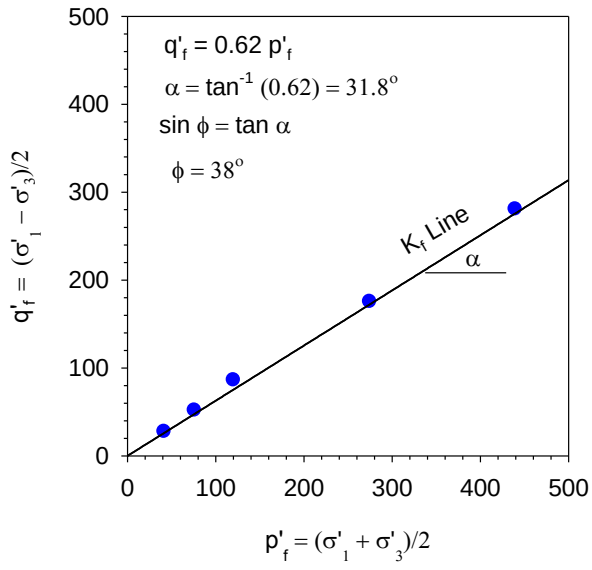

(d)

Figure 3.1 Material properties: (a) pervious concrete compressive strength and permeability for mixtures prepared using different aggregates with compaction time of 10 seconds, (b) gradation of the aggregate used for casting the test piles and for the soil used in the large soil box, (c) CD triaxial tests on sand samples with the same relative density used in the soil box, and (d) p'_f-q'_f diagram for the peak stresses of soil samples

3.4 TESTING FACILITY

The used experimental Soil-Structure Interaction (SSI) Facility had a reaction frame system, advanced sensors, state-of-the-art instrumentation and data acquisition and control system. The two stacked soil boxes and the vertical reaction frame test configuration are shown in Figure 3.2. The two soil boxes have dimensions of 1.5×1.5×1.5 m and 1.5×1.5×0.75 m and were designed to allow for flexible assembly.

The advanced sensors available in the SSI facility include customized flexible Shape Acceleration Arrays (SAA) deformation sensors, in-soil null pressure sensors, and tactile pressure sheets. The SAAs consists of a linked series of micro-machined electromechanical sensors that enabled gravity-based shape calculation over the sensed area. The sensors can measure three-dimensional (3D) movement based on a reference point. The SAAs were specially machined with segment lengths of 90 and 120 mm to fit the scale of the performed experiments. The in-soil null pressure sensors were designed in-house with a diameter of 42 mm and a thickness of 7 mm. Each null pressure sensor has an air pressure chamber with an embedded strain gauge. The null pressure sensors are connected to a closed loop system that controls the flow of air to maintain the strain measurement at zero. Talesnick (2005) and Talesnick et al. (2008) tested similar sensors within different soil types at several levels of pressure in a calibration chamber and reported that the difference between the measured and the applied pressure was smaller than 0.3 kPa. The tactile pressure sheets consist of a matrix of small point sensing cells (32×32 sensors) that provide discrete pressure measurements. Palmer et al. (2009) concluded that the accuracy of pressure

measurements using the tactile pressure sheets was higher than 90%. Suleiman et al. (2014b) studied the accuracy of the pressure measurements obtained in a lateral load test by comparing the applied load to the soil reaction obtained from measured pressures, which resulted in a difference smaller than 8%. The data acquisition and control system combines testing control and sensor monitoring. The system monitors several types of sensors, including load cells, strain gauges, null pressure sensors, tilt meters and displacement transducers. The SSI facility also has a soil storage and moving system, vibrating table to characterize granular material compaction properties, nuclear density gauge, and web broadcasting capability.

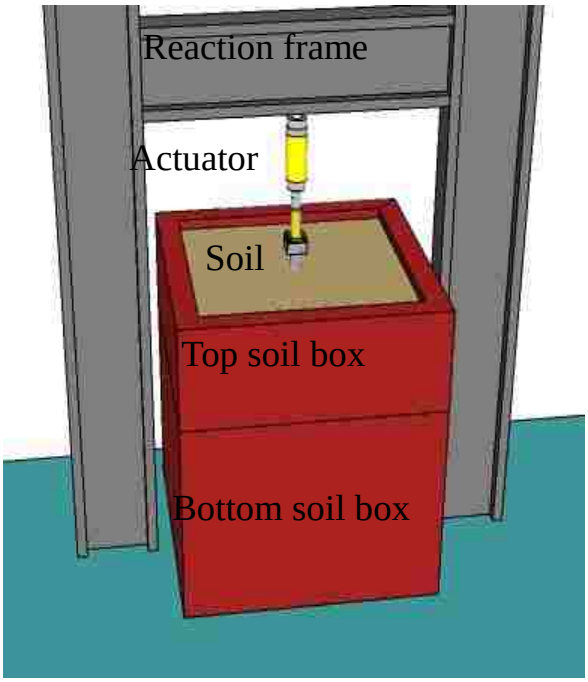

(a)

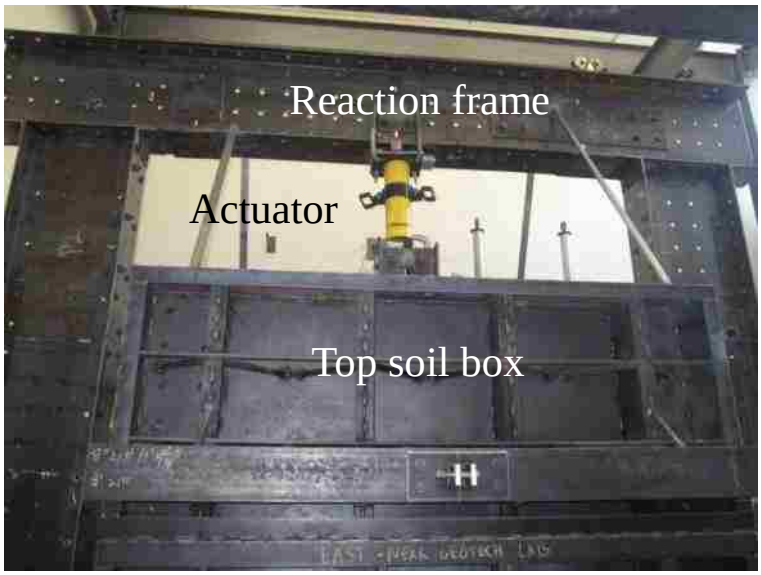

(b)

Figure 3.2 SSI facility and reaction frame system for vertical load tests: (a) schematic of the SSI facility, and (b) top soil box and reaction system of the SSI facility

3.5 TEST UNITS AND INSTRUMENTATION

3.5.1 Installation of Test Units

A laboratory installation method was developed by the research team to simulate a field construction method. Details of several stages of the laboratory installation method are shown in Figure 3.3. The developed installation system consists of a hollow steel mandrel with a specially designed cone at the tip. The mandrel can be vibrated into soil using an attached concrete vibrator (Figure 3.3a) or a Rhino pile driver placed on top of the mandrel. A bracing system was designed to ensure the verticality of the mandrel driving (Figure 3.3b and c). During mandrel advancement (mandrel penetration stage), the cone tip stays closed. Once the desired depth is reached, the pervious concrete or aggregate is placed inside the mandrel from the top (Figure 3.3d). Then, the mandrel is lifted upward (mandrel retrieval stage) at a

slow rate. During the mandrel retrieval stage, the cone tip opens and the pervious concrete or aggregate fills the created space (Figure 3.3e). This installation method is similar to the one used for sand piles described by Magnan (1983), which demonstrate that pervious concrete piles can be installed using available construction techniques.

Initially, a mandrel with 76 mm outside diameters was designed and fabricated. Test units 1 and 2 (one aggregate pier and one pervious concrete pile) were installed using the 76 mm mandrel utilizing the installation method described above. These two test units were tested under vertical loading and only the load and the displacement at the pile head were measured. To investigate the load transfer along the pile length, a steel rebar with mounted strain gauges is needed. With the 76 mm diameter mandrel, the installation of the steel rebar without damaging the strain gauges (or their wires) was difficult. So, a newer cone/mandrel setup was designed and fabricated with a diameter of 102 mm that allowed for easier installation of strain gauges. The 102 mm mandrel was used to install Test unit 4. Test unit 3 was a precast pervious concrete pile that has the same dimensions as Test unit 4.

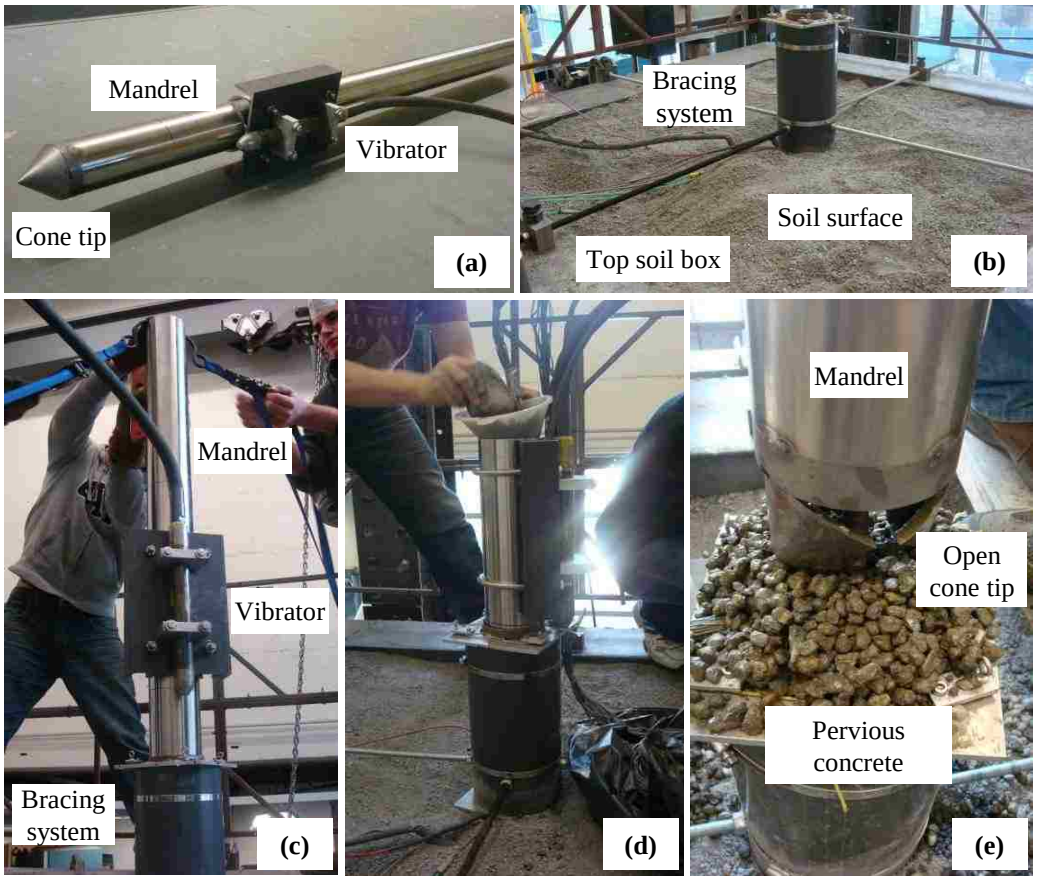

Figure 3.3 Summary of the developed pile installation method: (a) cone with vibrator, (b) bracing (guiding) system, (c) driving the mandrel, (d) casting the pile, (e) open cone during casting

3.5.2 Description of Test Units

Test units 1 and 2 were cast using the 76-mm diameter mandrel with an embedded length of 864 mm. Test unit 1 was a granular column and Test unit 2 was a pervious concrete pile; both used the same aggregate (Nazareth crushed aggregate) and were installed using the developed laboratory installation method described above. Test units 3 and 4 were pervious concrete piles, which were prepared using pea river gravel, with an embedded length of 1219 mm. Test unit 3 was a precast pile with a 102 mm diameter, which was placed vertically into the soil box and the soil was rained around it. Test unit 4 was installed using the 102-mm diameter mandrel.

Since the cone did not completely open during the installation of Test unit 4, the installed pile has a slightly tapered tip with a cross-sectional area of 4825 mm^2 and an average cross-sectional area along the pile length of 5935 mm^2.

3.5.3 Instrumentation of Test Units and Surrounding Soil

As mentioned previously, two soil boxes were stacked on top of the other, which provided a total height of 2.25 m, and a reaction frame was assembled for the vertical load tests (Figure 3.2a and Figure 3.4a). To produce a uniform soil, a soil storage and movement system was designed. This system consists of a bottom dump soil container with an attached sieve to rain the soil into the soil box. As shown in Figure 3.4b, the soil was placed in the soil boxes by raining the soil from a height of approximately 1.5 m.

Due to the large soil quantity needed in the large-scale experiments and because it is easier to rain sandy soils and to achieve uniform soil properties in the soil box, the testing program focuses on piles installed in sand. However, pervious concrete piles can be used in different soil types including very soft clays, and peat and organic soils.

Test unit 1 (granular column) and Test unit 2 (pervious concrete pile) were installed to assess the performance of the developed installation method and to compare the response of the granular column to that of the pervious concrete pile when subjected to vertical loading. These two Test units and the surrounding soil were not reinforced or instrumented and only the vertical applied load and displacement of the pile head were monitored during the load tests.

Test unit 3 (precast pervious concrete pile) and Test unit 4 (pervious concrete pile installed using the developed installation method or simply referred to as installed pervious concrete pile) were used to evaluate the effects of the installation method on the pile response when subjected to vertical loading. Test unit 3 was reinforced with a No. 4 (12.7 mm diameter) rebar instrumented with strain gauges and placed at the center of pile cross-section, as shown in Figure 3.5a. To evaluate the effects of the soil box boundaries on the installation and response of the pile, one tactile pressure sheet was mounted on the bottom of the soil box and another sheet on the side of the soil box (Figure 3.5a and b).

Test unit 4 was installed using the developed installation method. Similar to Test unit 3, Test unit 4 was reinforced with a No. 4 rebar with mounted strain gauges along the length of the pile. The surrounding soil was instrumented with three SAAs and six null pressure sensors as shown in Figures 3.4c, d and Figure 3.5. Two of the SAAs were installed at a distance of one pile diameter (1D or 102 mm) from the center of the pile and one SAA was installed at a distance of 2D from the center of the pile (203 mm). As shown in Figure 3.5, null pressure sensors 1, 2 and 3 were installed at 76, 178, and 279 mm (i.e., 0.75D, 1.75D, and 2.75D) below the tip of the pile. Null pressure sensors 4, 5 and 6 were installed at a horizontal distance of 1D from the center of the pile at either a depth of 914 mm or 1270 mm below the soil surface. Null pressure sensors 4 and 5 were installed at the same depth with a similar distance from the center of the pile to check the repeatability of the measured stress changes. Furthermore, one pressure sheet was mounted at the bottom of the soil box and one on the side wall of the soil box (Figure 3.5a and b) to assess the effect of the soil box

boundaries during installation and loading. The pressure sheets mounted on the side and at the bottom of the soil box recorded a maximum pressure change of 0.3 kPa and 1.4 kPa, respectively. These measurements illustrate that soil box boundaries has minimal or no effect on pile installation and soil-pile system response when subjected to vertical loading. It should be noted that several strain gauges used in the installed pile (Test unit 4) may have been damaged during installation and did not function properly during the vertical load test.

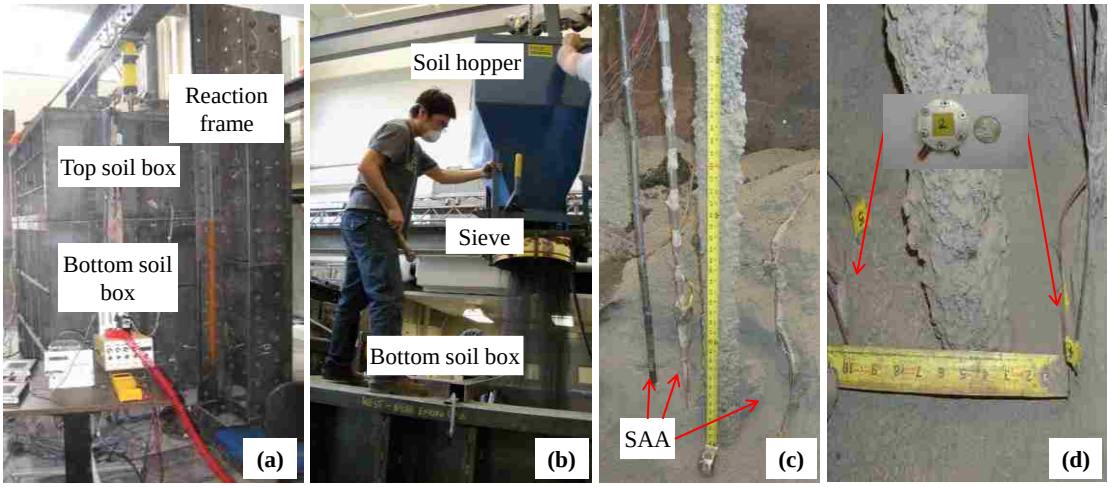

Figure 3.4 Set up of vertical load tests: (a) experiment set up showing the two soil boxes and the reaction system, (b) soil placement by raining the soil from an elevation of approximately 1.5 m, (c) SAAs used in the soil surrounding Test unit 4, and (d) in-soil null pressure sensors installed near the tip of Test unit 4 with a picture of the pressure sensor compared to the size of a quarter coin

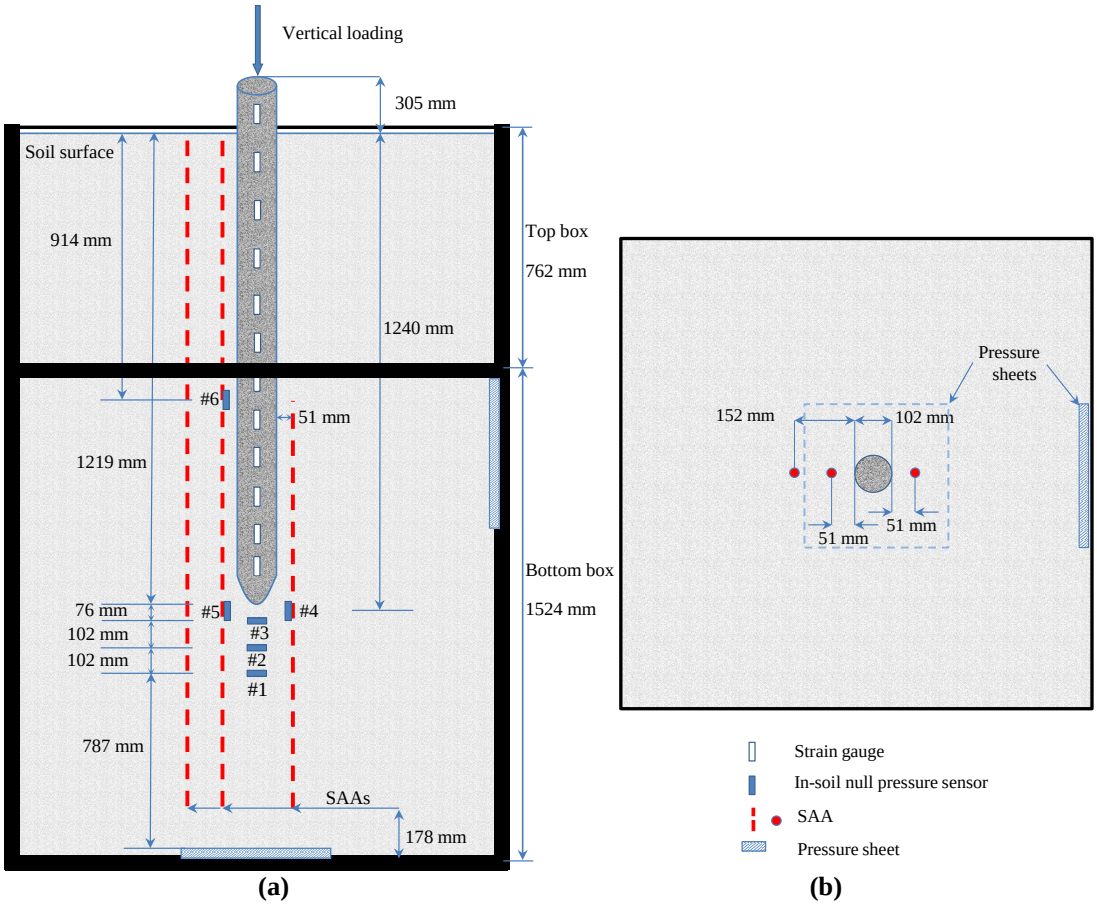

Figure 3.5 Instrumentation for Test unit 4: (a) side view, and (b) top view.

3.6 LOADING SEQUENCE

The four vertical load tests were conducted in general accordance with the fast procedure outlined in the ASTM D1143 (2009d). Each load level was held constant for at least 4 minutes or until the pile head displacement stabilized. The test was stopped when the pile displacement continued increasing without an increase in the applied load. During testing of Test units 1 and 2, a load increment of 222.4 N was used. For Test units 3 and 4, load increments of 222.4 N and 889.6 N were used.

3.7 TEST RESULTS

3.7.1 Experimental Pile Load-Displacement Response

Effect of Pile Type on Response

Figure 3.6a presents the measured vertical load-displacement responses for Test unit 1 (granular column) and Test unit 2 (pervious concrete pile). Both test units were made using the same aggregate and installed using the same installation method. The ultimate load of Test unit 1 was 2.2 kN and the ultimate load of Test unit 2 was 9.8 kN. Therefore, the ratio of the ultimate load of the pervious concrete pile to the ultimate load of the granular column was 4.4. After the ultimate load was reached during testing, the soil surrounding each pile was removed to expose the Test units. Figure 3.7a illustrates that Test unit 1 (granular column) failed by bulging into the surrounding soil due to the low confining pressure provided by the surrounding soil. The depth of the bulged zone was approximately 2.5D below the soil surface. For Test unit 2 (pervious concrete pile), the pile failed by punching vertically into the soil (Figure 3.7b). The observed failure types indicate that unlike granular piles, pervious concrete piles do not experience bulging into the surrounding soil allowing them to be used in different poor soil conditions including very soft, loose, and peat and organic soils.

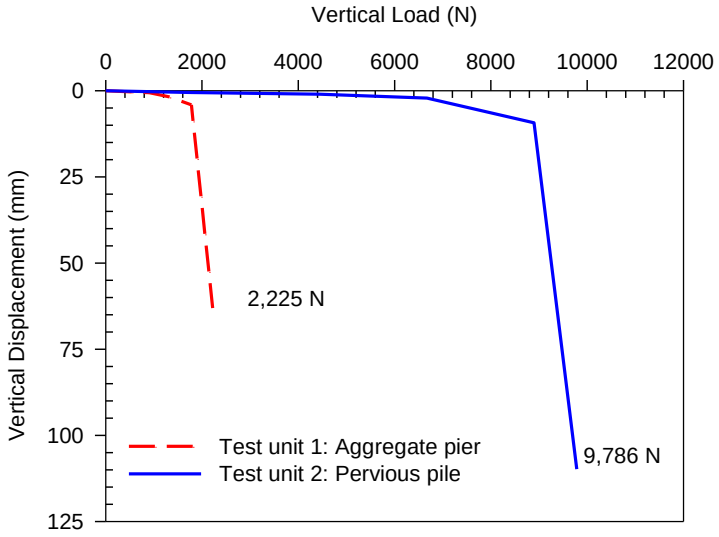

(a)

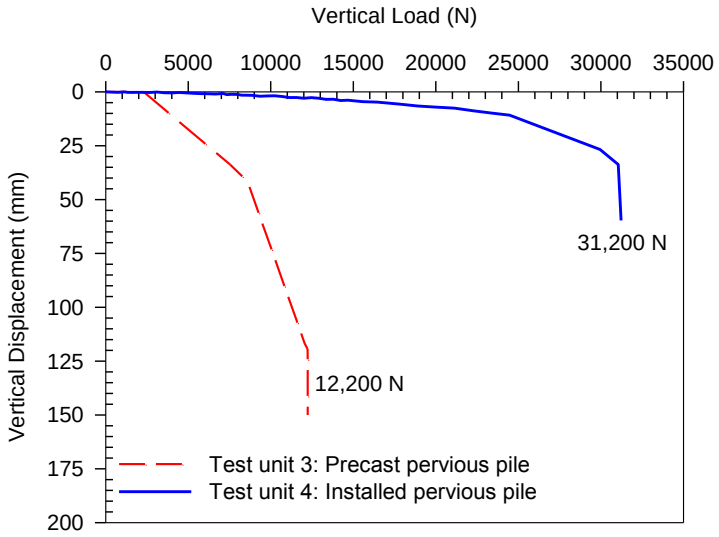

(b)

Figure 3.6 Vertical load versus displacement for all test units: (a) Test units 1 and 2 with a 76 mm diameter piles installed using the developed installation method, and (b) Test units 3 and 4 with a 102 mm diameter piles

Effect of Pile Installation Method on Response

Figure 3.6b presents the measured vertical load-displacement responses for Test unit 3 (precast pervious concrete pile) and Test unit 4 (installed pervious concrete pile). These tests were conducted to compare the load-displacement response

of two similar pervious concrete piles that were installed using different methods. The ultimate load of Test unit 3 was 12.20 kN and the ultimate load of Test unit 4 was 31.20 kN. Therefore, the ratio of the ultimate load of the installed pervious concrete pile to the ultimate load of the precast pile was 2.6. The difference between the ultimate loads of the two pervious concrete piles occurs because of the installation method, which has significant effects on the surrounding soil properties that will be briefly discussed later in this chapter. Similar to the failure experienced by Test unit 2, Test units 3 and 4 also experienced vertical punching failures as shown in Figure 3.7c and d.

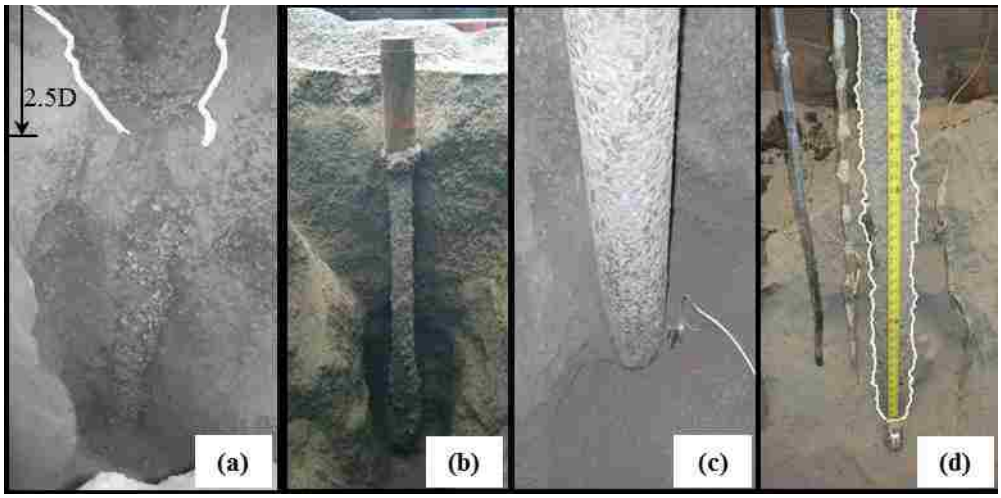

Figure 3.7 Test units after performing the vertical load test: (a) Test unit 1 with bulging failure, (b) Test unit 2, (c) Test unit 3, and (d) Test unit 4

3.7.2 Load Transfer along Pile Length

Using the strain gauge measurements along the pile length and the calculated initial elastic modulus of the pervious concrete composite section, including the steel reinforcing bar, the load transfer along the pile length for Test units 3 and 4 was calculated and compared at loading stages of 1.78 kN, 4.89 kN and 11.12 kN (Figure

3.8). These loading stages were selected for comparison because they represent the initial (linear) stage, transition stage and near the ultimate load for Test unit 3. The rate of load transfer shown in Figure 3.8 indicates that at the applied load of 11.12 kN, the maximum unit friction, which is the slope of the curve between depths of 381 mm and 965 mm, was 9.0 N/mm for Test unit 3 (precast pile) and 10.6 N/mm for Test unit 4 (installed pile). These unit friction values illustrate that the pile installed using the developed installation method had a 17.8% higher load transfer rate to the surrounding soil through shaft resistance than the precast pile at this loading step. Extending the load transfer curves in Figure 3.8 to the depth of the pile tip for the 11.12 kN loading stage results in tip resistances of 1.10 kN and 3.28 kN for Test units 3 and 4, respectively. At the ultimate load of Test unit 4 (31.20 kN), the tip resistance was approximately 35% of the applied load (i.e., shaft friction resisted 65% of the applied load). The difference in the ultimate load and load transfer between Test unit 3 and 4 is mainly attributed to the used installation method, which for the installed pile changes the soil density and soil stresses, as well as results in a rougher pile surface as shown in Figure 3.7 c and d.

Using the load transfer along the pile length and displacements back calculated using the strain measurements along the pile, the frictional soil-pile interface stress (interface shear stress)-displacement relationships at the soil-pile interface (i.e., t-z curves) were developed and are presented in Figure 3.9. The results illustrate that Test unit 4 (installed pile) had a higher maximum interface frictional stress transfer than that of Test unit 3 (precast pile). The ratio of maximum frictional stress at the soil-pile interface for Test unit 4 relative to that of Test unit 3 was 2.5 at

an average depth of 191 mm below the soil surface and 5.3 at an average depth of 635 mm. These ratios are consistent with those reported in the literature when comparing displacement and non-displacement piles (e.g., Colombi et al., 2006). The differences in ultimate load and load transfer clearly illustrate the significant effect that the installation method had on the soil-pile interaction for vertically loaded pervious concrete piles.

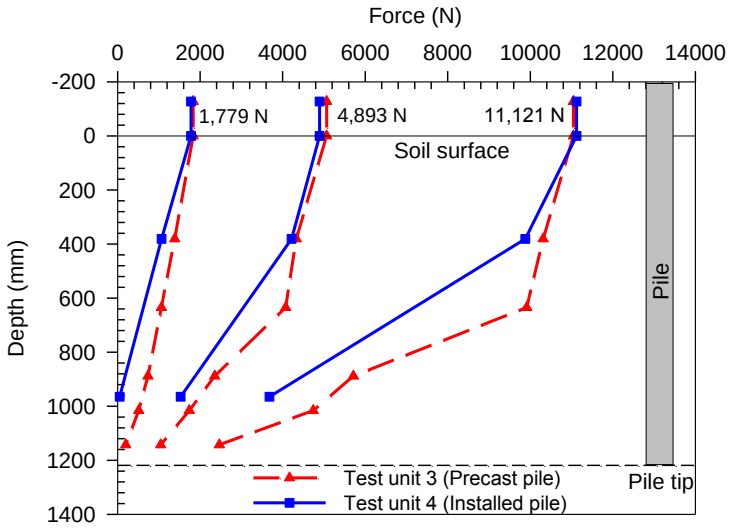

Figure 3.8 Comparison of the force transferred along the length of Test units 3 and 4 for different loading stages

3.7.3 Variation of Soil Stresses and Movement during Pile Installation

As the mandrel penetrates the soil, it pushes the soil downward and laterally (cavity expansion) resulting in a significant increase of vertical stress and a smaller increase of horizontal stress (Basu et al., 2011). For a soil element at a specific depth, the cavity expands until the mandrel, which has a constant diameter, starts to penetrate the location of the soil element. Vertical shearing is then applied to the soil element as the mandrel penetrates deeper. As discussed before, the effects of pile

installation on soil lateral displacement (movement) and stresses were monitored using SAAs and null pressure sensors for Test unit 4. The in-soil null pressure sensors were zeroed before starting the experiment which did not allow us to record the initial horizontal stresses (i.e., allowing the measurement of the change of stresses during installation and load testing). Null pressure sensor 2 did not function properly due to air leakage during installation.

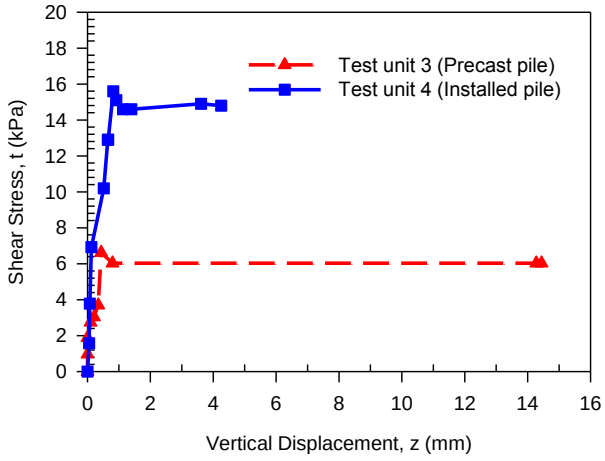

(a)

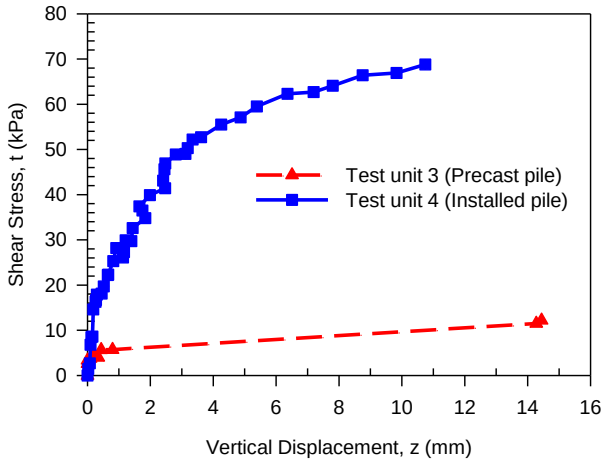

(b)

Figure 3.9 Shear stress versus displacement curves (t-z curves) for the soil-pile interface calculated using the strain gauge measurements for test units 3 and 4: (a) for average depth below soil surface of 191 mm, and (b) for average depth below soil surface of 635 mm

Lateral Soil Movement

The lateral soil movement due to pile installation measured using the SAAs are summarized in Figure 3.10. The SAAs measurements at 1D (102 mm) from the center of the pile, which was 51 mm from the surface of the pile, illustrate that the steel mandrel penetration resulted in a non-uniform lateral soil movement along the depth of the mandrel. The lateral movement near the soil surface was 17.6 mm, while the lateral movement near the pile tip was 8.2 mm. Therefore, the soil movement at the pile tip is only 50% of the soil movement near the soil surface. These non-uniform displacements along the depth of the pile are commonly modeled by researchers as uniform displacements that produce similar vertical load-displacement pile response (e.g., Chen et al., 2009; and Dijkstra et al. 2011). However, non-uniform displacement can also be simulated using the volumetric strain approach suggested by Thompson and Suleiman (2010); an approach that is currently being investigated further by the authors. During vertical loading, the soil at 1D experienced 1.7 to 5.8 mm additional lateral movement. At a distance of 2D (152.4 mm from the surface of the pile), the lateral soil movement was 4.1 mm at the soil surface with no lateral soil movement occurring below a depth of 500 mm (~5D).

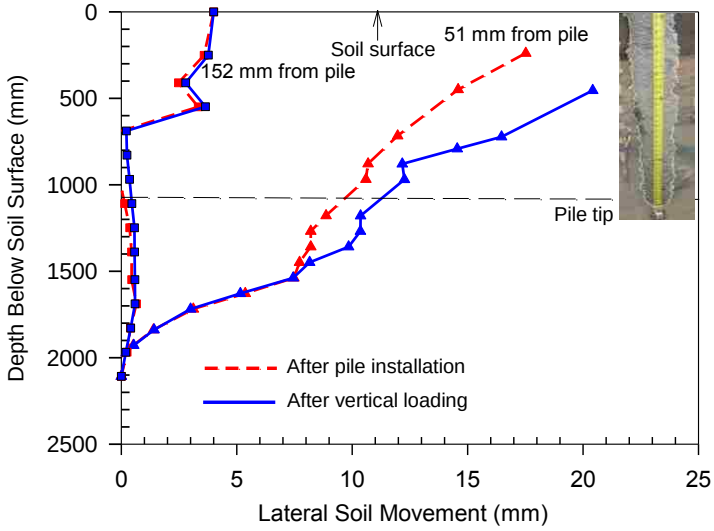

Figure 3.10 Soil lateral displacement at 51 mm (average) and at 152 mm from the surface of the pile measured using SAAs for Test unit 4

Horizontal Soil Stresses

The changes of horizontal soil stresses due to pervious concrete pile installation and during vertical loading, which were measured using null pressure sensors 4, 5 and 6, are summarized in Figure 3.11a. The following observations can be made regarding the changes occurring in the horizontal stresses: (1) due to mandrel advancement, the change of horizontal stresses measured by sensor 6 was 147 kPa at 914 mm below the soil surface; (2) the horizontal stress increased by 99 kPa at 1240 mm below the soil surface (i.e., near the tip of the pile); (3) sensors 4 and 5, located at the same depth and distance from the pile, showed similar horizontal stress increases during mandrel advancement, which confirms the repeatability of the stress measurements for the sensors.; (4) during the vertical load test, the horizontal stresses measured by sensor 6 increased, which is similar to the trend reported by Lehane et al. (1993); and (5) during the vertical load test, Test unit 4 with a slightly tapered tip (see Figure 3.5) penetrated the soil below the pile tip resulting in cavity

expansion at the location of sensors 4 and 5 approaching a condition similar to that at the location of sensor 6. Therefore, it was expected that at this stage the change of soil horizontal stress measured using sensors 4 and 5 would be similar to that of sensor 6, which is observed in Figure 3.11a. This measurement is another confirmation of the repeatability of the measured stresses.

The measured changes of soil horizontal stresses were compared with the elastic and elastic-plastic cavity expansion solutions presented by Yu (2000). Using the elastic and elastic-plastic solutions, the calculated changes of horizontal stress at the location of sensor 6 (914 mm below soil surface) were 182.9 kPa and 170.3 kPa, respectively, which are approximately 26% and 17% smaller than the measured change in soil horizontal stress at the same location (145 kPa). At the location of sensors 4 and 5 (depth of 1240 mm), the calculated changes in soil horizontal stress were 172.3 kPa and 177.5 kPa using the elastic and elastic-plastic cavity expansion analyses, respectively, which are approximately 12% and 10% smaller than the average measured pressure using sensors 4 and 5 (195.7 kPa).

Vertical Soil Stresses

For changes in vertical stresses, which were measured using sensors 1 and 3, the vertical stress increased by 180 kPa at 76 mm below the tip of the cone due to mandrel advancement. The increase of vertical stress is approximately 1.9 times the increase in horizontal stress measured using sensors 4 and 5 (located near sensor 3). The result of having the vertical stress significantly higher than horizontal stress during cone advancement was also reported by Salgado et al. (1997) and Salgado and

Prezzi (2007). Sensor 1 showed an increase of vertical stress of 57 kPa at the end of mandrel advancement. At the end of the load test, sensor 3, which was approximately 55 mm below the pile tip at this stage, recorded an increase of vertical stress of 638 kPa and sensor 1, which was approximately 60 mm below the pile tip at this stage, recorded an increase of 135 kPa (Figure 3.11a and b).

Figure 3.11b summarizes the development of measured pressures from sensor 6 during different installation stages focusing on the mandrel advancement stage. During mandrel advancement, the variation of horizontal stress measured using sensor 6 increased until the mandrel passed the location of the sensor. The horizontal stress measured by sensor 6 then decreased as the mandrel advanced deeper. This stress changing trend caused by the cavity expansion and shearing along soil-pile interface is consistent with the one-dimensional (1-D) finite element analytical results reported by Basu et al. (2011) for jacked piles.

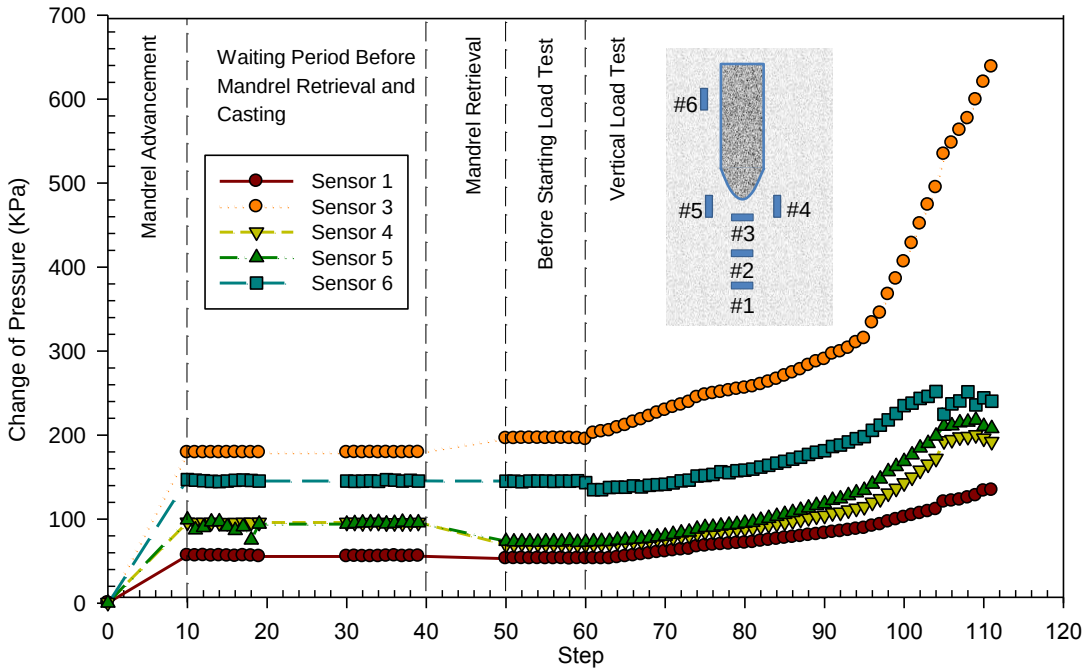

(a)

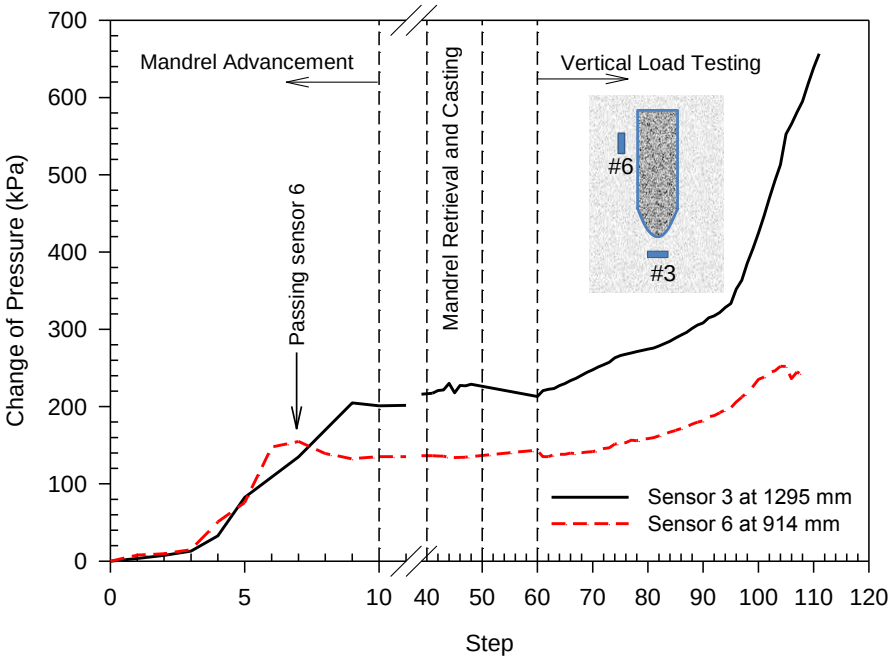

(b)

Figure 3.11 Effect of installation on the change of soil pressure: (a) summary of pressure changes developed at the end of installation and during load testing, and (b) details of changes of horizontal pressure measured using sensor 6 and changes of vertical pressure measured using sensor 3 focusing on the changes during installation (Note: the x axis represent different stages (steps) including mandrel advancement, waiting period, casting and mandrel retrieval and vertical load testing)

3.8 SUMARY AND CONCLUSIONS

A new ground improvement method has been developed using pervious concrete piles. This chapter summarizes the material properties of the pervious concrete and the response of four different vertical load tests performed using the SSI Facility. Initially, Test unit 1 (granular column) and Test unit 2 (pervious concrete pile) were installed to investigate the effectiveness of the designed laboratory installation method and to compare the vertical load-displacement response of the granular column to that of the pervious concrete pile. Then two instrumented vertical load tests were performed on a precast pervious concrete pile (Test unit 3) and an installed pervious concrete pile (Test unit 4) to evaluate the effects of the installation

method on the soil-pile interaction. Although the testing program focuses on piles installed in loose sand, pervious concrete piles can be used in different soil types including very soft clays, and peat and organic soils. Based on the experimental results obtained from the four vertical load tests and the discussion of the results presented in this chapter, the following conclusions were made:

1. Pervious concrete piles have a compressive strength that is more than 10 times that of granular piles, while providing similar permeability to granular piles.
2. The pervious concrete pile (Test unit 2), which had the same dimensions, aggregate type, and installation method, as the granular column (Test unit 1), had an ultimate load that was 4.4 times greater than the ultimate load of the granular column. Furthermore, the pervious concrete pile failed by vertically punching into the soil at the pile tip, while the granular column failed by bulging outward into the surrounding soil.
3. The installation method had significant effects on the response of the pervious concrete piles. When comparing the response of the two pervious concrete piles installed using different methods [precast pile (Test unit 3) and installed pile (Test unit 4)], the ultimate load of the installed pile was 2.6 times greater than the ultimate load of the precast pile.
4. Installation of the pervious concrete pile resulted in an increase of the maximum frictional stress transferred at the soil-pile interface. The

ratio of the maximum frictional stress calculated using the strain gauges for the installed pile compared to the precast pile ranged from 2.5 to 5.3.

5. The lateral soil displacements measured at a distance of 1D from the pile center during installation were not uniform along the length of the pile. The installation of the pile also resulted in significant increases of the soil vertical stress and a smaller increase of the soil horizontal stress. The measured change of the vertical and horizontal soil stresses showed trends similar to those reported in the literature.

CHAPTER 4

BEHAVIOR AND SOIL-STRUCTURE INTERACTION OF PERVIOUS CONCRETE GROUND IMPROVEMENT PILES UNDER LATERAL LOADING

4.1 INTRODUCTION

Granular columns are commonly used to resist vertical and lateral loads and to improve soft and loose soils. Granular columns include stone columns, sand compaction piles, and rammed aggregate piers. With higher stiffness, strength, and higher permeability than surrounding soils, granular columns have been used to improve soil strength, increase consolidation rate, reduce liquefaction potential, improve bearing capacity, reduce settlement, improve embankment stability, and stabilize slopes (Barksdale and Bachus 1983; Mitchell 1981; Aboshi and Suematsu 1985; Bergado et al. 1994; Baez 1995; Terashi and Juran 2000; Okamure et al. 2006; Elgamal et al. 2009; and Stuedlein and Holtz 2013). For typical granular column length to diameter (L/D) ratios, the most common failure mechanism when subjected to vertical loading is bulging, which is usually observed over a distance of 2 to 3 diameters below the soil surface (Barksdale and Bachus 1983; Bergado et al. 1994; Suleiman et al. 2014a). When subjected to lateral loading, such as to stabilize slopes, granular columns fail in direct shear at the location of loading or along the slope failure surface (i.e., do not transfer loads to deeper stable soils as in the case of concrete or steel piles used to stabilize slopes) (Barksdale and Bachus, 1983; Mitchell 1981; Bergado et al. 1994; White and Suleiman 2005; Suleiman et al. 2014b).

Compared to other pile types (concrete and steel piles), granular columns have lower strength and stiffness, which depend on the properties of the surrounding soil. Therefore, granular columns have limited use in very soft clays and silts, and organic and peat soils. The research team has recently developed a new ground improvement pile made of pervious concrete material. In addition to providing adequate permeability comparable to granular columns, pervious concrete ground improvement piles have higher stiffness and strength, which are independent of the surrounding soil properties.

The behavior of vertically loaded pervious concrete piles compared to granular columns has been studied using a series of fully-instrumented tests. The results and analysis of pervious concrete piles subjected to vertical loading were presented by Suleiman et al. (2014a). The vertical load tests included one granular column test and three pervious concrete pile tests installed using two different methods. Comparison of the behavior of the granular column and the pervious concrete pile that had the same dimensions and installation method showed that the ultimate load of the pervious concrete pile was 4.4 times that of the granular column. In addition, the pervious concrete pile failed by punching into the soil at the pile tip, while the granular column failed by bulging into the surrounding soil.

To further characterize the behavior of the pervious concrete ground improvement piles, this chapter focuses on experimentally investigating the behavior of pervious concrete piles and the effects of pile installation on the soil-structure interaction when subjected to lateral loading. It is worth noting that there is a lack of knowledge related to the effects of pile installation on the soil-structure interaction of

laterally loaded piles in general (Fan and Long, 2005; Kim and Jeong, 2011); a knowledge gap that is partially addressed in this chapter. To achieve the goal of the chapter, two fully-instrumented lateral load tests were performed using the soil-structure interaction (SSI) testing facility at Lehigh University. One of the test piles was a precast pervious concrete pile with sand rained around it, while the other was a cast-in-place pile installed using the method developed by the research team to simulate field installation. To investigate the soil-structure interaction of laterally loaded pervious concrete piles, the piles and surrounding soil were instrumented with advanced sensors. In addition to comparing the lateral load responses of the precast and installed piles, the soil-structure interaction pressure and displacement in the surrounding soil were analyzed. Furthermore, the effects of the pile installation methods on measured responses were briefly discussed. This chapter presents: (1) the material properties of the pervious concrete and the installation methods used for pervious concrete piles; (2) the lateral load behavior of pervious concrete piles, including pile response, soil-pile interaction and surrounding soil displacements; and (3) the effects of the installation methods on the response of pervious concrete piles and on surrounding soil. The research team is currently conducting a detailed analytical study to evaluate the effects of installation on the response of pervious concrete piles subjected to vertical and lateral loading; the results of which will be presented in a separate future paper.

4.2 MATERIAL PROPERTIES

4.2.1 Soil Properties

The soil used in the two lateral load tests was classified as poorly graded sand (SP) using the Unified Soil Classification System (Figure 4.4.1a). The minimum and maximum unit weights of sand at oven dry condition obtained from minimum and maximum relative density tests (ASTM D4253, 2009g and ASTM D4254, 2009h) were 14.54 kN/m^3 and 16.75 kN/m^3, respectively (maximum void ratio of 0.79 and a minimum of 0.55). In order to provide homogeneous soil conditions, the sand was rained from a height of approximately 1.5 m through a bottom-dump container fitted with a sieve. The soil placed in the box had an average unit weight of 15.24 N/m^3 and water content of 0.4%, which were measured by a nuclear density gauge (Humboldt HS-5001EZ). A series of consolidated drained (CD) triaxial tests with different confining pressures (15 kPa, 25 kPa, 50 kPa and 100 kPa) targeting the same relative density (35%) as the soil in the box were conducted. The results showed that the average peak friction angle of soil was 39 ° with a critical state friction angle of 36 °. The initial soil modulus (E_i) was evaluated as a function of confining pressure (σ_3) as $E_i=kP_a(\sigma_3/P_a)^n$ (Janbu, 1963), where P_a is the atmospheric pressure of 101 kPa and *k* and *n* are calculated as 506.7 and 0.445, respectively (Figure 4.1b).

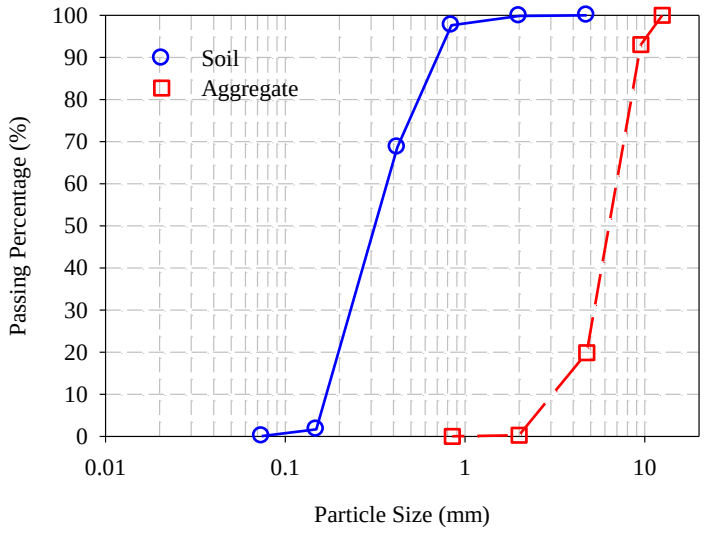

(a)

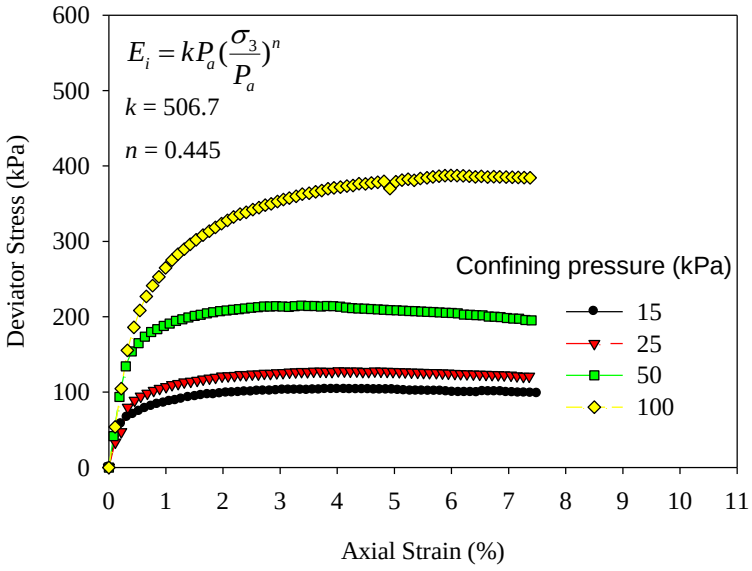

(b)

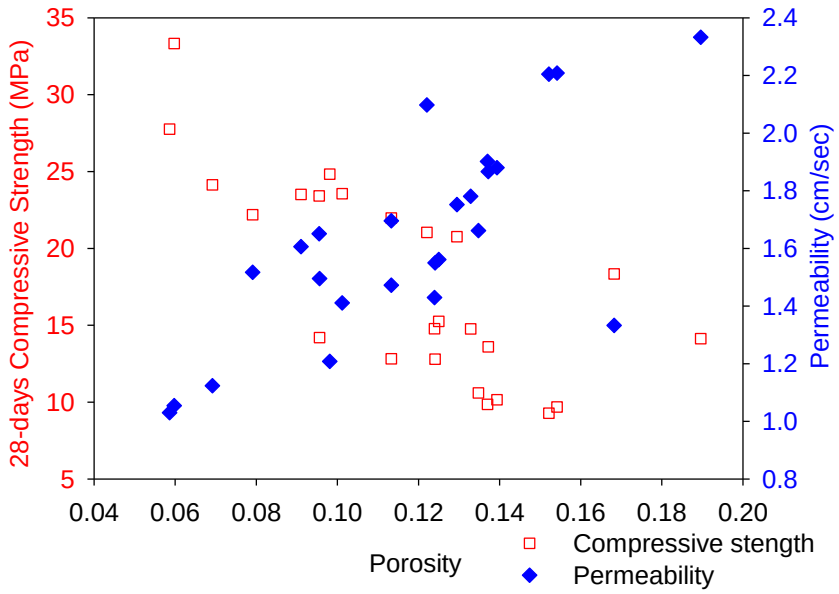

(c)

Figure 4.1 Material Properties: (a) Gradation of soil and aggregate used in lateral loading tests, (b) CD triaxial tests on sand with same relative density measured in the lateral load tests, (c) pervious concrete compressive strength and permeability vs. the porosity

4.2.2 Pervious Concrete Properties

To achieve adequate compressive strength and permeability, a series of pervious concrete mixtures were prepared. Pervious concrete cylindrical samples were tested to measure the pervious concrete properties including the compressive strength (ASTM C39, 2009b), permeability, porosity, spilt tensile strength (ASTM C496, 2009i), and elastic modulus (ASTM C469, 2009j). The effects of aggregate type, size and compaction time were investigated to optimize the pervious concrete mix. The 28-day compressive strength, porosity and permeability of tested mixtures are summarized in Figure 4.1c. Based on the results presented in Figure 4.1c, the mixture with 0.21 water/cement ratio, 0.11 sand/aggregate ratio, 377 kg/m^3 cement and 1440 kg/m^3 coarse aggregate (pea gravel, available at home improvement stores) was used for casting the test piles. The pea gravel for pile casting was washed and

sieved, and the portion passing the 9.5 mm sieve (3/8 in. sieve) and retained on the 4.75 mm sieve (No.4 sieve) was used. The pervious concrete mixture used in preparing the test piles had average porosity of 10.7%, permeability of 1.44 cm/sec., 28-day compressive strength of 22.8 MPa, split tensile strength of 2702 kPa, and elastic modulus of 15.1 GPa. Samples cut from the test piles were used to measure the porosity and permeability of the two piles. The permeability and porosity for the precast pile were 1.33 cm/sec. and 10.4%, respectively. For the installed pile, the permeability and porosity were 1.51 cm/sec. and 11.3%, respectively. By comparing the material properties of the pervious concrete piles with the granular columns, it was found that the unconfined compressive strength of the pervious concrete material was more than 10 times greater than that of the confined granular columns; and the permeability coefficient of the pervious concrete piles and granular columns were comparable (Suleiman et al. 2014a).

4.3 TESTING FACILITY

The Soil-Structure Interaction (SSI) testing facility at Lehigh University, which includes soil boxes, a reaction frame system, advanced sensors, state-of-the-art instrumentation and data acquisition and control systems, has been used for the pervious concrete lateral load tests. As shown in the Figure 4.2, a soil box with dimensions of 1.8 × 1.8 × 1.8 m (width × length × height) and a reaction frame were assembled for the two lateral load tests.

The advanced sensors available at the SSI facility included customized flexible Shape Acceleration Arrays (SAAs) deformation sensors and tactile pressure

sheets. The SAAs consist of a series of micro-machined electromechanical sensors capable of measuring three-dimensional (3D) movement based on a reference point. These SAAs were specially designed with segment lengths of 90 and 120 mm to fit the scale of the performed laboratory experiments. The tactile pressure sheets (0.7 mm thickness) consist of a matrix of small point sensing cells that provide discrete pressure measurements. The accuracy of pressures measured by the tactile pressure sheets was discussed by Palmer et al. (2009) who concluded that the error was smaller than 10%. In addition to using these sensors, bender elements were fabricated in-house using two-parallel-layer piezoelectric transducer to measure the soil shear wave velocity in the soil box (Lee and Santamarina, 2005; Brandenberg et al., 2008). The SSI facility also uses data acquisition and control systems that combine testing control and sensor monitoring of several types of sensors, including load cells, strain gauges, tiltmeters and displacement transducers. In addition, the SSI facility includes a soil storage and moving system, pile driving system, nuclear density gauge to measure the soil properties, and web broadcasting system.

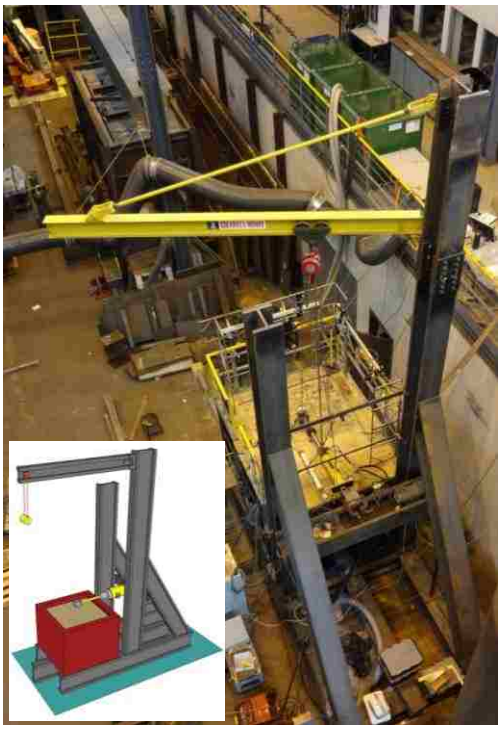

Figure 4.2 Laboratory Soil-Structure Interaction (SSI) testing facility with lateral loading set up and a 3D system sketch (bottom left).

4.4 TEST UNITS AND INSTRUMENTATION

4.4.1 Test Units and Installation

The two test piles were prepared using the designed pervious concrete mix with a diameter of 102 mm and a length of 1321 mm below the soil surface. The precast pile (Test unit 1) was cast using a 102 mm-inside diameter PVC pipe. The pile was then placed vertically in the soil box and soil was rained around it. To produce soil with uniform properties, a soil storage and movement system was used. The system (shown in Figure 4.3a) consisted of a bottom-dump soil container with an attached sieve to rain the soil into the soil box from a height of 1.5 m. Due to the needed large soil quantity and because it is easier to rain sandy soils to achieve uniform soil properties, the testing program focused on piles installed in sand.

However, pervious concrete piles can be used in different soil types, including very soft clays, and organic and peat soils.

The installed pile (Test unit 2) was constructed using a laboratory installation system after filling the soil box. The laboratory installation system was developed to simulate field installation methods. As shown in Figure 4.3b, the laboratory installation system consists of a hollow steel mandrel (102 mm inside diameter) with a specially designed cone at the tip and an air-operated driver (Rhino PD-200) placed on top of the mandrel. A bracing system was designed to ensure accurate pile position and the verticality of the pile installation. Through the hollow cylinder of the bracing system (Figure 4.3b), the mandrel was driven into the soil. Once the designed depth was reached, the pervious concrete was placed inside the mandrel from the top. As the mandrel was lifted upward at slow rate, the cone was separated from the mandrel and the pervious concrete filled the cavity created by the mandrel retrieval. This installation method is similar to the one described by Magnan (1983) for installing sand compaction piles, which demonstrates that pervious concrete piles can be installed using currently available construction techniques. It is worth noting that similar to displacement piles, the used installation method results in lateral compression and densification of the surrounding sand as well as increase lateral soil stresses (e.g., Lundberg et al. 2013; Dijkstra et al. 2011). These changes are expected to affect the soil-structure interaction and response of laterally loaded pervious concrete piles.

4.4.2 Instrumentation of Test Units and Surrounding Soil

As discussed previously, one soil box with height of 1.8 m and a reaction frame were assembled for the lateral load tests. As shown in Figure 4.3c and 3d, the lateral loads were applied to the pile by a hydraulic jack, which was attached to the pile head by a free rotation plate to create a free head loading condition. The load cell and displacement transducers were attached to the pile head with the loading point located at 235 mm above the soil surface.

The advanced sensors described previously were used to instrument the pile and surrounding soil as shown in Figure 4.4. In the precast pile test (Test unit 1), one steel rebar with 11 strain gauges was installed on the tension side of the pile at 25.4 mm from the pile center. Three SAAs were installed in the pile and within the passive wedge (on the front side as shown in Figure 4.4) to measure the pile and soil movement. SAA1 and SAA2 were installed at 51 mm and 153 mm (0.5 D and 1.5 D) from pile surface. SAA3 was installed in the pile to measure the lateral displacement along the pile length at one side of the central line. Three tactile pressure sheets were wrapped along the pile length between the soil surface and a depth of 1111 mm to measure the soil-pile interface pressure. One additional pressure sheet was mounted on the inside surface of soil box to independently monitor the boundary effects of the soil box during the lateral load test.

For the installed pile test (Test unit 2), one steel rebar, with strain gauges installed at the same locations as the precast pile, was used. Due to the installation method, it was not possible to install the pressure sheets around the pile or the SAA in the pile. Therefore, three SAAs (SAA1, SAA2 and SAA3) were placed on the front

side of pile at 51 mm, 153 mm and 254 mm (0.5 D, 1.5 D and 2.5 D) from pile surface. Four bender element pairs were installed around the pile at a depth of 508 mm. The bender element pairs 1, 2 and 3 were installed beside the SAAs [i.e. on the front side of the pile with a distance of 51 mm, 153 and 254 mm (0.5D, 1.5D and 2.5D) from the pile surface]. Bender element pair 4 was installed 51 mm (0.5D) from the pile surface similar to bender element pair 1 but on the back side of the pile. In addition, one pressure sheet was mounted on the inside surface of the soil box to monitor the boundary effects during installation and lateral load test. During both tests, the pressures measured by the pressure sheets on the inside surface of the box were less than 1 kPa, which confirmed that the soil box boundaries had no effect on the measurements during pile installation and lateral load tests.

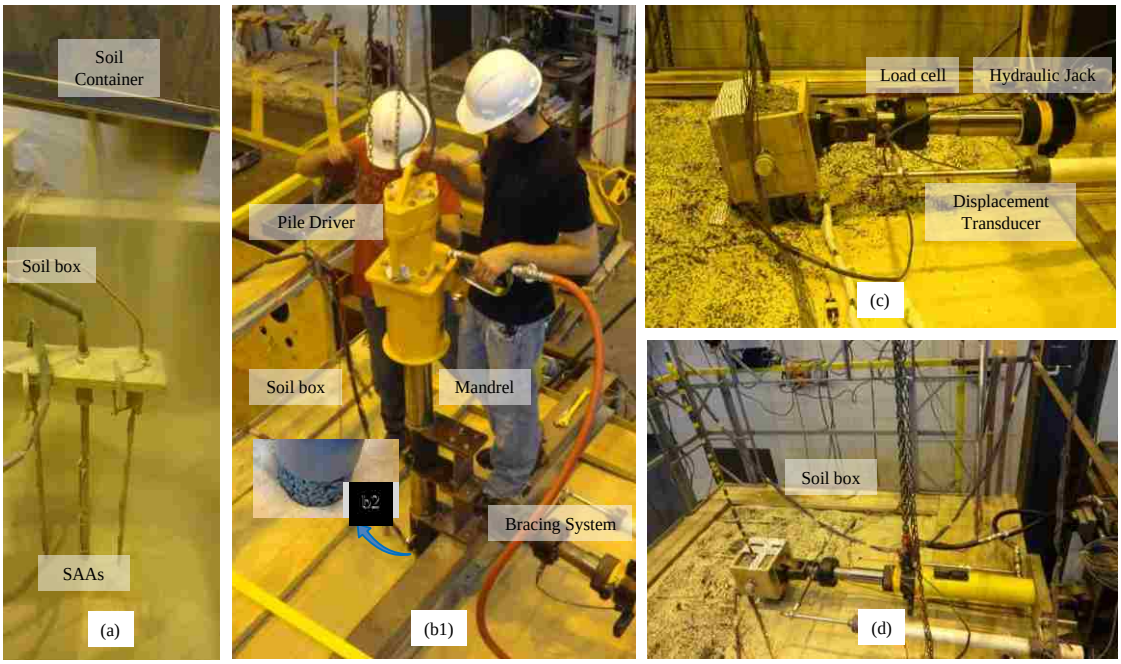

Figure 4.3 Lateral loading tests set up: (a) soil raining in preparation for installed pile test, (b1) pervious pile installation in the installed pile test, (b2) pile casting at the soil surface, (c) loading of the precast pile, (d) loading of the installed pile.

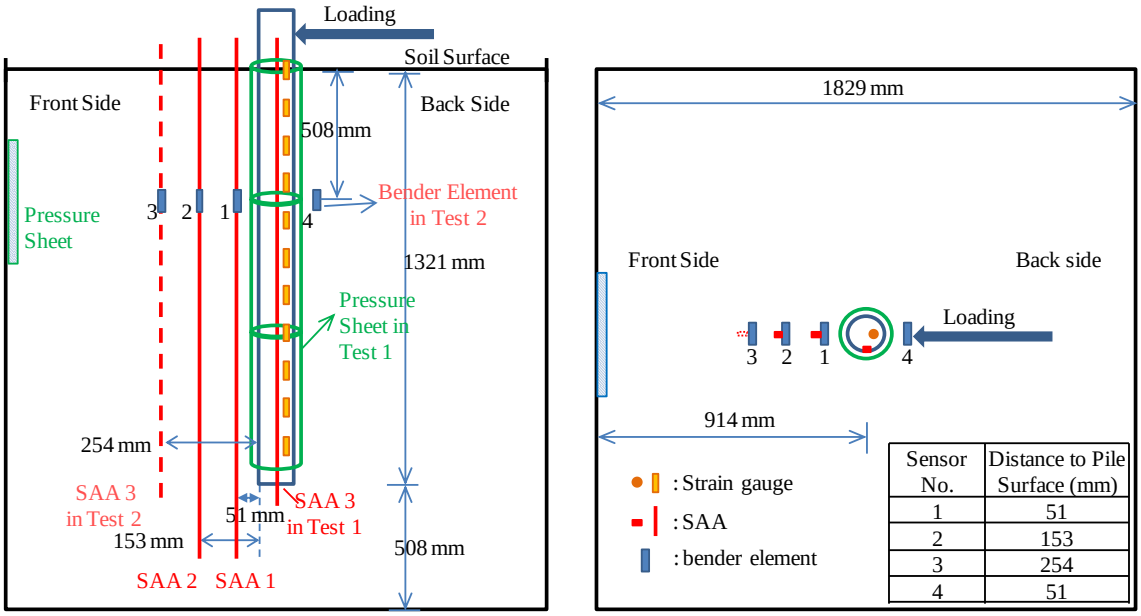

(a) **(b)**

Figure 4.4 Instrumentation for lateral loading tests: (a) Side View, (b) Top view (Notes: the strain gauge with rebar was installed on the tension side of pile at 25 mm from pile center; SAA3 was installed in the precast pile and was installed in the soil at 254 mm from pile for the installed pile test).

4.5 LOADING SEQUENCE

The two lateral load tests were conducted in general accordance with the procedure outlined in ASTM D3966 (2009i). The loading procedure, however, included two stages; a loading-control stage and a displacement-control stage. During the loading-control stage, loading was held constant for at least 5 minutes or until the pile head displacement stabilized. When the pile reached ultimate load (observed by a large increase of lateral displacement under constant load), the control was shifted to displacement-control by applying a constant lateral displacement at the pile head. The tests were stopped when the displacement at the pile head reached approximately 125 mm. For the precast pile test, a load increment of 111 N was used for loads smaller than 1780 N and a load increment of 222 N was used for larger loads. When the

ultimate load was reached at a displacement of 72.3 mm, the procedure shifted to displacement-control with an increment of 10 mm and 2 minute holding time. For the installed pile test, load-control with an increment of 222 N was used, and displacement-control with 10 mm increment and 2 minute holding time was applied after reaching the ultimate load at a displacement of 39.7 mm.

4.6 TEST RESULTS

4.6.1 Lateral Load-Displacement at Pile Head

Figure 4.5 illustrates the lateral load-displacement response of the precast and installed pervious concrete piles. The results show that the ultimate loads of the precast and installed pervious concrete piles were 3225 N and 3440 N, respectively, indicating that the installation method had small effect on the ultimate (maximum) load for laterally loaded piles, which is consistent with the results reported by Lundberg, et al. (2013). This result could be attributed to the fact that the ultimate lateral load is controlled by the structural resistance of the pile as concluded by Suleiman et al. (2014b). However, ultimate loads were reached at a pile head displacement of 39.7 mm for the installed pile, which is 55% of the displacement of the precast pile (72.3 mm) at ultimate load. In addition, the stiffness of the soil-pile system (i.e. the slope of the initial part of the load-displacement curve) for the precast pile was 75.2 N/mm, which is 32% of the stiffness of the installed pile (233.2 N/mm). These differences between the pile head displacement at ultimate load and stiffness of the soil-pile system are mainly attributed to the effect of pile installation method, which alters soil stresses and properties as will be discussed later.

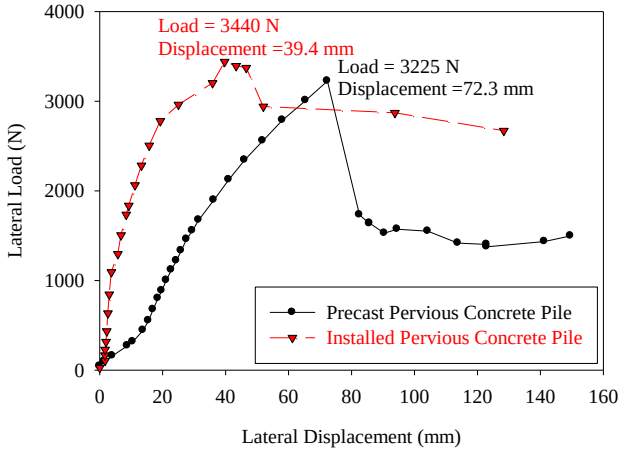

Figure 4.5 Lateral load vs. displacement at the loading point.

4.6.2 Strain along the Pile

The strain measurements along the pile length from the two tests are summarized in Figure 4.6. The strains are presented at four loading stages that represent the beginning of the test, the linear part of the load-displacement response, the nonlinear part of the load-displacement response, and the ultimate condition. Figure 4.6 shows that the strains along the pile increased with lateral load. In both pervious concrete piles, the strain increased along the depth and reached a peak value at depth of 444 mm (4.4 D) below the soil surface; then the strain started to decrease reaching zero at the pile tip. At ultimate load, the maximum strain occurred at the depth of 444 mm, which indicates that the maximum moment was at this depth. After the tests, the piles were retrieved and inspected (Figure 4.7). The precast and installed piles cracked on the tension side at depths ranging from 460 mm (4.5 D) to 470 mm (4.6 D) below the soil surface and the concrete was crushed on the compression side at similar depth locations. These results are consistent with measurements of strain gauges in the piles. The strain profiles and inspection of the piles after the tests

confirm that pervious concrete ground improvement piles behave as flexible laterally loaded piles (i.e., similar to long concrete or steel piles), while still having a permeability similar to granular columns. For the case of stabilizing slopes, this behavior can help in transferring lateral loads to stable soils below the failure surface, which improves the stability of slopes compared to granular columns that fail along the slope failure surface (Suleiman et al. 2014b).

Based on the strain measurements and the moment-curvature relationship of the pile cross-section, the bending moment along the pile length was calculated for both piles and the soil-pile interaction force versus pile lateral displacement relationships (p-y curves) at different depths were calculated using the procedure outlined in several references (e.g., Naggar and Wei, 1999; Yang and Liang, 2006; Kim et al. 2004). The p-y curves based on strain data for both piles will be further discussed in the following sections of the chapter.

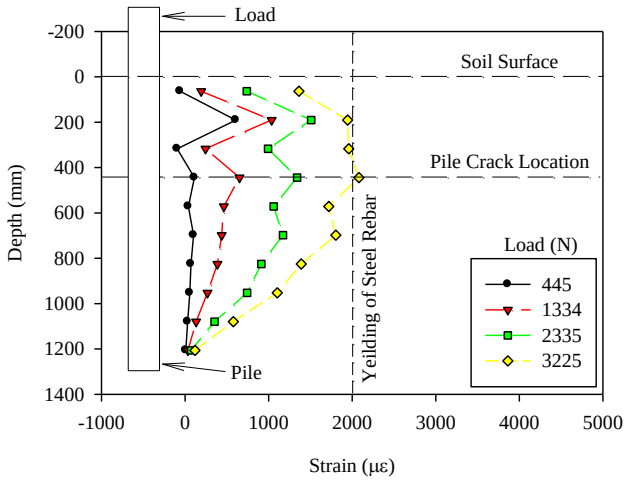

(a)

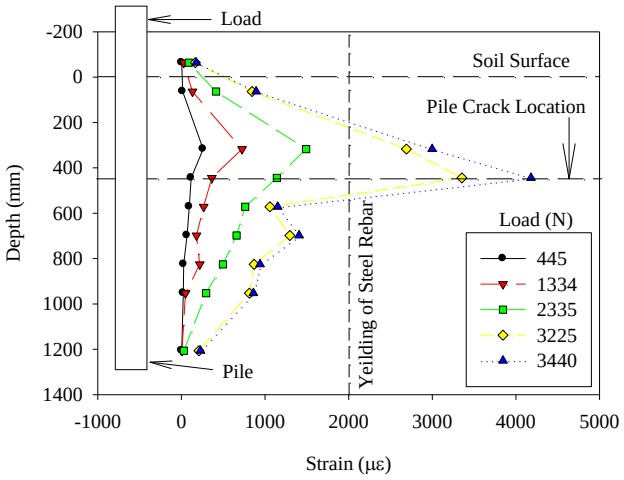

(b)

Figure 4.6 Strain profile along the pile during lateral load tests: (a) precast pervious concrete pile, and (b) installed pervious concrete pile.

(a) **(b)**

Figure 4.7 Test units after lateral load tests: (a) precast pervious concrete pile (the tape measurement from the bottom of pile head, the depth of crack is at 470 mm below the soil surface), and (b) Installed pervious concrete pile (the tape measurement from the top of pile head, the depth of crack is 460 mm below the soil surface).

4.6.3 Soil-Pile Interaction

Pile and Soil Lateral Displacement

The pile and soil lateral displacements measured by the SAAs and displacement transducers at an applied lateral load of 3225 N, which is the ultimate

load of the precast pile, are presented in Figure 4.8. As shown in the Figure 4.4 for the precast pile, the SAAs were installed in the pile, at 51 mm and at 152 mm (0.5D and 1.5D) from pile, while the SAAs were placed at 51 mm, 152 mm and 254 mm (0.5D, 1.5D and 2.5D) from pile surface for the installed pile test. Based on the SAA measurements at the applied load of 3225 N, the following observation can be made: (1) the precast pile had a displacement of 61.8 mm at the soil surface while the displacement of the installed pile was 27.7 mm; (2) at a distance of 51 mm (0.5D) from the pile surface, the soil in precast pile test had a displacement of 24.4 mm at a depth of 115 mm and decreased to 0 mm at a depth of 900 mm, while the soil had a lateral displacement of 20.0 mm at a depth of 115 mm and decreased to 0 mm at a depth of 640 mm for the installed pile test; (3) at 152 mm (1.5 D) from the pile surface, the soil lateral displacement was small in both tests (less than 6 mm); and (4) for the installed pile test, the soil at a distance of 254 mm (2.5D) on the front side of the pile showed minimal lateral displacement during the test. These results indicate that the soil lateral displacements on the front side of the installed pile were smaller than those measured during the precast pile test, which reflects the effects of soil densification and lateral compression during pile installation on the surrounding soil and soil-pile interaction.

Figure 4.9 summarizes the lateral displacement of the precast pile along its length. Figure 4.9 shows that the pile lateral displacement increased as the load increased. The pile experienced no or minimal movement at the pile tip indicating a long, flexible pile behavior when subjected to lateral loading. The displacement

profile indicates that a plastic hinge forms at a depth of approximately 440 mm, which is consistent with the strain measurements (Figure 4.6).

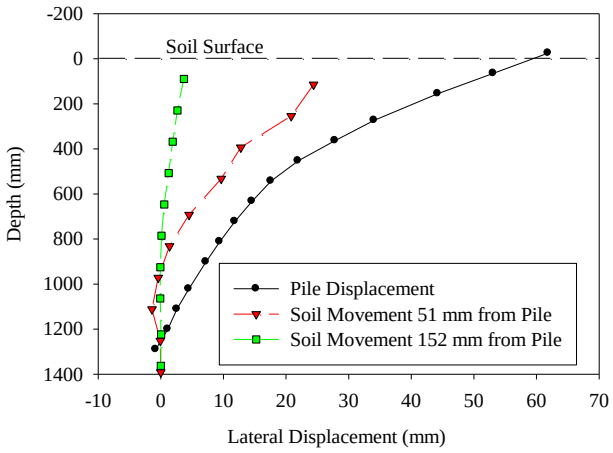

(a)

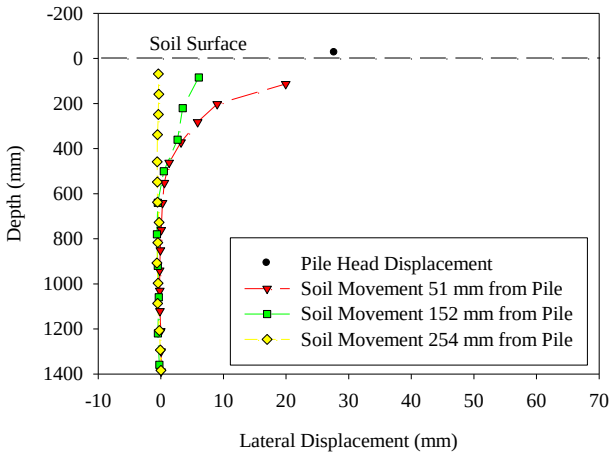

(b)

Figure 4.8 The pile and soil lateral displacement under lateral loading of 3225 N: (a) precast pervious concrete pile, and (b) installed pervious concrete pile

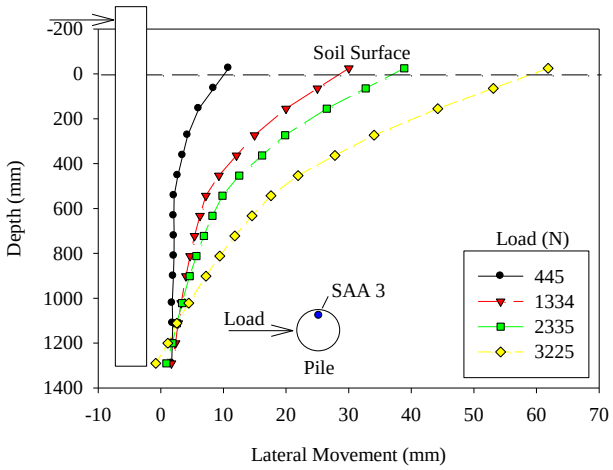

Figure 4.9 Precast pile displacements under lateral loading

Soil-Pile Interaction Pressure along the Precast Pile

During the precast pile test, the interaction pressures between the pile and surrounding soil were measured using tactile pressure sheets. As mentioned in the instrumentation section, three pressure sheets were wrapped around the pile from the soil surface to the depth of 1111 mm (the bottom pressure sheet didn't function properly during the test due to a wire connection problem). The soil reaction (i.e. the soil-pile interaction force per unit length, p in N/mm) along the pile is shown in Figure 4.10 at the four loading stages previously defined. The soil reaction was calculated using the measured soil-pile interaction pressures utilizing the following two steps: (1) integrate the soil-pile interaction measured pressures to produce a force (in N); and (2) divide the calculated force by the integrated length to produce the soil-pile interaction force (p in N/mm). As shown in Figure 4.10, as the lateral loading increased, the soil reaction (p) along the pile increased and the maximum value of soil reaction reached 2.5 N/mm between depths of 388 mm and 453 mm (3.8 D and 4.5 D) at ultimate load in the precast pile test.

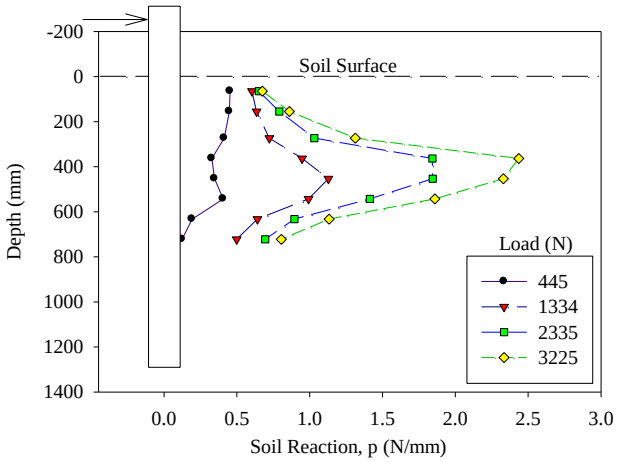

Figure 4.10 Soil reactions (soil-pile interaction force per unit length) along the pile for the precast pile test unit

Soil-Pile Interaction Force-Displacement Relationships (P-Y Curves)

Based on the measured pressures (Figure 4.10) and pile displacements (Figure 4.9), the p-y curves based on direct measurement at several depths along the precast pile were generated (Figure 4.11a). The curves show that the initial slope (or stiffness) and ultimate soil reaction (pu) increased as the depth increased.

The directly-measured p-y curves for the precast pile were compared with the p-y curves calculated using the strain measurements and those developed using the procedures suggested by Reese et al. (1974). For the precast pile, the p-y curves calculated using the measured strains show higher initial stiffness (i.e. the slope of the initial part of the curve) and ultimate soil reaction than the directly-measured curves. An example of the compared p-y curves is presented in Figure 4.11b for a depth of 364 mm and comparisons at other depths show similar trends. Along the length of the precast pile, the differences in the p-y curve initial stiffness and ultimate soil reaction between the directly-measured curves and those calculated using measured strains ranged from 20% to 53% and 31% to 73%, respectively. The p-y curves error was

calculated using the procedure suggested by Yang and Liang (2006). The error is defined as the summation of the ratios of the difference between the measured and the calculated p divided by the measured p at deflections of 0.25ym, 0.5 ym, 0.75 ym and ym (ym is the maximum measured y). For different p-y curves along the pile length, the calculated errors ranged from 3 to 8, which are similar or smaller than that those reported by Yang and Liang (2006) who mainly attributed these errors to the inaccurate determination of moment profiles from strain gauges. When compared to the procedures suggested by Reese et al. (1974), the initial stiffness and ultimate soil reaction of the directly measured p-y curves show differences up to 95% and 82%, respectively.

The p-y curve of the installed pile at a depth of 364 mm has an initial stiffness that is 95% of the value calculated using the method suggested by Reese et al. (1974). The ultimate soil reaction is 98% of that calculated using Reese et al. (1974) method. Along the pile length, the difference between values of initial stiffness and ultimate soil reaction ranges from 1% to 58% and 0% to 17%, respectively. The better match of the method suggested by Reese et al. (1974) to the installed pile results was expected since the Reese method was developed for driven piles, which is an installation method similar to the method used in the installed pile.

It is noteworthy that when comparing the p-y curves of the precast and installed piles (i.e., effect of installation) using the strain measurements at the same depth, the p-y curves of the installed pile shows a higher stiffness and ultimate soil reaction. Along the pile, the ratio of the ultimate soil reaction of the installed pile to the precast pile ranges from 1.4 to 5.9 at different depths. For smaller diameter piles

(12 mm), Kim et al. (2004) reported that this ratio range from 2 to 4 for laterally loaded piles installed in medium dense sand.

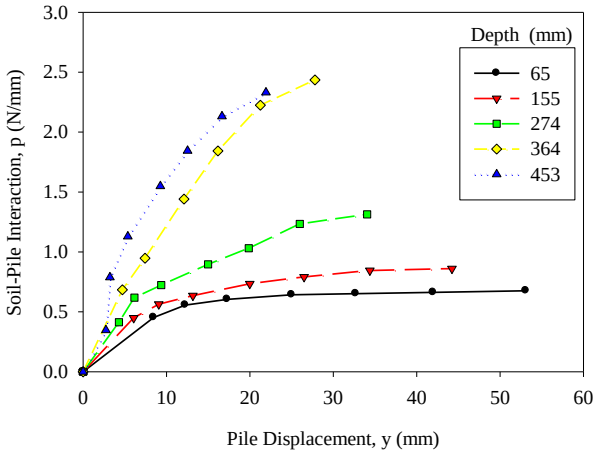

(a)

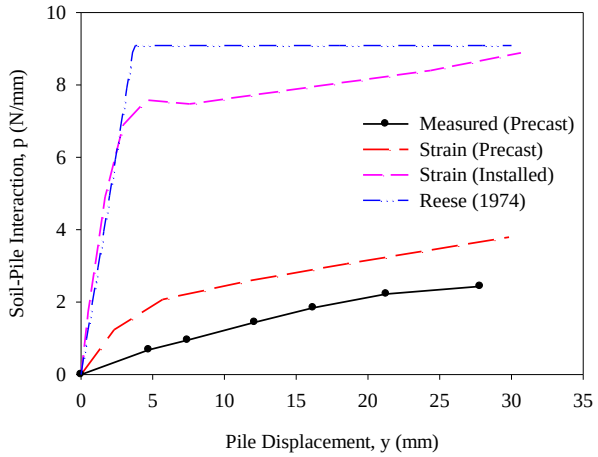

(b)

Figure 4.11 Soil-pile interaction force-displacement relationships: (a) directly-measured soil-pile interaction force-displacement relationship (i.e. p-y curves) at several depths along the precast pile, and (b) comparison of p-y curves at a depth 364 mm

4.6.4 Shear Wave Velocity Change during Pile Installation

To further characterize the effects of pile installation, bender elements were installed to measure the change of shear wave velocity due to pile installation. The bender elements were installed at a depth of 508 mm (5 D) with distances of 51 mm, 153 mm and 254 mm (0.5D, 1.5D, and 2.5D from pile surface) on the front side of the

pile and 51 mm (0.5 D) from the pile on the back side. Based on the measurements, the ratios of shear wave velocity (i.e., shear wave velocity/initial shear wave velocity) at the end of pile installation are presented in Figure 4.12. These results show that the shear wave velocity close to the surface of the installed pile (within 0.5D) increased by 25% (30 m/s) during pile installation and that this effect decreased with distance. Figure 4.12 also illustrates that the velocity change due to pile installation extend to a distance of 254 mm (2.5D) from the pile surface. The measured increase in shear wave velocity due to pile installation is mainly attributed to the increase of soil density and lateral stresses in the soil (Lee et al. 2007). The measured zone of soil affected by pile installation (2.5D from the pile surface) is consistent with the analytical results reported by Dijkstra et al. (2011) and experimental results reported by Lundberg et al. (2013), Vesic (1977), and Salgado (2014).

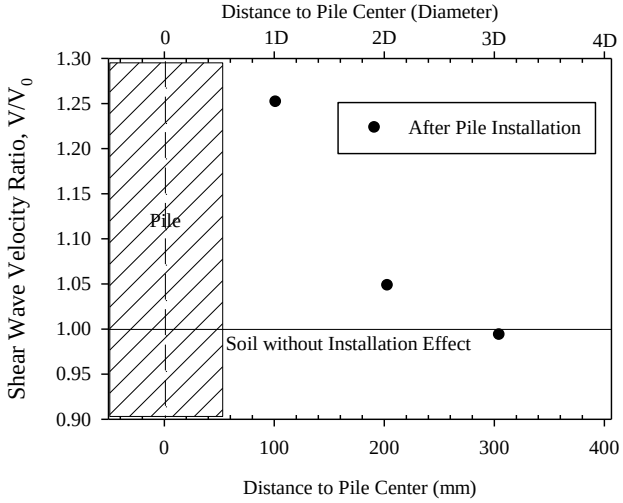

Figure 4.12 Change of shear wave velocity during pile installation at depth 550 mm

4.7 SUMMARY AND CONCLUSIONS

A new ground improvement method has been developed using pervious concrete piles. This chapter summarizes the material properties of pervious concrete

and the pile and soil responses obtained from two lateral load tests performed using the SSI facility at Lehigh University. Fully-instrumented lateral load tests were performed on a precast pervious concrete pile and an installed pervious concrete pile to investigate the pile and soil behavior, to study the soil-pile interaction, and to evaluate the effects of installation methods on pile behavior under lateral loading. Based on the experimental results obtained from the two lateral load tests and the discussion of the results presented in this chapter, the following conclusions are drawn:

1. A pervious concrete mixture prepared using proportions of 0.21 water/cement ratio, 0.11 sand/aggregate ratio, 377 kg/m^3 cement and 1440 kg/m^3 coarse aggregate provided an average compressive strength of 22.8 MPa, modulus of 15.1 GPa, and permeability of 1.44 cm/sec. at an average porosity of 10.7%. These properties show that pervious concrete piles have a compressive strength that is more than 10 times that of granular columns, while having permeability similar to granular columns.
2. The used installation method results in lateral compression and densification of surrounding sand as well as lateral stress increase. These changes significantly affect the pile and soil responses and the soil-structure interaction of pervious concrete ground improvement piles when subjected to laterally loading.
3. The ultimate lateral loads for the precast and installed pervious concrete piles were similar but the lateral displacements at ultimate load were significantly different. The displacement of the installed pile was 55% of the precast pile.

4. For both the precast and installed piles, the maximum strain and moment occurred at a similar depth of 444 mm below the soil surface, which is consistent with the locations of major tensile cracks (460 to 470 mm). Regardless of the installation method, pervious concrete ground improvement piles behave similar to long concrete or steel piles (i.e., long, flexible piles) when subjected to lateral loading, while providing permeability similar to that of granular columns. Unlike granular columns, this behavior helps in transferring lateral loads to stable deeper soils below the failure surface when used to stabilize slopes, which improve the response of stabilized slopes.
5. The installation of pervious concrete piles affects the surrounding soil response. A comparison of the soil displacements illustrates that the lateral displacements around the installed pile are smaller than the displacements around the precast pile.
6. The soil-pile interaction was directly measured for the precast pile using tactile pressure sheets and SAAs, which provided the information needed to develop directly measured p-y curves. The p-y curves obtained based on direct measurements show that the initial slope and ultimate soil reaction increased as the depth increased.
7. The p-y curves developed using the strain measurements of the installed pile more closely matched the curves produced using the Reese et al. (1974) method than the curves developed for the precast pile.

8. The installation method significantly affects the p-y curves for laterally loaded piles. Along the pile, the ratio of the ultimate soil reaction of the installed pile to the precast pile ranged from 1.4 to 5.9.
9. Shear wave velocity changes measured in the soil surrounding the installed pervious concrete pile during installation demonstrate that the zone of soil affected by installation extended to 2.5D from the pile surface.

CHAPTER 5

NUMERICAL SIMULATION OF PERVIOUS CONCRETE PILE TESTS

5.1 INTRODUCTION

Pervious concrete piles have recently been developed as an innovative ground improvement method (Suleiman et al. 2014; Ni et al. 2014). The behaviors of pervious concrete piles when subjected to vertical loading have been investigated using state-of-art Soil-Structure Interaction (SSI) facility. As part of this research, the piles and surrounding soil were instrumented and the effects of pile installation on soil-pile interaction and pile responses have been evaluated using the experimental tests. To improve the understanding of the installation effects on soil-pile interaction, 2D finite element modeling has been used. This study focuses on validating the finite element analytical models that can be used to simulate the installation effects of pile and the behaviors of pervious concrete piles under vertical loading.

However, developing a proper numerical model to accurately simulate the pile installation and behavior under vertical loading is a challenging task. In finite element method modeling, the large deformations, which occur during pile installation and at the soil-pile interface during loading, lead to severe mesh distortion in the finite element analysis. In addition, pile installation may change the soil properties and stresses, which significantly affect the behavior of piles when subjected to vertical loading.

Researchers have used different modeling approaches to simulate the effects of installation methods and effect on vertical load behavior, including 1D, 2D and 3D

finite element methods(Dijkstra et al. 2006; Pham and White 2007; Gennaro et al. 2008; Chen et al. 2009; Said et al. 2009; Basu et al. 2010; Dijkstra et al. 2011; Pucker and Grabe 2012). These approaches utilized defining soil-pile interaction properties by interface model and using special calculation steps to modeling the pile installation effects, the pile and soil behavior under vertical loading.

In this chapter, numerical analysis method has been developed to investigate the behavior of the pervious concrete piles subjected to vertical loading. The vertical load tests of pervious concrete piles are simulated using 2D axisymmetric finite element model with Plaxis 2D. An approach used to take into account the installation effects are proposed and discussed. The comparison between calculation results from the numerical simulations and measured results from experimental testing were conducted to validate the numerical simulations.

5.2 BACKGROUND

During the process of pile installation, the soil experience large displacement and its properties and stress will change. These installation effects influence the load-displacement response of the pile. Several laboratory and field tests have been conducted to investigate the installation effects of different types of pile. Measurements included the change of soil density, soil deformation along the pile and at the tip of the pile, cone penetration tests before and after installation, and shear wave velocity (Shublaq 1992; Klotz and Coop 2001; Hunt et al. 2002; Lee et al. 2004; White and Bolton 2004; Suleiman and White 2006; Ambily and Ganhdi 2007; Yi et al. 2010; Frikha et al. 2013; and Lundberg et al. 2013).

Numerical simulations of pile installation have been developed by several researchers (Wehnert and Vermeer 2004a, 2004b; Dijkstra et al 2006; Ambily and Gandhi 2007; Guetif et al. 2007; Pham and White 2007; Gennaro et al 2008; Chen et al. 2009; Said et al. 2009; Basu et al. 2010; Castro and Karstunen 2010; Thompson and Suleiman 2010; Dijkstra et al. 2011; and Pucker and Grabe 2012). These approaches include 1D (one dimension), 2D and 3D finite element modeling of different pile types (i.e. stone column, rammed aggregate pier, displacement pile, and bored pile).

To consider the installation effects of bored piles, Wehnert and Vermeer (2004a and 2004b) concluded that the soil stiffness (i.e. soil Young's modulus) needed to be increased 25% within 1D at the tip of pile.

In the numerical analysis of stone columns, Ambily and Gandhi (2007) didn't consider the installation effect, Guetif, et al. (2007) used an elastic-perfectly plastic soil model and the improvement of the soil Young's modulus was considered due to column installation. Castro and Karstunen (2010) improved the simulation by using a hardening-soil model and modeling the pile installation as the expansion of a cavity.

The behavior of rammed aggregate piers installed in a prebored hole was simulated by Pham and White (2007), Chen, et al. (2009), and Thompson and Suleiman (2010). In the study of Pham and White (2007), the pier installation process was modeled by applying 5 to 10% of the nominal diameter of cavity outward displacement along the shaft and downward uniform displacement at the bottom of the cavity based on measurement (Pham 2005). Chen et al. (2009) used same concept of cavity expansion to develop a 3D (diameter) model and investigate the effect of

different installation method of aggregate pier. Thompson and Suleiman (2010) used prescribed cavity volumetric strain expansion to simulate stress-dependent stiffness behavior of the aggregate, instead of using the prescribed displacement method proposed by Pham and White. In addition, the interface elements with hardening soil model were used to improve the modeling.

The displacement pile (normal concrete pile compared with granular pile) has been investigated using numerical method by several researchers. Dijkstra et al (2006) studied the effects of soil model on the behavior of pile, recommended the interface element with reduction factor as 0.75 for modeling and proposed the cavity expansion method with 3.75% of the pile diameter horizontally expansion and 3.75D (diameter) vertical expansion to simulate the displacement pile installation effects. Gennaro, et al. (2008) and Said et al. (2009) simulated the soil pile interaction by special interface constitutive model and proposed an approach to account for the pile installation effects due to jacking and driving in a 2D finite element model. In this approach, empirical correlations based on field data have been used to reproduce the soil stress, shaft friction and base resistance due to pile installation. The numerical models mentioned above only take into the installation effects without simulating the installation process. Few researchers have simulated the installation process to improve the understanding of changes during the installation process. Basu et al. (2011) used 1D finite element model to investigate the shaft capacity development for a displacement pile installed in sand. A small initial radius (<10% of pile diameter) has been selected for cavity expansion to simulate the pile installation. Dijkstra, et al. (2011) used a 2D finite element model capable of large displacement to simulate the

pile installation phase. The simulation results showed a soil zone with 2D around pile and 4D × 2D at the pile tip in axisymmetric model was effected by pile installation and the soil property (density) had been changed in the pile installation process. Pucker, et al. (2012) develop a 3D finite element model to simulate the pile installation process. The pile installation effects on the soil stress state and the soil density was investigated. However, because of the complexity of installation process simulation, the further validation of these models is still needed.

Based on the previous research work, a proper numerical model to simulate the pile installation and behavior under vertical loading should include:

1. Proper soil constitutive model to simulate the soil behavior
2. Interface element to consider the soil pile interaction
3. A Cavity expansion procedure to simulate the soil stress development due to pile installation
4. Changes of soil properties caused by the pile installation

These requirements were used in the numerical simulations presented in this chapter. The next sections provide the details of the numerical models and the experimental measurements used for validation.

5.3 EXPERIMENTAL PROGRAM

5.3.1 Soil Properties

The soil used in vertical load test was classified as well-graded sand (SW) according to the Unified Soil Classification System. The sand was rained into the soil box to produce a homogeneous soil profile along the total depth of the pile. The

minimum and maximum unit weights of the sand were 15.1 and 20.8 kN/m^3, respectively (i.e., maximum void ratio of 0.720 and minimum void ratio of 0.250). The rained sand had average relative density of 32%, unit weight of 16.5 kN/m^3, and water content of 2%.

To characterize the soil properties, consolidated drained (CD) triaxial tests were performed. The soil samples were prepared with similar properties for vertical load tests, (i.e., relative density of 32% and unit weight of 16.5 kN/m^3). The samples were tested under confining pressures of 15, 25, 100 and 160 kPa. The K_f line indicates that the peak friction angle of the soil is 38 °. The critical friction angle is the same as the peak friction angle, which is consistent with the results presented by Mitchell and Soga (2005) for loose sand. Based on the triaxial data, the sand at low confining pressure has the friction angle as 42 °which is higher than the friction angle calculated using all confining pressure. Low confining pressure presents the stress range within the soil box; therefore, it is more suitable to use the friction angle at low confining pressure to represent the initial condition.

5.3.2 Vertical Load Tests

The pervious concrete pile tests used to validate the numerical analysis are two instrumented vertical load tests. Both piles were prepared using pea river gravel, with diameter of 102 mm and embedded length of 1,219 mm. The first test unit was a precast pile, which was installed vertically into soil box with soil raining afterward. The second test unit (installed pile) was a cast-in-place pile installed using a 102-mm-diameter mandrel as shown in Figure 3.3. A bracing system was designed to ensure

accurate pile position and the verticality of the pile installation. Through the hollow cylinder of the bracing system, the mandrel was driven into the soil. Once the targeted depth was reached, the pervious concrete was placed into the mandrel from the top. As the mandrel was lifted upward at a slow rate, the cone would open to fill the created cavity with pervious concrete during retrieval. It is worth noting that similar to displacement piles, the used installation method results in lateral compression and densification of the surrounding sand as well as increase lateral soil stresses (Dijkstra et al. 2011; Lundberg et al. 2013).

The vertical load tests generally followed the fast procedure outlined in the ASTM D1143 (ASTM 2009d). In tests, the loads were applied by successive increments of 222.4 N for precast pile test and 889.6 N for installed pile test. Each load was held constant for 4 min or until the pile head displacement stabilized. The tests were stopped when the pile displacement continued increasing without an increase in the applied load. The load-displacement responses were shown in the Fgiure 3.6b.

In the vertical load test of installed pile, the surrounding soil was instrumented with three SAAs and six null pressure sensors, as shown in Figure 3.5. Two SAAs were installed at 102 (1D) from the center of pile, and one SAAs was installed at 203 mm from the center of pile (2D). The null pressure sensor 1, 2 and 3 were installed at 76, 178 and 279 mm (i.e., 0.75 D, 1.75 D, and 2.75 D) below the tip of the pile to measure the vertical soil pressure. The null pressure sensor 4, 5 and 6 were installed at the same horizontal distance of 102 mm (1D) from the pile center with different depth of 1,270, 1,270 and 914 mm below the soil surface, respectively. The soil

movement during the pile installation and vertical test are shown in Figure 3.10 and the soil pressure changes are summarized at Figure 3.11.

5.4 MATERIAL CONSTITUTIVE MODELS

5.4.1 Hardening-Soil Model

The hardening-soil (HS) constitutive model is used to describe the behavior of sand used in the tests. This HS model has been recommended by Wehnert and Vermeer (2004a) and Dijkstra et al. (2006) to simulate sand behaviors. The parameters for the model are derived from triaxial consolidated drained (CD) tests which are summarized in Table 5.1. In this constitutive model, the soil initial stiffness E_i is determined by E_{50}, which is the confining stress dependent modulus given by the equation (1):

$$E_{50} = E_{50}^{ref} \left(\frac{c\ cos\varphi - \sigma_3' sin\varphi}{c\ cos\varphi + p^{ref} sin\varphi} \right)^m \quad (1)$$

The parameters are defined in Table 5.1 and are calculated based on Brinkgreve et al. (2014). The dilatant behavior of sand needs to be considered in the modelling for its influence on the shaft resistance (Wehnert and Vermeer 2004a; Dijkstra et al. 2006; Gennaro et al. 2008). A dilatation angle of 12 ° was selected for modeling. This value was determined based on the difference of 30 ° between the friction angle and the dilatation angle as recommended by Gennaro et al. (2008) and Brinkgreve et al. (2014). The stress dependency value m is 0.725 in the range given by Von Soos (1990) and the unloading-reloading modulus E_{ur}^{ref} is set as three times of E_{50}^{ref} based on the recommendation by Schanz et al. (1999).

Table 5.1 The constitutive model parameters for sand used in vertical load tests

Name	Symbol	HS model	Unit
Unsaturated unit weight	γ_{unsat}	16.5	kN/m^3
Saturated unit weight	γ_{sat}	19.8	kN/m^3
Initial void ratio	e_{ini}	0.606	-
Reference stiffness	E_{50}^{ref}	4878	kN/m^2
Oedometer reference modulus	E_{oed}^{ref}	4878	kN/m^2
Unloading/reloading stiffness	E_{ur}^{ref}	14634	kN/m^2
Power for stress-level dependency of stiffness	m	0.725	-
Cohesion	c'_{ref}	0	kN/m^2
Friction angle	φ	42	° (degree)
Dilatation angle	ψ	42	° (degree)
Poisson ratio	ν'_{ur}	0.2	-
Reference stress for stiffness	p^{ref}	100	kN/m^2
Interface strength reduction factor	R_{inter}	0.75 (0.8)	-

To validate the soil parameters used in the hardening soil model, the triaxial tests was modeled in Plaxis. The measured from consolidated drained (CD) triaxial test and calculated (from Plaxis) stress-strain responses for sand are presented in the Figure 5.1. The similarity between measured and calculated soil behavior indicates that the soil behavior is well simulated by HS constitutive model.

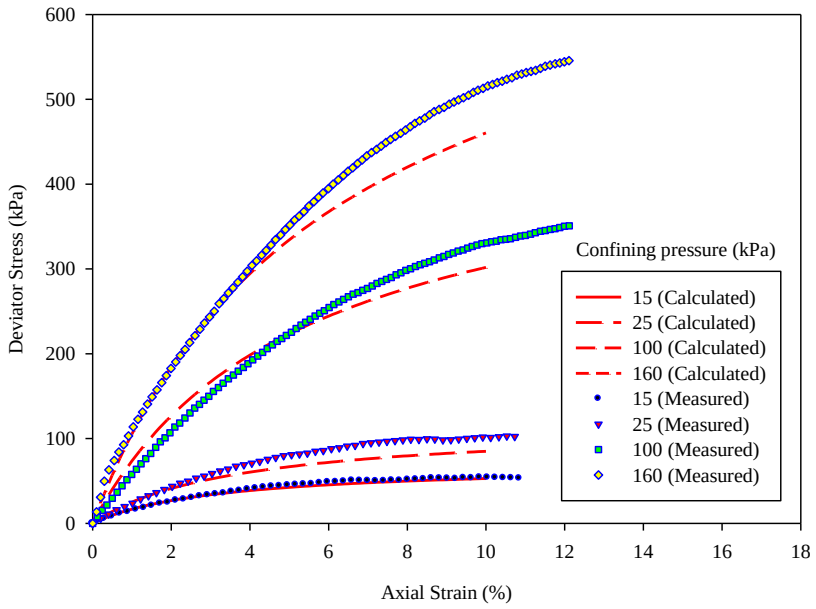

Figure 5.1 The measured and calculated triaxial deviator stress vs. strain curves under different confining pressure

5.4.2 Interface Soil Element Model

The soil-pile interaction is included in the model by utilizing the interface element between the pile and surrounding soil. The interface element is modelled using the Mohr-Coulomb friction failure criterion. The displacement is allowed to occur within the interface element to simulate the relative movement between the pile and soil, where the small displacements are controlled by elastic behavior and large displacement are described by plastic behavior. In Plaxis, the interface properties are functions of the adjacent soil strength properties associated with strength reduction factor (R_{inter}). The value of R_{inter} is set as 0.75 for precast pile interface as recommended by Dijkstra et al. (2006) and set as 0.8 for installed pile interface with rough pile surface based on the match between the calculated and measured results.

5.4.3 Pile Element Model

The pile is simulated by linear elastic model (Wehner and Vermeer 2004; Dijktra et al. 2006) with Young's elastic modulus of 15.4×10^6 kN/m^3, and Poisson ratio of 0.3, which are obtained from experimental results of pervious concrete sample.

5.5 FINITE ELEMENT MODEL

The model dimension is set the same as the soil box that was used for vertical load tests with height of 2286 mm and half width of 762 mm as shown in Figure 5.2. The pile and soil are modeled by 15-noded triangular elements in axisymmetric model. The interface between pile and soil has been set along the pile length using R_{inter} values mentioned before.

In vertical load tests, the pervious concrete piles have radius of 51 mm and embedded length of 1219 mm. The precast pile is directly modeled with this dimension. For the installed pile, the model accounted for the installation effects, which will be discussed in further details in the next section. The previous analysis by Wehnert and Vermeer (2004a) and Dijkstra et al. (2006) pointed out that, in order to avoid the effect of element size on calculation results, the pile needed to be meshed with at least 16 elements along the pile and at least 2 elements over the radius of the pile tip. Therefore, the local element size factor of pile was reset to 0.1 instead of 1.0. And the local element size factor of soil near the pile was reset to 0.25. The smaller size of element is able to provide better prediction of the soil behavior. The mesh of two models with the refined zone near the pile is shown in the Figure 5.3.

As shown in Figure 5.2a and 5.3a, three soil zones were used around the precast pile for near the pile are set for mesh refinement. According to the investigation of Dijkstra et al. (2008), Said et al. (2009), Dijkstra et al. (2011) and Lundberg et al. (2013), the soil within 2D around the pile and 4D below the pile tip was effected by the vertical loading. Therefore, Zone 1 is adjacent to the pile along its length (1219 mm) and has a width of 203 mm (2D). Zone 2 is below the pile with height of 406 mm (4D) and width of 51 mm (0.5 D). Zone 3 is below the soil adjacent to the pile with height of 406 mm (4D) and width of 203 mm (2D). Zone 4 represents the soil away from pile, which is less affected by the vertical load, with boundary of soil box. The model includes 2119 elements totally.

For the installed pile model shown Figure 5.2b and 5.3b, the soil area surrounding the installed pile was divided into additional six zones to take account for the installation effects on surrounding soil. Research on the installation effects of displacement pile demonstrated that the area affected by pile installation at the tip is approximately 4D × 2D (height × width) (Shublaq 1992; Dijkstra et al. 2008; Said et al. 2009; Dijkstra et al. 2011; and Lundberg et al. 2013). This affected zone is confirmed by the measured vertical stress below the pile tip presented in Chapter 3. In addition, the measured soil movements around the pile show that the zone affected by pile installation extended to 2D along the pile (Lundberg et al. 2013). Therefore, the soil area affected by installation is set in a horizontal distance of 2D along the pile and a vertical distance of 4D below the pile tip. As shown in Figure 5.2b and 5.3b, two zones beside the pile have been set, which are zone 1 of 1019 mm × 147 mm (height × width) and zone 2 of 1019 mm × 102 mm (height × width). In addition, two

bottom zones, which are zone 3 of 403 mm × 152 mm (height × width) and zone 4 of 606 mm × 254 mm (height × width, and expect zone 3), have been used. The Zone 5 is set with dimension of 203 mm (2D) below the zone 4 and 203 mm (2D) beside the zone 1 and 4. Zone 5 is set for the further study the effected zone of pile installation. Zone 6 represents the dimension of the soil box in vertical load test. The total number of the meshed element is 1784. The effects of installation on soil properties will be discussed in the next section.

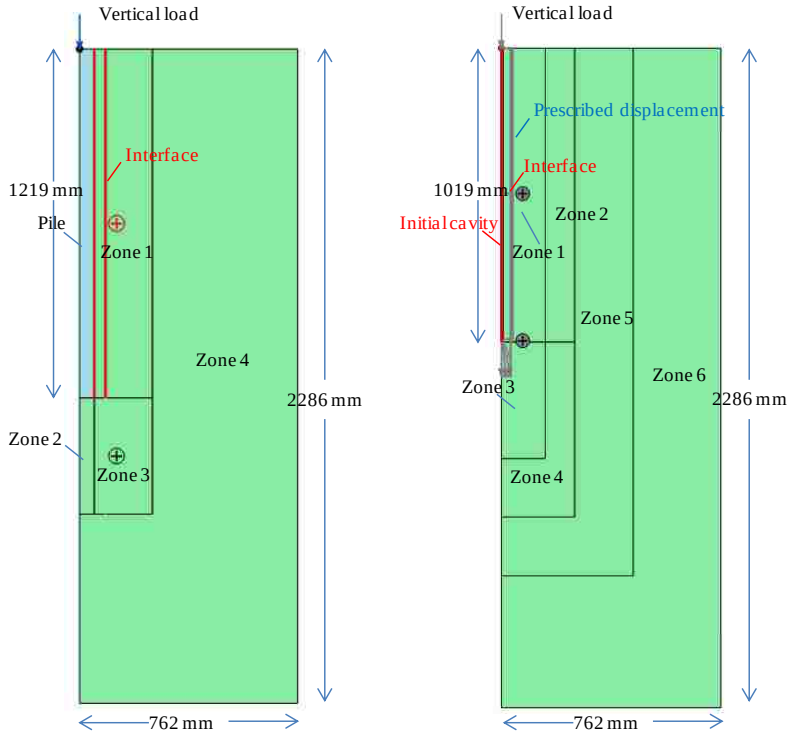

Figure 5.2 The geometry of finite element model: (a) Precast pile; (b) Installed pile.

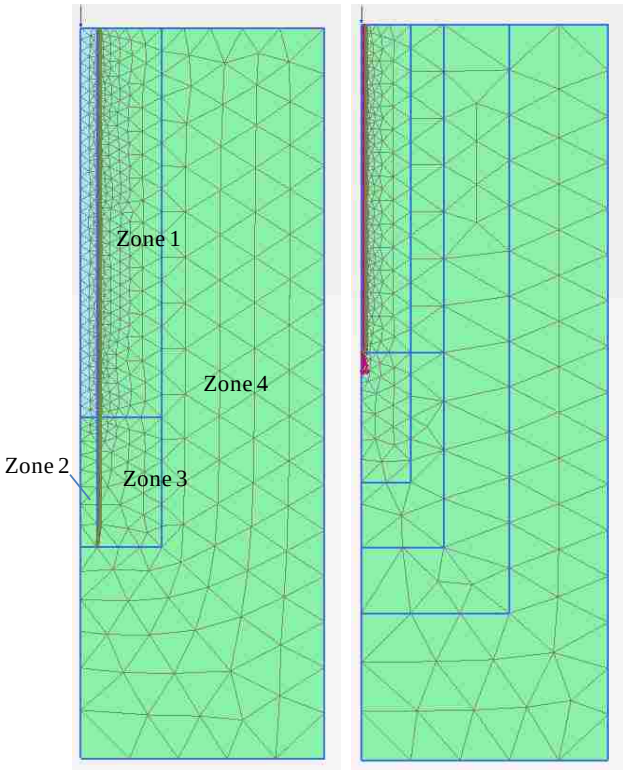

(a) **(b)**

Figure 5.3 The mesh of finite element model: (a) Precast pile; (b) Installed pile.

5.6 MODELING PROCEDURE

For the precast pile, the modeling procedure includes the initial phase to generate initial stress and a series of loading phases. In order to consider the installation effects on the vertical load test of the installed pile, installation phases were included between pr the initial phase and the loading phases. The section below provides the details of different modeling phases.

5.6.1 Initial Phase

The initial stress condition is established to generate the initial vertical and horizontal soil stresses. The vertical stresses are calculated using the unit weight of

the soil. Initial horizontal stresses are generated using the K_0 procedure, in which the in-situ horizontal effective stresses are calculated using the vertical effective stress and the predefined K_0 value (based on the soil friction angle).

5.6.2 Installation Phase

For the installed pile, the zone representing the pile with the initial size which is 10% of the pile diameter (5.1 mm width) is deactivated initially. The 10% size of the initial cavity was recommended by Basu et al. (2011). In pile installation, the cavity is mainly expanded vertically with the pile driving into deeper depth. However, the simulation of only vertical cavity expansion in finite element model will cause mesh distortion at the tip of pile. Therefore, the numerical approach focuses on simulating the final installation effects rather than the installation procedure itself.

The installation effects are considered by applying prescribed displacements at the pile-soil boundary of initial cavity. The prescribed displacement method was recommened by Broere and Van Tol (2006) and Said et al. (2009). The total cavity expansion includes horizontal prescribed displacement of 45.7 mm and vertical prescribed displacement of 200 mm (2D) as shown in Figure 5.4. The implementation of cavity expansion is divided into four expansion steps. Each step has 25% increment of horizontal displacement (11.4 mm) and vertical displacement (50 mm). For each expansion step, the mesh is updated (i.e. to consider large displacement) to avoid mesh distortion. This expansion procedure of cavity in model is different from the actual cavity creation process during pile penetration.

During the experimental test, the horizontal displacement of the soil (cavity expansion) starts from zero lateral soil displacement (i.e., no initial cavity). However, the cavity expansion from a zero radius in finite element model may cause numerical instability and errors. Therefore, researches investigating pile installation effects using cavity expansion (e.g., Salgado and Prezzi 2007; Basu et al. 2011) recommended that instead of creating a cavity from zero radius, the cavity expansion from a sufficient small initial cavity radius (~10% of the final radius) lead to a reasonable results. Therefore, the initial horizontal expansion in this model is set as 5.1 mm, which is 10% of final pile radius.

For the vertical direction, the cavity was expanded by a displacement that results in vertical stress change similar to the measured value during the test. Several trials were performed for the vertical expansion to match measured stress. It was found that the vertical expansion of 200 mm (i.e., after expansion the length of cavity is the same as the pile length of 1219 mm) produce similar soil stress at the tip of the pile as the measured pressure at the same location in the experimental test.

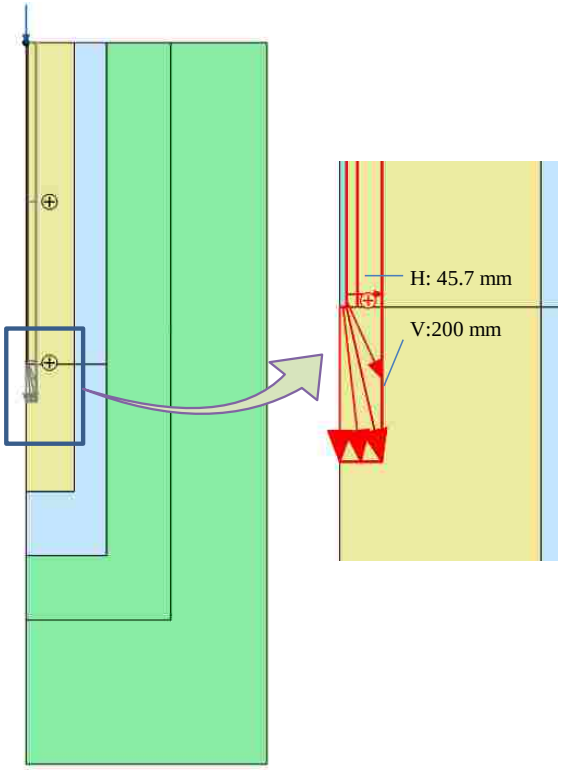

Figure 5.4 The prescribed displacement on soil boundary to simulate the cavity expansion in pile installation

5.6.3 Activation Phase

Before applying the vertical load on the installed pile, the pile elements were reactivated in the expanded cavity and the prescribed displacement was deactivated.

For the installed pile, the pile installation will not only densify the soil and increase the soil stress, but also will improve the soil stiffness. Wehnert and Vermeer (2004a, and 2004b) recommended improving the soil stiffness by 25% in the effected zone below the pile tip of 1D. Gennaro (1999) presented an equation to quantify the increase of the soil modulus after pile installation, which is confirmed by Said, et al. (2009). The equation of the modified soil modulus as a function of confining pressure is presented as:

$$E_{ur} = m\sigma_c^{0.55} \quad (2)$$

where the m value is calculated as 1.16 from the initial value of E_{ur} under reference confining pressure (100 kPa) from measurements of CD triaxial test. The modified value of E_{ur} at pile tip is calculated as 21.96 MPa using Equation (2) and the measured radial stress close to the pile tip as 210 kPa (i.e. the stress measured by sensor 4 and 5), which is about 50% increase compared to initial soil modulus. Therefore, the soil modulus in the installation effected zone (2D around the pile, 4D below the pile tip) should increasing 25 to 50% compared to initial modulus.

According to the previous studies (Suleiman et al. 2014) on soil stiffness change during pile installation and the experimental analysis of soil stress and movement during vertical load tests in Chapter 3, the soil modulus (including the parameter of E_{50}^{ref}, E_{oed}^{ref}, and E_{ur}^{ref}) are reactivated with increased value due to pile installation is shown in the Figure 5.5. Zone 1 (within 1D to pile) and zone 3 (within 2D to pile tip) has modulus 1.5 times of the initial value. Zone 2 (1D to 2D beside the pile) and zone 4 (2D to 4D below the tip of pile) has modulus 1.25 times of the initial value.

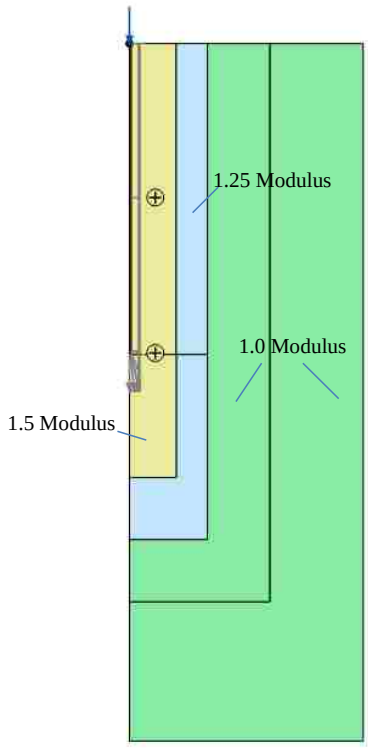

Figure 5.5 The soil stiffness change after pile installation

5.6.4 Loading Phase

The vertical loading procedure was modeled by applying a sequence of vertical loads on the pile head. The vertical loads on the top of the pile were simulated by point loads at the axis of symmetry. The input value of loads was the force acted on the angle of one radian (i.e., the point load should be multiplied by 2π to give load on physical pile). Mesh updating was also used for each load step to minimize any numerical instability that could be caused by large displacement, and to obtain more accurate results.

5.7 RESULTS ANALYSES

5.7.1 Model Validation

The model validation focuses on the comparison between the calculated and measured values, including the load-displacement relationship, soil movement and stress development near the pile tip.

The calculated and measured vertical load-displacement relationships were shown in Figure 5.6. For the precast pile, the calculated initial slope of load displacement curve is 149 N/mm and the displacement at ultimate load is 113 mm, which are similar with the measured initial slope of 155 N/mm and displacement of 119 mm (i.e., the calculated slope and displacement under ultimate load is 96% and 95% of the measured value, respectively). For the installed pile, the calculated initial slope of load displacement curve is 2,427 N/mm and displacement at ultimate load is 37 mm, which is 84% of the measured initial slope (2,883 N/mm) and 109% of the measured displacement (34 mm), respectively. The very good match between the model prediction and test results indicates that procedure used to model the response of pervious concrete piles and the effects of installation is reasonable and the soil parameter selection is appropriate.

The major difference between precast pile model and installed pile model is the additional of two calculation phases to consider the pile installation effects. The increases of load capacity and slope of the load-displacement curve attributed to the pile installation effects have been well simulated by the proposed approach, which confirmed that this modeling approach of pile installation effects is reasonable.

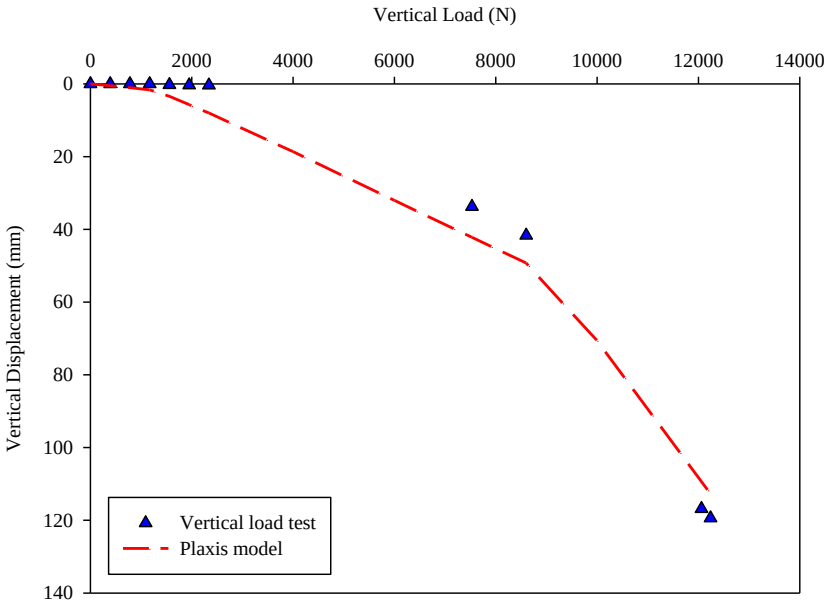

(a)

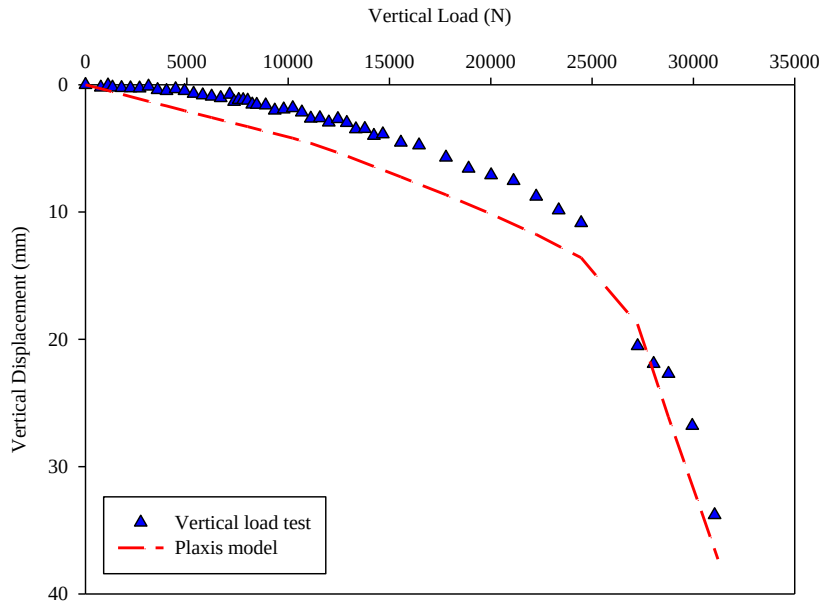

(b)

Figure 5.6 Comparison of vertical load versus displacement: (a) Precast pile; (b) Installed pile

The soil horizontal movement (U_x) at distance 51 mm (0.5 D) from pile surface along the pile is compared with the measured SAAs data in Figure 5.7. The maximum difference between the calculated and measured movement value along the

pile is 3.7 mm (34%), which further validates that the initial set of prescribed displacement with 45.7 mm on a small diameter (5.1 mm) cavity.

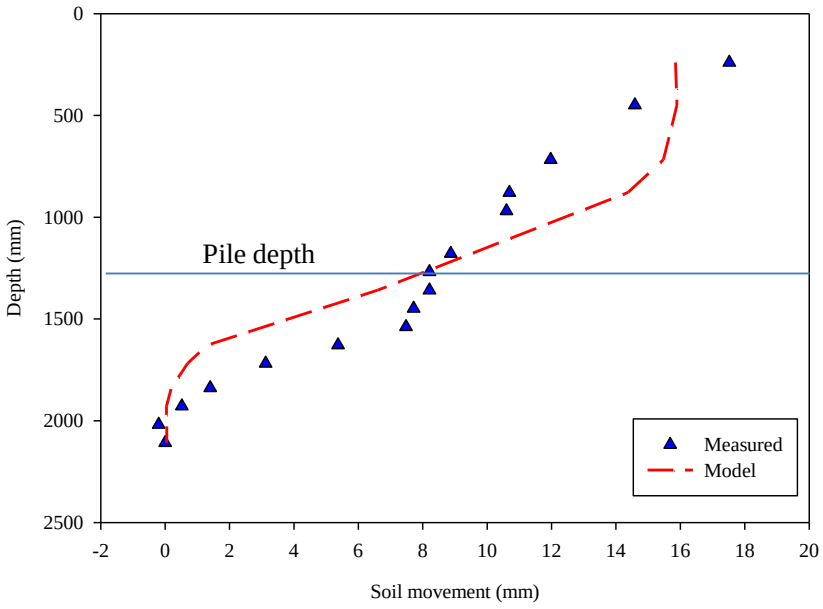

Figure 5.7 The comparison of calculated and measured soil lateral movements at 51 mm from surface of installed pile

During the vertical loading stage, the soil stress development at 76 mm (0.75D) below the pile tip is plotted and compared with the measured soil stress at this point (i.e., the pressure sensor 3 measurement in Figure 3.11a). As shown in Figure 5.8, after pile installation, the calculated pressure (the 1st point) is 214 kPa, which is very close to the measured pressure of 215 kPa after installation. This confirms that the prescribed displacement of 200 mm (2D) in the vertical direction is appropriate. When comparing the measured final pressure of 644 kPa under ultimate vertical load, the calculated pressure (the last point) of was 512 kPa has difference to the measured pressure value less than 20%.

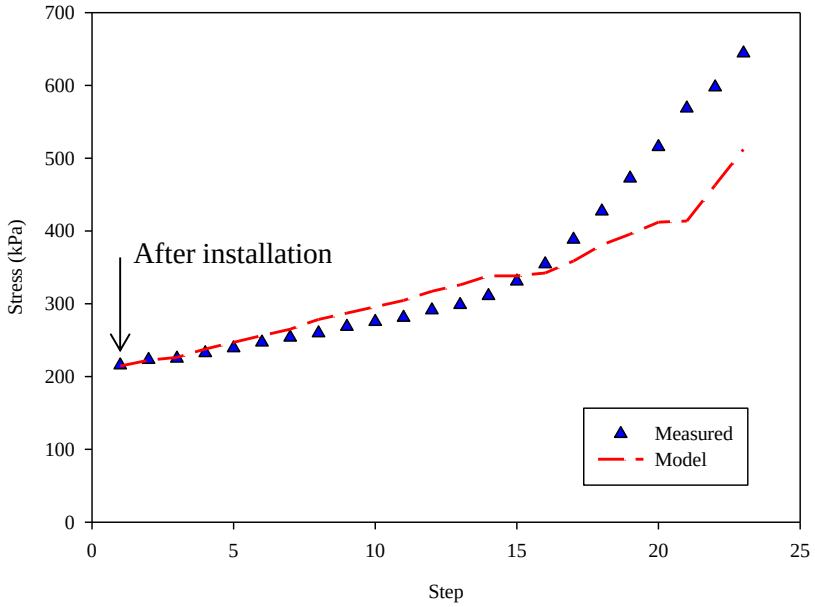

Figure 5.8 The comparison of calculated and measured soil vertical pressure 76 mm below the pile tip during the vertical load test

5.7.2 Soil Movement and Stress Distribution

The distribution of soil movement under ultimate load is plotted in Figure 5.9, including total soil movement (|U|), vertical movement (U_y) and horizontal movement (U_x) for both the precast pile and the installed pile. As shown in the Figure 5.9, the soil movements in both vertical and horizontal direction mainly occur in the zone of 406 mm × 203 mm (4D × 2D as height × width) below the pile tip. This range is consistent with the observation of soil properties change around the tip of pile under vertical load by other researchers (Dijkstra et al. 2008; Said et al. 2009; Dijkstra et al. 2011; and Lundberg et al., 2013).

Comparing the soil horizontal movement (U_x) beside the pile, the soil beside the precast pile has very little horizontal movement along the pile depth, while the soil has apparent movement along the installed pile within the range of 2D distance to

the pile surface. The difference of soil horizontal movement next to the pile between precast pile and installed pile indicates that the vertical load will not produce significant soil horizontal movement along the pile shaft and the pile installation is the main factor of soil horizontal movement development.

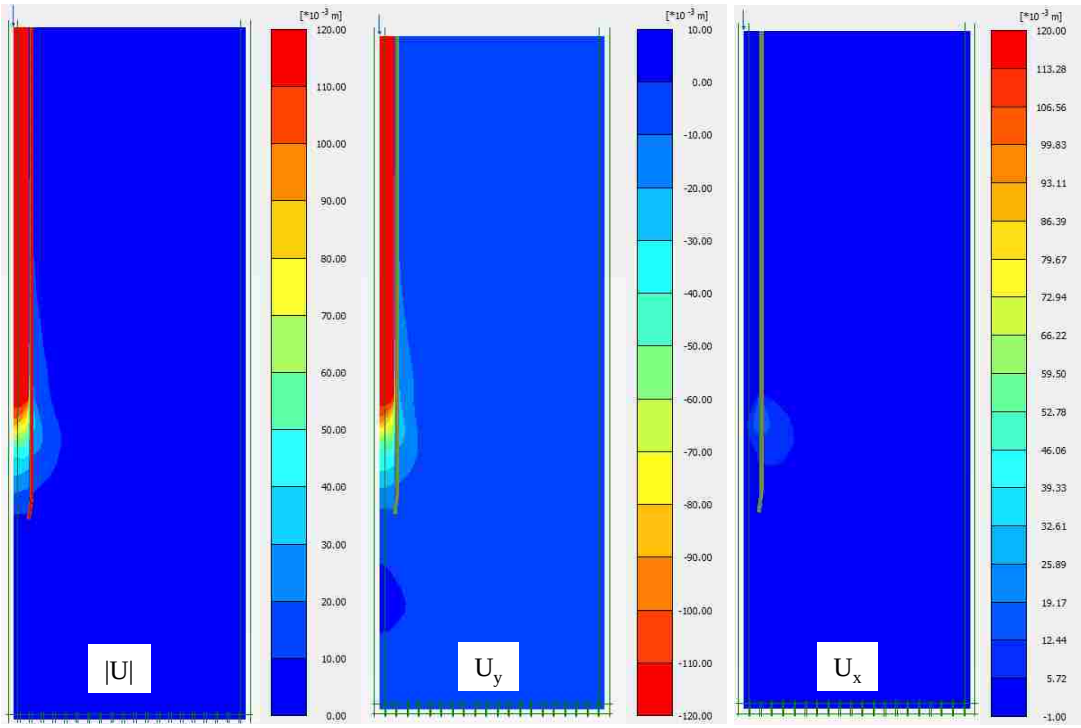

(a)

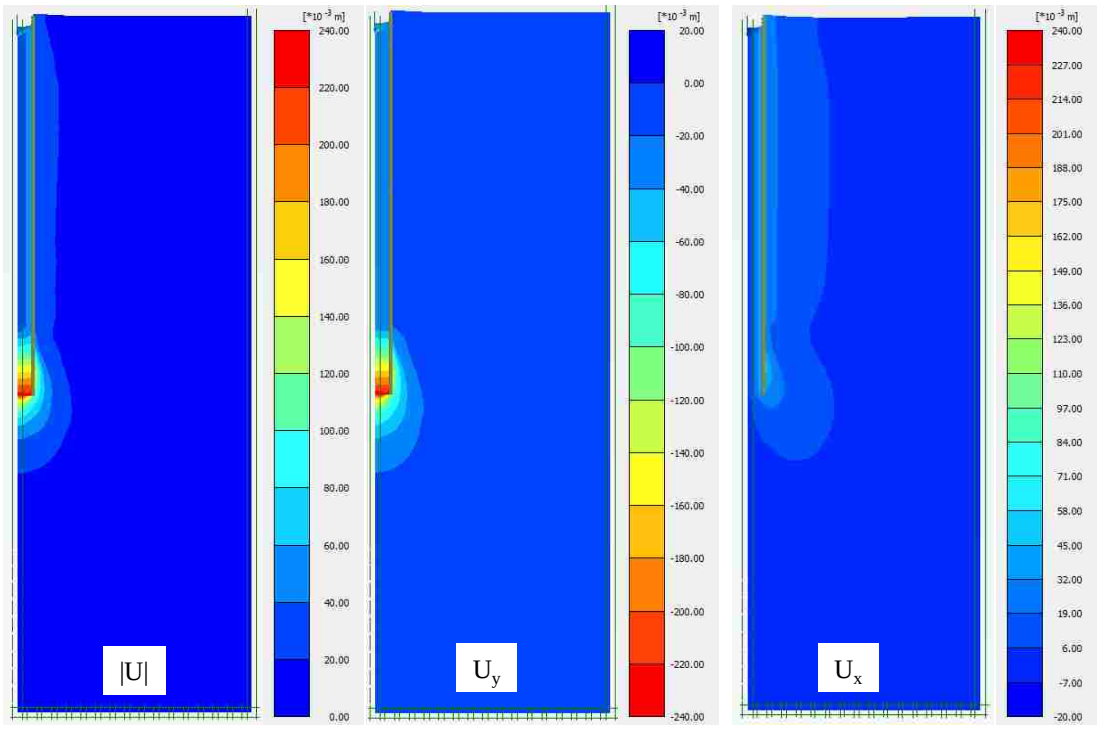

(b)

Figure 5.9 distribution of displacement under vertical load: (a) Precast pile; (b) Installed pile

The soil stress distributions in vertical and horizontal direction at the final loading step of 31,200 N are shown in Figure 5.10. The stress contours show that the zone of main stress change is below the pile tip that extend is 4.5 D × 3D for installed pile model and 4 D × 2D for the precast pile model. This effected soil area is consistent with the area of soil properties changes observed by other researchers (Said et al. 2009; Dijkstra et al. 2011) and confirms the geometry setting of soil zone in both model.

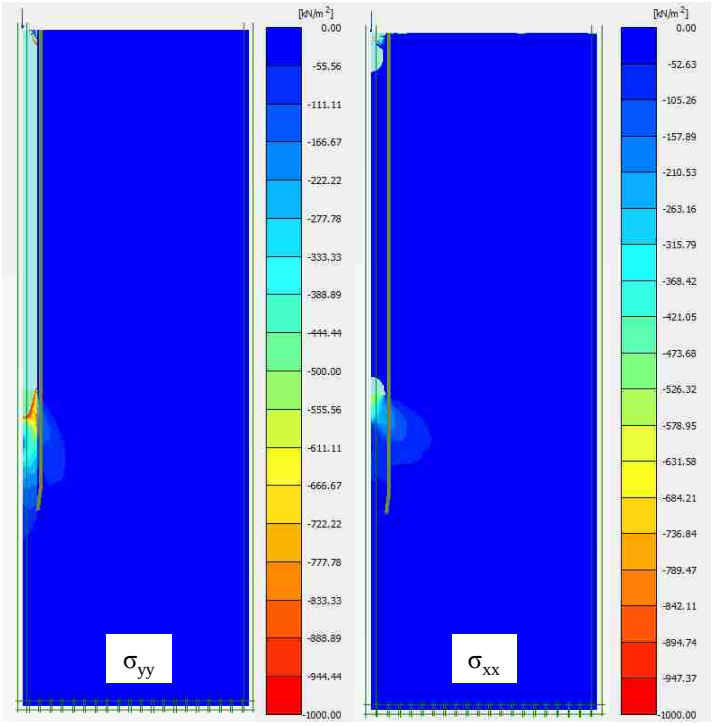

(a)

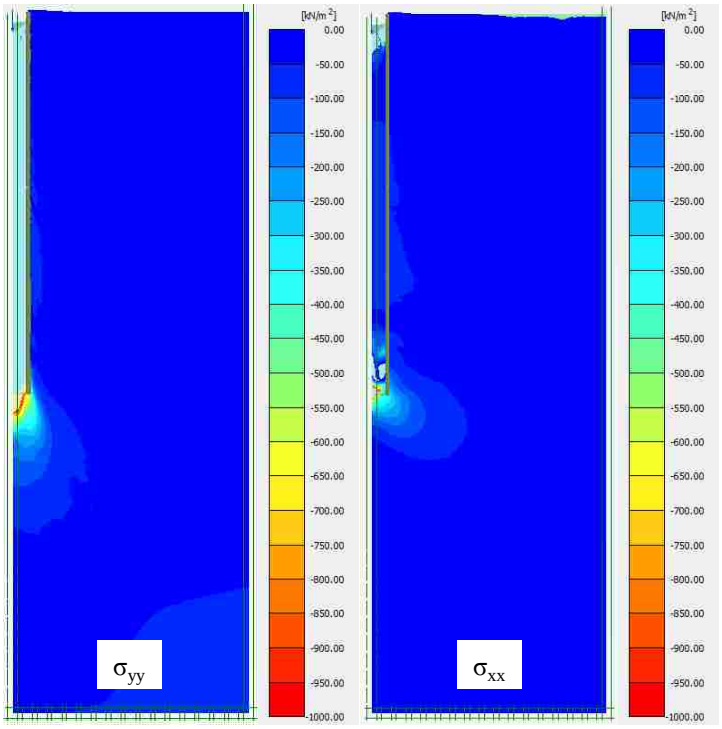

(b)

Figure 5.10 Distribution of soil stress under vertical load: (a) Precast pile; (b) Installed pile

5.7.3 Influence of the Interface Model

The influence of the interface model on the simulation results of the vertical load tests is investigated by two calculation cases. In the first calculation case, the soil-pile interface behavior is modeled using interface element created between soil and pile. For the second case, the soil and pile were perfectly attached to each other (i.e., no interface element).

The calculation results of load-displacement relationship are compared in the Figure 5.11. And the properties of load-displacement curve are summarized in the Table 5.2. For the precast pile, the model without interface element has initial slope of 295 N/mm and failed at a small displacement of 30 mm under an ultimate load of 10,000 N. Compared to the measured response, the model without interface element has much higher (around 2 times as high as the measured one) initial load-displacement slope with an underestimated the displacement and ultimate load at failure. Moreover, when large vertical displacement occurs at large vertical load, the model needs extended interface to simulate the large soil movement below the tip of pile. As showed in Figure 5.10a, when the displacement is larger than 51 mm (0.5D), the model without extended interfaces cannot well estimate the vertical load behavior, while the model with original interface along the pile and extended interface can accurately simulate the pile under vertical load.

For the installed pile, without using interface element does not have significant influence at the stage with small displacement increment as show in Table 5.2. However, when the large displacements occur (>17 mm), the soil in model without interface collapsed under lower vertical load.

In both vertical load tests, the finite element model without interface failed at small displacement. This phenomenon is expected because that the finite element model doesn't allow large displacement to occur.

Table 5.2 The load-displacement properties of model with/without interface

Type		Initial slope (N/mm)	Ultimate load (N)	Displacement (mm)
Precast pile	Test	155	12, 200	119
	Model with two interfaces	149	12, 200	113
	Model without extended interface	149	12, 200	88
	Model without interface	295	10, 000	30
Installed pile	Test	2883	31, 222	34
	Model with interface	2427	31, 222	37
	Model without interface	2600	28, 770	17

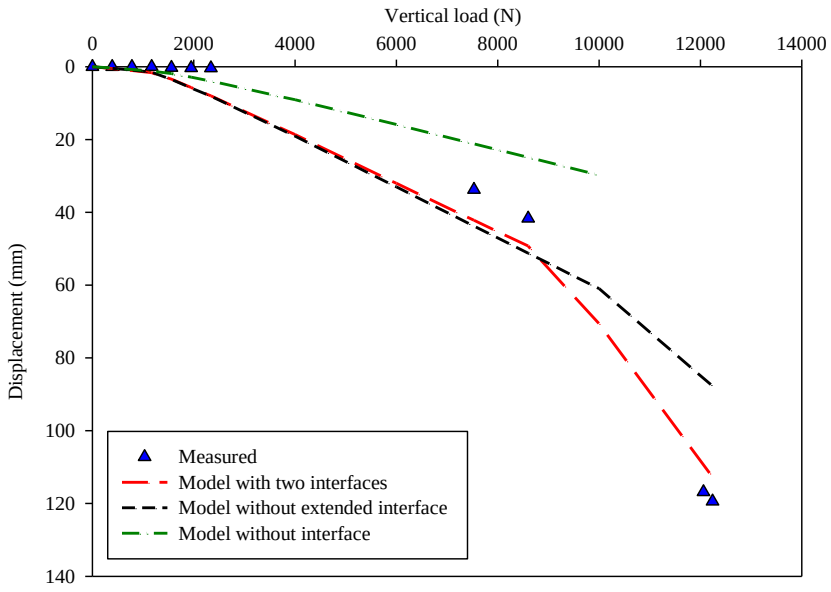

(a)

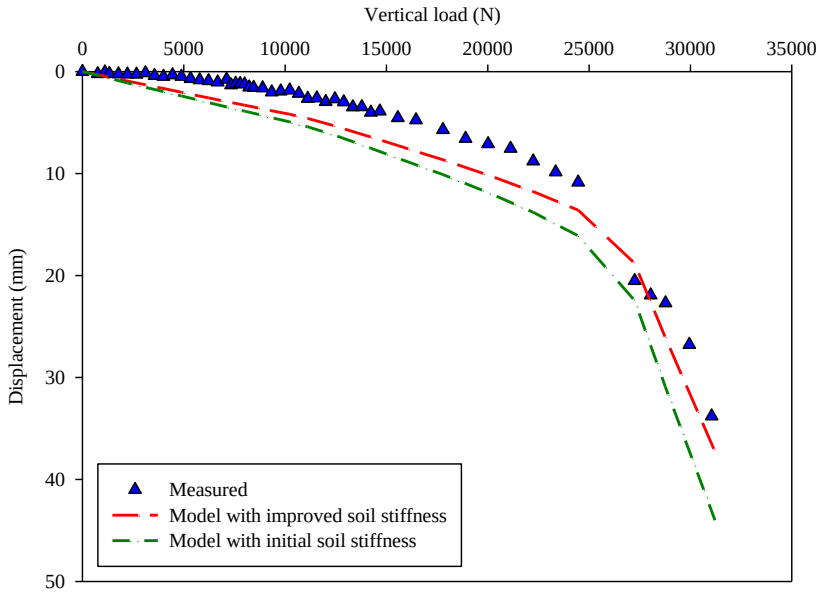

(b)

Figure 5.11 Influence on the interface: (a) Precast pile; (b) Installed pile

5.7.4 The Influence of Soil Stiffness

As mentioned in background, the soil stiffness has been improved by the pile installation, which will affect the load-displacement response of pile. To evaluate the effects of soil stiffness change, the results of two models, one without changes of soil stiffness and one with changes, were compared. As shown in the Figure 5.12, the initial slope of the model without considering the changes of soil stiffness around the pile is 2067 N/mm, which is 72% of the slope of the measured response; and the displacement under ultimate load (44 mm) is 29% larger than the measure value. Therefore, the results of the model with initial soil stiffness overestimate the displacement of pile under vertical load around 30% compared to the test results. In addition, the effect of soil stiffness 1D beside the pile and 2D below the pile tip was investigated by increasing 30%, 40% and 60% after pile installation. The results show that the displacements under ultimate load with 30%, 40% and 60% soil stiffness

increase are 5.5% bigger, 2.1% bigger and 2.5% smaller than the one with 50% soil stiffness increase, which indicate that the soil stiffness increase indeed effect the pile load-displacement behavior.

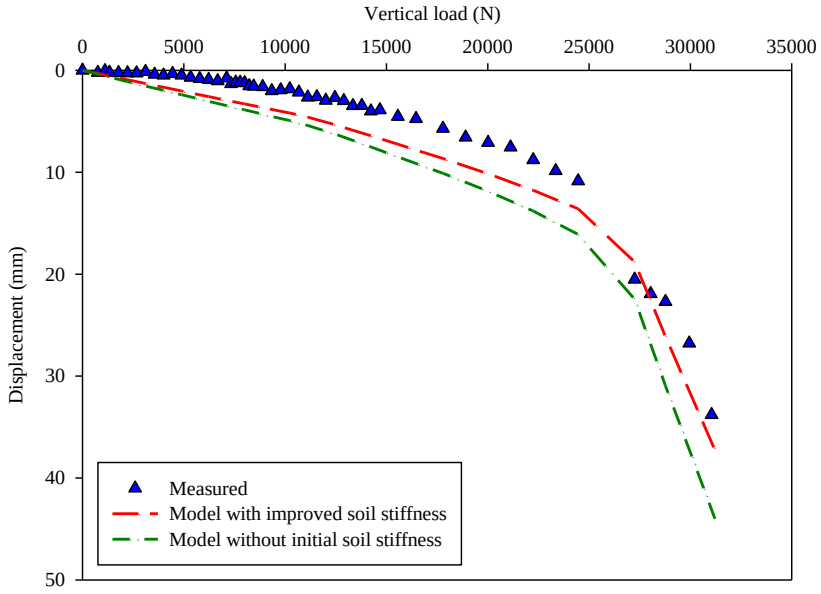

Figure 5.12 Influence of soil stiffness for vertical load of installed pile

5.7.5 Soil Movement during Installation

In the installed pile model, the pile installation is taken into account using installation and activation phases. In the installation phase, the cavity expansion due to the pile installation is applied using a prescribed displacement on soil. During the prescribed displacement process, the soil is pushed to create the cavity. The corresponding soil movement caused by pile installation is presented in Figure 5.13. The range of the soil movement is mainly in the zone of 406 mm (4D) below the tip of the pile and 203 mm (2D) beside the pile. The affected soil zone is consistent with the soil movement zone measured by Lundberg et al. (2013) and the SAAs measurements in the tests presented in chapter 3.

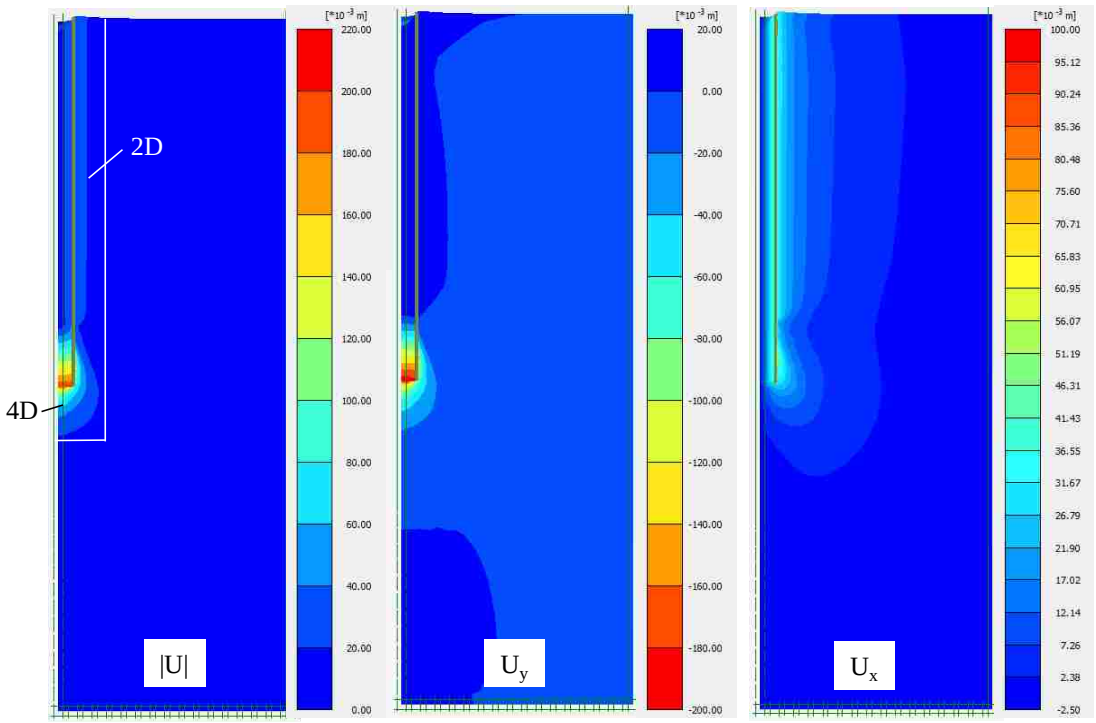

Figure 5.13 Soil movements during pile installation

5.8 SUMMARY AND CONCLUSIONS

In this chapter, the behaviors of pervious concrete piles and surrounding soil were investigated using Plaxis 2D. The pile installation effects have been taken into account. The analysis results confirm that the installation effects significant influence the pile and soil behaviors.

Two finite element models have been created to simulate the installation effects and behavior of pervious concrete piles subjected to vertical loading. The pile responses in modeling have been compared with the measured response. The major findings of the numerical study include:

1. A finite element simulation approach is proposed to account for the effects of pile installation. The approach includes two additional calculation phases: installation phases with prescribed displacement (2D in vertical direction and

0.45 D in horizontal direction); and activation phase with soil stiffness increased.

2. The modeling results of both precast and installed pile show good agreement with the measurement results. The difference of the initial load-displacement slope and the displacement under ultimate load is less than 16%, the difference of the displacement under ultimate load is less than 9%.
3. The pile installation effect on soil movement (1D from pile center) has difference less than 34% between the modeling results and measurements. After pile installation, the soil stress development at pile tip in model has less than 20% difference to the measured pressure value.
4. The soil properties improvement is taken into consideration of modeling the pile installation effect. The analytical results show that within the range of 2D horizontal distance to pile and 4D vertical distance to tip of pile, the soil stiffness based on the needs to be increased by 25%~50% as consequence of pile installation.

CHAPTER 6

SUMMARY AND CONCLUSIONS

6.1 SUMMARY AND CONCLUSIONS

An innovative ground improvement method using pervious concrete piles has been created and studied in this research. In addition, the installation effects are investigated by various advanced experimental and numerical methods. The important conclusions from this research are summarized as follow:

1. Pervious concrete piles have a compressive strength that is more than 10 times that of granular piles, while providing similar permeability to granular piles.
2. The pervious concrete pile, which had the same dimensions, aggregate type, and installation method as the granular pile, had an ultimate load that was 4.4 times greater than the ultimate load of the granular piles.
3. The installation method had significant effects on the response of the pervious concrete piles and surrounding soil.
4. The ultimate vertical load of the installed pile was 2.6 times greater than that of the precast pile.
5. Installation of the pervious concrete pile resulted in an increase of the maximum frictional stress transferred at the soil-pile interface.
6. The lateral soil displacements measured at a distance of 1D from the pile center during installation were not uniform along the length of the pile.
7. The ultimate lateral loads for the precast and installed pervious concrete piles were similar but the lateral displacement at ultimate load of the installed pile was 55% of the precast pile.

8. The installation method significantly affects the p-y curves for laterally loaded piles. Along the pile, the ratio of the ultimate soil reaction of the installed pile to the precast pile ranged from 1.4 to 5.9.
9. Shear wave velocity changes measured in the soil surrounding the installed pervious concrete pile during installation demonstrate that the zone of soil affected by installation extended to 2.5D from the pile surface.
10. A new finite element simulation approach is proposed to account for the effects of pile installation. The approach includes two additional calculation phases: installation phases with prescribed displacement and activation phase with soil stiffness increased.
11. 2D axisymmetric finite element simulations that account for the effects of installation show good agreement with the measured response of test piles.
12. The zone of soil affected by the pile installation and loading is 2D × 4D (Width × height) below the tip of the pile and 2D along the pile length.

6.2 FUTURE RESEARCH

The author suggests that the following of pervious concrete ground improvement pile needs further study:

1. Parametric study on pervious concrete pile in different soils using finite element models proposed by author.
2. The pervious concrete pile has high permeability comparing to surrounding soil. The pore water pressure dissipation is worth to investigate to further understand the ground improve process by using pervious concrete piles.

3. Instead of single pile, the further investigation should include the pile and soil behavior of group piles. And the 3D model will be more benefit for investigation the soil-pile interaction and group piles behavior.
4. The field tests on pervious concrete pile will be helpful for investigate the pervious concrete piles behavior and industrial application.

REFERENCE

Aboshi, H., Ichimoto, E., Harada, K., and Emoki, M. (1979). The Compozer: A Method to Improve Characteristics of Soft Clays by Inclusion of Large Diameter Sand Columns. *International Conference on Soil Reinforcement, Reinforced Earth and Other Techniques, Vol.1, Paris*, pp 211−216.

Aboshi, H., and Suematsu, N. (1985). Sand Compaction Pile Method: State-of-art Paper. *3rd International Seminar on Soil Improvement Methods*, Singapore, pp. 1−12.

Adalier, K., Elgamal, A., Meneses, J. and Baez, J. I. (2003). Stone Columns as Liquefaction Countermeasure in Non-plastic Silty Soils, *Soil Dynamics and Earthquake Engineering*. Vol.23, No. 7, pp. 571−584.

Adalier, K. and Elgamal, A. (2004). Mitigation of Liquefaction and Associated Ground Deformations by Stone Columns. *Engineering Geology*, Vol.72, No. 3-4, pp. 275−291.

Ambily, A. P. and Gandhi, S. R. (2007). Behavior of Stone Columns Based on Experimental and FEM Analysis, *Journal of Geotechnical and Geoenvironmental Engineering*, Vol. 133, No. 4, pp. 405−415.

ASTM. (2009a). Standard Practice for Making and Curing Concrete Test Specimens in the Laboratory. *C192*, West Conshohocken, PA.

ASTM. (2009b). Standard Test Method for Compressive Strength of Cylindrical Concrete Specimens. *C39*, West Conshohocken, PA.

ASTM. (2009c). Standard Test Methods for Deep Foundations under Lateral Load. *D3966*, West Conshohocken, PA.

ASTM. (2009d). Standard Test Methods for Deep Foundations under Static Axial Compressive Load. *D1143*, West Conshohocken, PA.

ASTM. (2009e). Standard Test Method for Density and Void Content of Freshly Mixed Pervious Concrete. *C1688*, West Conshohocken, PA.

ASTM. (2009f). Standard Test Method for Flexual Strength of Concrete (Using Simple Beam with Third-Point Loading). *C78*, West Conshohocken, PA.

ASTM. (2009g). Standard Test Methods for Maximum Index Density and Unit Weight of Soils Using a Vibratory Table. *D4253*, West Conshohocken, PA.

ASTM. (2009h). Standard Test Methods for Minimum Index Density and Unit Weight of Soils and Calculation of Relative Density. *D4254*, West Conshohocken, PA.

ASTM. (2009i). Standard Test Methods for Splitting Tensile Strength of Cylindrical Concrete Specimens. *C496*, West Conshohocken, PA.

ASTM. (2009j). Standard Test Methods for Static Modulus of Elasticity and Poisson's Ratio of Concrete in Compression. *C469*, West Conshohocken, PA.

Ashford, S. A., Rollins, K. M., Bradford V, S. C., Weaver, T. J., and Baez, J. I. (2000). Liquefaction Mitigation Using Stone Columns Around Deep Foundations: Full Scale Test Results. *Transportation Research Record 1736*, pp 110-118.

Baez, J. I. (1995). A Design Model for the Reduction of Soil Liquefaction by Vibro-stone Columns. *Ph.D. Dissertation, University of Southern California*, Los Angeles, CA.

Barksdale, R. D., and Bachus, R. C. (1983). Design and Construction of Stone Columns. *Federal Highway Administration*, FHWA/RD 83/026, Vol. 1, Report No.1.

Basu, P., Loukidis, D., Prezzi, M. and Salgado, R. (2011). Analysis of Shaft Resistance of Jacked Piles in Sands. *International Journal for Numerical and Analytical Methods in Geomechanics*, Vol. 35, pp. 1605−1635.

Beeldens, A., Gemert, D. V. and Caestecker, C. (2003). Porous Concrete: Laboratory Versus Field Experience. *9th International Symposium on Concrete Roads*, Istanbul, Turkey.

Bergado, D. T., Miura, N., Panichayatum, B. and Sampaco, C. L. (1988). Reinforcement of Soft Bangkok Clay using Granular Piles. *Proceedings of the International Geotechnical Symposium on Theory and Practice of Earth Reinforcement*, pp. 179 – 184.

Bergado, D. T., Chai, J. C., Alfaro, M. C., and Balasubramaniam, A. S. (1994). *Improvement Techniques of Soft Ground in Subsiding and Lowland Environment*, A.A. Balkema, Rotterdam/Brookfield VT USA.

Brandenberg, S. J., Kutter, B. L. and Wilson, D. W. (2008). Fast Stacking and Phase Corrections of Shear Wave Signals in a Noisy Environment. *Journal of Geotechnical and Geoenvironmental Engineering*, Vol. 134, No. 8, pp. 1154 – 1165.

Brinkgreve, R. B. J., Broere, W. and Waterman, D. (Edited). *PLAXIS 2014*, PLAXIS, Delft, Netherlands.

Castro, J. and Karstunen, M. (2010). Numerical Simulation of Stone Column Installation. *Canadian Geotechnical Journal,* Vol. 47, pp. 1127 – 1138.

Chen, J. F., Jan, J., Oztoprak, S., and Yang, X. M. (2009). Behavior of Single Rammed Aggregate Piers Considering Installation Effects. *Computers and Geotechnics*, Vol. 36, pp. 1191−1199.

Colombi, A., Fioravante, V., and Jamiolkowski, M. (2006). Displacement vs. Non-displacement Axially Loaded Pile Behaviour in Sand from Centrifuge Tests. *Proceedings of the 6th International Conference on Physical Modeling in Geotechnics*, Hong Kong, pp. 815 – 820.

Dijkstra, J., Broere, W. and Heeres, O. M. (2011). Numerical Simulation of Pile Installation. *Computer and Geotechnics*, Vol. 38, pp. 612 – 622.

Dijkstra, J., Broere, W. and Tol A. F. V. (2006). Numerical Investigation into Stress and Strain Development around A Displacement Pile in Sand. *6th European Conference on Numerical Methods in Geotechnical Engineering*, Graz, Austria, pp. 595 – 600.

Dijkstra, J., Broere, W. and Tol, A. F. V. (2008). Density Changes Near An Advancing Displacement Pile in Sand. *Proceeding of 2nd International Conference on Foundations*, pp. 545 – 554.

Elgamal, A., Lu, J. and Forcellini, D. (2009). Mitigation of Liquefaction-Induced Lateral Deformation in a Sloping Stratum: Three-dimensional Numerical Simulation. *Journal of Geotechnical and Geoenvironmental Engineering*, Vol. 135, No. 11, pp. 1672 – 1682.

Elias, V., Welsh, J., Warren, J., Lukas, R., Collin, J. G. and Berg, R. R. (2006). *Ground Improvement Methods I & II*. National Highway Institute, Federal Highway Administration, U.S. Department of Transportation, FHWA NHI-06-019.

Elshazly, H. A., Hafez, D. H., and Mossaad, M. E. (2008). Reliability of Conventional Settlement Evaluation for Circular Foundations on Stone Columns. *Geotechnical and Geological Engineering*, Vol. 26, No. 3, pp. 323−334.

Fan, C. C., and Long, J. H. (2005). Assessment of Existing Methods for Predicting Soil Response of Laterally Loaded Piles in Sand. *Computers and Geotechnics*, Vol. 32, No. 4, pp. 274 – 289.

Frikha, W., Bouassida, M. and Canou, J. (2013). Observed Behaviour of Laterally Expanded Stone Column in Soft Soil, Geotechnical and Geological Engineering, Vol. 31, No. 2, pp. 739−752.

Gennaro, V. D., Frank, R. and Said, I. (2008). Finite element analysis of model piles axially loaded in sands, *Italian Geotechnical Journal*, Vol. 2, pp. 44 – 62.

Geopier Foundations Company. (2014). Rammed Aggregate Pier System. http://www.geopier.com/Geopier-Systems

Guetif Z., Bouassida M. and Debats J. M. (2007). Improved Soft Clay Characteristics Due to Stone Column Installation. *Computers and Geotechnics*, Vol. 34, No. 2, pp. 104 − 111.

Han, J. and Gabr, M. (2002). Numerical Analysis of Geosynthetic-Reinforced and Pile-Supported Earth Platforms over Soft Soil. *Journal of Geotechnical and Geoenvironmental Engineering*, Vol. 128, No. 1, pp. 44 − 53.

Handy, R. L. (2001). Does Lateral Stress Really Influence Settlement. *Geotechnical and Geoenvironmental Engineering*, Vol. 127, No. 7, pp. 623 − 626.

Hoevelkamp, K. K. (2002). Rammed Aggregate Pier Soil Reinforcement: Group Load Tests and Settlement Monitoring of Large Box Culvert. *M.S. Thesis, Iowa State University*, Ames, Iowa.

Hughes, J. M. O. and Withers, N. J. (1974). Reinforcing of Soft Cohesive Soils with Stone Column. *Ground Engineering*, Vol.7, No. 7. pp. 42 − 49.

Hunt, C. E., Pestana, J. M., Bray, J. D. and Riemer, M. F. (2002). Effect of Pile Installation on Static and Dynamic properties of Soft Clay. *Journal of Geotechnical Engineering*, Vol. 128, No. 1, pp. 199 − 212.

Janbu, N. (1963). Soil Compressibility as Determined by Oedometer and Triaxial Tests. *European Conference on Soil Mechanics and Foundation Engineering*, Wiesbaden, Germany, Vol. 1, pp. 19 − 25.

Kajio, S., Tanaka, S., Tomita, R., Noda, E. and Hashimoto, S. (1998). Properties of Porous Concrete with High Strength. *8th International Symposium on Concrete Roads*, pp. 171 − 177.

Kevern, J. T., Schaefer, V. R., Wang, K., and Suleiman, M. T. (2008). Pervious Concrete Mixture Proportions for Improved Freeze-Thaw Durability. *Journal of ASTM International*, Vol. 5, No. 2.

Kim, B. T., Kim, N. K., Lee, W. J. and Kim, Y. S. (2004). Experimental Load-Transfer Curves of Laterally Loaded Piles in Nak-Dong River Sand. *Journal of Geotechnical and Geoenvironmental Engineering*, Vol. 130, No. 4, pp. 416 – 425.

Kim, Y., and Jeong, S. (2011). Analysis of Soil Resistance on Laterally Loaded Piles Based on 3D Soil-pile Interaction. *Computers and Geotechnics*, Vol. 38, No. 2, pp. 248 – 257.

Klotz, E. U. and Coop, M. R. (2001). An Investigation of the Effect of Soil State on the Capacity of Driven Piles in Sands. *Geotechnique*, Vol. 51, No. 9, pp. 733 – 751.

Krishna, A. M., Madhav, M. R., and Latha, G .M. (2006). Liquefaction Mitigation of Ground Treated with Granular Piles: Densification Effect. *Journal of Earthquake Technology*, Vol. 43, No. 4, pp. 105 – 120.

Lawton, E. C. (1999). *Performance of Geopier Foundation during Simulated Seismic Tests at South Temple Bridge on Interstate 15*, Salt Lake city, Utah, Interim Report, No. UUCVEEN 99-06, University of Utah, Salt Lake City, Utah.

Lawton, E. C. (2000). Performance of Geopier Foundations During Simulated Seismic Tests on I-15 Bridge Bents. *Transportation Research Record 1736*, No. 00-1307, pp. 3 – 11.

Lee, F. H., Juneja, A., and Tan, T. S. (2004). Stress and Pore Pressure Changes Due to Sand Compaction Pile Installation in Soft Clay. *Geotechnique*, Vol. 54, No.1, pp. 1 − 16.

Lee, J. S. and Santamarina, J. C. (2005). Bender Elements: Performance and Signal Interpretation. *Journal of Geotechnical and Geoenvironmental Engineering*, Vol. 131, No. 9, pp. 1063 – 1070.

Lee, J. S., Guimaraes, M., and Santamarina, J. C. (2007). Micaceous Sands Microscale Mechanics and Macroscale Response. *Journal of Geotechnical and Geoenvironmental Engineering*, Vol. 133, No. 9, pp. 1136 – 1143.

Lehane, B. M., Jardine, R. J, Bond, A. J., and Frank, R. (1993). Mechanisms of Shaft Friction in Sand from Instrumented Pile Tests. *Journal of Geotechnical Engineering, ASCE*, Vol.119, No. 1, pp. 19 – 35.

Lehane, B. M. and White, D. J. (2005). Lateral Stress Changes and Shaft Friction for Model Displacement Piles in Sand. *Canadian Geotechnical Journal*, Vol. 42, No. 4, pp. 1039 – 1052.

Lin, K. Q., and Wong I. H. (1999). Use of Deep Cement Mixing to Reduce Settlement Bridge Approaches. *Journal of Geotechnical and Geoenvironmental Engineering*, Vol. 125, No. 4, pp. 309 – 320.

Lundberg, A. B., Dijkstra, J., and Tol, A. F. V. (2013). Displacement Pile Installation Effects in Sand. *Installation Effects in Geotechnical Engineering*, Hicks Editor, Taylor and Francis Group, London, UK.

Magnan J. P. (1983). Théorie et pratique des drains verticaux. *Edition Technique et Documentation-Lavoisier*. Paris.

Magnan J. P. (1983). *Théorie et pratique des drains verticaux*. Edition Technique et Documentation-Lavoisier. Paris.

Mitchell J.K. (1981). State-of-the-art Report, Session 12. *10th International Conference on Soil Mechanics and Foundation Engineering*, Stockholm, Sweden, pp. 506 − 565.

Mitchell, J. K., Baxter, C. D. P., and Munson, T. C., (1995). Performance of Improved Ground During Earthquakes. *Proceedings of Soil Improvement for Earthquake Hazard Mitigation*, ASCE Geotechnical Publication No.49, pp. 1 – 36.

Mitchell, J. K., and Soga, K. (2005). *Fundamentals of Soil Behavior*, Third Edition, Wiley, Hoboken, NJ.

Moseley, M. P., and Kirsch, K. (2004). *Ground Improvement*. Spon Press, Taylor and Francis Group, New York, NY.

Ni, L., Suleiman, M. T. and Raich, A. (2013). Pervious Concrete Pile: An Innovative Ground Improvement Alternative. *Geo-Congress 2013*, pp. 2051 – 2058.

Naggar, M. H. EI and Wei, J. Q. (1999) Response of Tapered Piles subjected to Lateral Loading. *Canadian Geotechnical Journal*, Vol. 36, No. 1, pp. 52 – 71.

Ohtsuka, T., Aramaki, G., and Koga, K. (2004). Soil Improvement of Soft Ground around Pile Foundation in Earthquake-Resistant Design. *Lowland Technology International*, Vol. 6, No. 1, pp. 42 – 54.

Okamura, M., Ishihara, M., and Ohshita, T. (2003) Liquefaction Resistance of Sand Deposit Improved with Sand Compaction Piles. *Soils and Foundations*, Vol. 43, No.5, pp.175 – 187.

Okamura, M., Ishihara, M., and Tamura, K. (2006). Degree of Saturation and Liquefaction Resistances of Sand Improved with Sand Compaction Pile.

Journal of Geotechnical and Geoenvironmental Engineering, Vol. 132, No. 2, pp. 258 – 264.

Palmer, M. C., O'Rourke, T. D., Olson, N. A., Abdoun, T., Ha, D. and O'Rourke, M. J. (2009). Tactile Pressure Sensors for Soil-Structure Interaction Assessment. *Journal of Geotechnical and Geoenvironmental Engineering*, Vol. 135, No.11, pp. 1638 – 1645.

Park, S. and Tia, M. (2004). An Experimental Study on the Water-purification Properties of Porous Concrete. *Cement and Concrete Research*, Vol. 34, No. 2, pp. 177 – 184.

Pham, H. T. V. (2005). *Support mechanism for rammed aggregate piers*. Ph.D Dissertation, Iowa State University, Ames, Iowa.

Pham, H. T. V. and White, D. J. (2007). Support Mechanisms of Rammed Aggregate Piers. II: Numercial Analyses. *Journal of Geotechnical and Geoenvironmental Engineering*, ASCE, Vol. 133 No. 12, pp. 1512 – 1521.

Pucker, T., Grabe, J. (2012). Numerical Simulation of the Installation Process of Full Displacement Piles. *Computers and Geotechnics*, Vol. 45, pp. 93 – 106.

Reese, L. C., Cox, W. R., and Koop, F. D. (1974). Analysis of Laterally Loaded Pile in Sand. *In Proceedings of the Six Annual Offshore Technology Conference*. Houston, TX, No. 2080, pp. 671 – 690.

Said, I., Gennaro, V. D. and Frank, R. (2009). Axisymmetric Finite Element Analysis of Pile Loading Tests, *Computer and Geotechnics*, Vol. 36, PP. 6 – 19.

Salgado, R., Mitchell, J. K., and Jamiolkowski, M. (1997). Cavity Expansion and Penetration Resistance in Sand. *Journal of Geotechnical and Geoenvironmental Engineering*, ASCE, Vol. 123 No. 4, pp. 344 – 354.

Salgado, R. and Prezzi, M. (2007), Computation of Cavity Expansion Pressure and Penetration Resistance in Sands. *International Journal of Geomechanics*, ASCE, Vol. 7 No. 4, pp. 251 – 265.

Salgado, R. (2014). Experimental Research on Cone Penetration Resistance. *Keynote Lecture. GeoCongress 2014*, Atlanta, GA, Feb 23 – 26.

Schaefer, V. R., Abramson, L. W., Drumheller, J. C., Hussin, J. D., and Sharp, K. D. (1997). *Ground Improvement, Ground Reinforcement, Ground Treatment: Development 1987−1997*. Geotechnical special publication No. 69, ASCE, Logan, Utah.

Schaefer V. R., Wang K. J., Suleiman M. T., and Kevern J. T. (2006). *Mix Design Development for Pervious Concrete in Cold Weather Climates*. National Concrete Pavement Technology Center, Iowa State University, Ames, Iowa.

Schanz, T., Vermeer, P. A., Bonnier, P. G. (1999). The Hardening-Soil Model: Formulation and Verification. *Beyond 2000 in Computational Geotechnics (Brinkgreve, R. B. J. edited)*, Balkema, Rotterdam, pp. 281 – 290.

Shao, L., Taylor, D., Koelling, M. (2013). Stone Columns and Earthquake Drain Liquefaction Mitigation for Federal Center South in Seattle, *Washington. Geo-Congress 2013*, San Diego, CA, pp. 864 – 878.

Shenthan, T., Nashed, R., Thevanayagam, S. and Martin, G. R. (2004). Liquefaction Mitigation in Silty Soils Using Composite Stone Columns and Dynamic

Compaction. *Earthquake Engineering and Engineering Vibration*, Vol.3, No. 1, pp. 39 – 50.

Shublaq, E. W. (1992). Soil Disturbance due to Installation of Model piles and Pile Groups. *Soils and Foundations*, Vol. 32, No. 4, pp. 17 – 26.

Stuedlein, A. W. and Holtz, R. D. (2013). Bearing Capacity of Spread Footings on Aggregate Pier Reinforced Clay. *Journal of Geotechnical and Geoenvironmental Engineering*, Vol. 139, No. 1, pp. 49 – 58.

Suleiman, M. T., Pham, H., and White, D. J. (2003). Numerical Analyses of Geosynthetic-Reinforced Rammed Aggregate Pier-Supported Embankments. *Report No. ISU-ERI-03598*, Iowa State University, Ames, Iowa.

Suleiman, M. T. and White, D. (2006). Load Transfer in Rammed Aggregate Piers. *International Journal of Geomechanics*, Vol. 6, No. 6, pp. 389 – 398.

Suleiman, M. T., Kevern, J., Schaefer, V. R., and Wang, K. (2006). Effect of compaction energy on pervious concrete properties. *Concrete Technology Forum–Focus on Pervious Concrete*, National Ready Mix Concrete Association, Nashville, TN.

Suleiman, M. T., Gopalakrisnan, K., and Kevern, J. (2011). Structural Behavior of Pervious Pavement Systems. *Journal of Transportation Engineering*, Vol. 137, No. 12, pp. 907 – 917.

Suleiman, M. T. Ni, L. and Raich, A. (2014a). Development of Pervious Concrete Pile Ground Improvement Alternative and Behavior under Vertical Loading. *Journal of Geotechnical and Geoenvironmental Engineering*, under review.

Suleiman, M. T. Ni, L., Helm, J. D. and Raich, A. (2014b). Soil-Pile Interaction for Small Diameter Pile Embedded in Granular Soil Subjected to Passive Loading. *Journal of Geotechnical and Geoenvironmental Engineering*, Accepted.

Suleiman, M. T., Ni, L., Raich, A. M., and Ghazanfari, E., (2013). Measured Soil-Structure Interaction for Piles Subjected to Lateral Loading. *Journal of Geotechnical and Geoenvironmental Engineering*, Under Review.

Talesnick, M. (2005). Measuring Soil Contact Pressure on a Solid Boundary and Quantifying Soil Arching. *Geotechnical Testing Journal*, Vol.28, No. 2, pp. 171 – 179.

Talesnick, M., Horany, H., Dancygier, A. N. and Karinski, Y. S. (2008). Measuring soil pressure on a buried model structure for the validation of quantitative frameworks. *Journal of Geotechnical and Geoenvironmental Engineering*, Vol. 134, No. 6, pp. 855 – 865.

Tamai, M., and Yoshida, M. (2003). Durability of Porous Concrete. *Proceeding in 6th International Conference on Durability of Concrete*, American Concrete Institute, Detroit, MI.

Tennis P. D., Leming, M. L. and Akers, D. J. (2004). *Pervious Concrete Pavements*. EB302, Portland Cement Association, Skokie, IL, and National Ready Mixed Concrete Association, Silver Spring, MD.

Terashi, M., and Juran, I. (2000). Ground Improvement - State-of-the-art. *International Conference on Geotechnical and Geological Engineering*. Melbourne, Australia.

Thompson, M. J. and Suleiman, M. T. (2010). Numerical Modeling of Rammed Aggregate Pier Construction. *GeoFlorida 2010: Advances in Analysis, Modeling & Design*, pp 1460-1469.

Vesic, A. S. (1977). Design of Pile Foundations. *Transportation Research Board National Cooperative Highway Research Program, National Research Council*, ed., Washington, D.C.

Von Soos, P. (1990). *Porperties of Soil and Rock* (in German). In Grundbautaschenbuch Part 4, Edition 4, Ernst & Sohn, Berlin.

Wehnert, M. and Vermeer, P. A. (2004a). Numerical Analyses of Load Tests on Bored Piles. *Proceeding of 9th numerical models in Geomechanics*, Ottawa, Canada, pp. 505 – 511.

Wehnert, M. and Vermeer, P. A. (2004b). Numerische Simulation von Probebelastungen an Grobbohrpfahlen (in German). *Proceeding of the 4th Kolloqium Bauen in Boden und Fels*, Ostfildern, pp. 555 – 565.

Welsh, J. P., (1987). *Soil Improvement -A Ten Year Update*, ASCE Geotechnical Publication No.12.

White, D. J. and Bolton, M. D. (2004). Displacement and Strain Paths During Plane-Strain Model pile installation in sand. *Geotechnique*, Vol. 54, No. 6, pp. 375 – 397.

White, D. J. and Suleiman, M. T. (2004). Design of Short Aggregate Piers to Support Highway Embankments. *Journal of the Transportation Research Board*. No. 1868, Transportation Research Board, National Research Council, Washington D. C., pp. 103 – 112.

White, D. J., and Suleiman, M. T. (2005) "Full Scale Direct Shear Tests for Rammed Aggregate Piers." *Report No. ISU-ERI-05416*, Iowa State University, Ames, Iowa.

Yang, K. and Liang, R. (2006). Methods for Deriving p-y Curves from Instrumented Lateral Load Tests. *Geotechnical Testing Journal*, Vol. 30, No. 1, pp. 49 – 58.

Yasuda, S., Ishihara, K., Harada, K., and Shinkawa, N. (1996). Effectiveness of the Ground Improvement on the Susceptibility of Liquefaction Observed During the 1995 Hyogo-ken Nambu (Kobe) Earthquake. *World Conference on Earthquake Engineering*, Mexico.

Yi, J. T., Goh, S. H. and Lee, F. H. (2010). Centrifuge Study on the "Set-up" Effect Induced by Sand Compaction Pile Installation, *Physical Modeling in Geotechnics – Springman*, Laue &Seward (eds), pp. 1383 – 1388.

Yu, H. S. (1990). *Cavity Expansion Theory and its Application to the Analysis of Pressuremeters*, Dissertation, University of Oxford, British.

Yu, H. S. (2000). *Cavity Expansion Methods in Geomechanics*. Kluwer Academic Publishers, Dordrecht, Netherlands.

VITA

Lusu Ni was born on August 12, 1985 at Yushan, Jiangxi Province of China. He received his Bachelor Degree of Civil Engineering in 2007 and Master Degree of Underground Engineering in 2010 at Beijing Jiaotong University, Beijing, China. He started research on this doctoral dissertation at Lehigh University in August 2010.